EFFECTIVENESS OF SUBSURFACE DRAINAGE AND VEGETATION IN ENHANCING THE SLOPE STABILITY: A COMPREHENSIVE CASE STUDY ON BADULUSIRIGAMA LANDSLIDE

Lilanka Udayana Matarambha Kankanamge

(168963X)

Thesis submitted in partial fulfilment of the requirements for the degree Master of Engineering in Foundation Engineering and Earth Retaining Systems

Department of Civil Engineering

University of Moratuwa

Sri Lanka

July 2020

Statement of Authentication

I declare that this is my own work and this thesis does not incorporate without acknowledgement any material previously submitted for a Degree or Diploma in any other University or institute of higher learning and to the best of my knowledge and belief it does not contain any material previously published or written by another person except where the acknowledgement is made in the text.

Also, I hereby grant to University of Moratuwa the non-exclusive right to reproduce and distribute my thesis/dissertation, in whole or in part in print, electronic or other medium. I retain the right to use this content in whole or part in future works (such as articles or books).

Name of the candidate: Lilanka Kankanamge

Signature of the candidate: Date:

The above candidate has carried out research for the Master thesis under my supervision.

Signature of the supervisor: Date:

Professor S.A.S Kulathilaka,
BSc. Eng. Hons (Moratuwa), PhD (Monash), CEng, MIE (SL)
Senior Professor,
Department of Civil Engineering,
University of Moratuwa,
Sri Lanka

Acknowledgement

This accomplishment would not have been a reality without the tremendous support I received from my supervisor, Senior Professor S.A.S. Kulathilaka. I am deeply grateful to him for setting a strong platform for me to pursue my career in geotechnical engineering and for building- up confidence in me to engage in innovative research activities. He not only encouraged but also facilitated the pathway for me to connect with other researchers from different parts of the world, to gain inspiration and to work on new research ideas. Professor Kulathilaka has been a true mentor and an exceptional role model to me throughout my research candidature.

Next, I would like to acknowledge Prof. Apiniti Jotisankasa of Kasetsart University, Thailand, for his suggestions, insightful comments and his generosity in sharing knowledge. My sincere thanks also extend to Dr. U.P. Nawagamuwa, Dr. Nalin de Silva, all the lecturers of the M.Eng programme and staff of the geotechnical engineering division of University of Moratuwa, for their assistance during my candidature.

It is my obligation to acknowledge the guidance and the support given by Eng. (Dr.) Asiri Karunawardena, the director general of NBRO and Mr. K.N. Bandara, the director of the Geotechnical Engineering Division (GED) of NBRO. Also, the support from all the staff of GED, especially from Eng (Ms). Nanthini Vasanthan, Mr. Chandima, Mr. Abeysinghe, Mr. Prasad and Ms. Sewwandi is thankfully appreciated.

The continuous assistance, kindness and the understanding from my mother, father and brother has helped me to come a long way and it meant a lot to me during my research career as well. I would also like to thank my friends and colleagues who never failed to cheer me up when it is most needed.

Last but not least, I would like to express my gratitude to Eng. (Dr.) Manasi Wijerathna for being with me in every ups and downs and supporting me on the way to this great achievement that I am proud of.

Abstract

Slope instability, triggered by excessive rainfall, is one of the common geo –hazards that geotechnical engineers are challenged with in tropical countries such as Sri Lanka. Typically, these slope failures are initiated in colluvial layers derived from former landslides or planes of low shear strength in differently weathered zones in the thick soil overburden. Improvement of surface and subsurface drainage has proven to be effective in improving the slope stability by lowering the ground water table as well as preventing near surface perched water table conditions. Badulusirigama Landslide in central highlands of Sri Lanka is an example for a slow moving long rotational slip that activates after heavy rainfall events.

The landslide was rectified with over 45 m long individual sub-horizontal drains that are arranged into a network of radial drainage groups at different elevations along the long sliding mass. This site is also well equipped with monitoring instruments and thus provides a great case history to further our understanding on contribution of surface and subsurface drains in mitigating landslides. In this study, the effectiveness of the introduced subsurface drainage measures in enhancing the stability of the Badulusirigama Landslide was investigated using 2D and 3D numerical models. The numerical models were then used to predict the behaviour of the landslide during different anticipated rainfall events.

The results show that the subsurface drains system enhances the initial near failure condition of the site to a stable slope with a factor of safety of over 1.25 within one month. After initial drop down of the ground water table, the sub-horizontal drains still remain effective by rapidly draining out any infiltration. The analysis also shows that the width of the influence zone of radial horizontal drains should be carefully selected when simplifying the problem into 2D plane strain models because the influence can be very much localised in a low permeable medium. Possibility of introducing surface vegetation as a hybrid measure along with subsurface drainage was also investigated. A factor of safety improvement of 38% and 16.3% was achieved after the simulation of construction of the drains in 2D plane strain and 3D finite element analyses separately. Also, it was found that, vegetation could result in increasing the hydraulic conductivity of the root zone, leading to development of perched water table conditions.

Table of Contents

List of Figures

List of Tables

Chapter 1

1 INTRODUCTION

1.1 Background

Slope instability is one of the major geo –hazards, in geotechnical engineering which creates number of disastrous situations including fatalities and damages to infrastructure facilities. Not only the natural slopes, but also the manmade slopes are liable to failures, and most of the times this is triggered by excessive rainfall. Typically, the type of slope failure encountered in tropical climatic regions are shallow translational movements occurred in the thick soil overburden through planes of low shear strength. In addition, slope failures also occur due to increased demand of shear strength to maintain the stability of the slope, due to human interventions. Apart from the rainfall events, additional surcharges applied on the slope, steepening of the slope, and drawdown of water level in front of the slope would demand mobilization of additional shear stress within the slope to maintain the stability. Inability of soil mass to mobilize the excess shear strength required to maintain the equilibrium, causes movements and subsequent slope failure in the soil mass.

Soil slopes in arid and semi-arid regions of the world have distinct characteristics; deep phreatic surface, thick soil overburden composed of in–situ weathering of the

parent rock and sometimes colluvium deposits which are reminisce or remains of former earth slips. Near surface soil profile of these slopes are dominated by negative pore water pressures or the suction, during the dry periods. The magnitude of the suction prevails in a soil depends on the type of soil, pore size distribution and the degree of saturation. The apparent cohesion provided by the effect of matric suction has a direct impact on the shear strength of the soil. Beside the aforementioned internal factors, the nature of the vegetation overlying the slope has its own effects on the stability criteria of the slope. Plant roots provide an additional support to keep the soil mass intact and also some plant roots increase the suction within the soil pores through the mechanisms of evapotranspiration.

Introduction of surface and subsurface drainage is one of the popular rectification techniques in landslide prone slopes. The main idea behind such drainage improvements is to lower the natural ground water table as well as to avoid the creation of near surface perched conditions. A sound combination of surface and subsurface drainage network could be effective in even mitigating slopes of large extent which are prone to failures.

Badulusirigama landslide is located in the Badulla administrative district of Sri Lanka. It is about 4 kilometres away from the city centre of Badulla and towards Batticaloa highway. A part of the landslide is situated within the premises of Uwa–Wellassa University. The width of the landslide is about 120 m, length is around 500 m, and the slip surface has been identified at a depth of around 10 – 15 m. Sliding had occurred in a zone of weak strength in the slope. Further, the cracks formed in the body of the sliding mass had promoted deep infiltration of rain water and development of pore water pressures in the slide area. This landslide poses considerable risk to residential areas around the lower part of the slope.

Subsurface and surface drainage improvements have been implemented at the site with the objective of lowering the ground water table and directing the surface flow paths. In addition to those drainage systems, some bio–engineering measures are proposed to be introduced to control the surface run–off, strengthen the top soil by

means of root reinforcement, increase the scenic and aesthetic value, and to gain some commercial benefits.

In this study, the effectiveness of the introduced hybrid mitigation measures in enhancing the slope stability of the Badulusirigama landslide was analyzed using numerical models. Soil strength properties were determined using the field investigation conducted at the site and experience under similar conditions. The effect of sub surface drainage and vegetation were studied using different cases of analysis.

1.2 Scope of the research

The scope of this study is to analyze the effects of structural and bio-engineering mitigation measures in stabilizing the Badulusirigama landslide. The impact of both measures in stabilizing the slope is separately addressed and assessed. Effectiveness of sub surface drainage in mitigating the risk of a slow moving landslide was evaluated using numerical models and was compared with the data obtained from field instrumentation. Effectiveness of surface vegetation in eliminating the formation of shallow slip surfaces was also studied, incorporating the principals of soil- bio engineering and unsaturated soil mechanics.

1.3 Thesis objectives

The main objectives of this thesis are to:

- Study the impact of subsurface drainage improvement in stabilizing a deep seated failure at Badulusirigama
- Quantify the effect of different vegetation in slope stabilization.
- Incorporate the effect of surface vegetation in geotechnical modelling of slope stability.
- Study the effectiveness of installed drainage measures in ensuring the stability of the slope in response to anticipated critical rainfalls.

1.4 Research methodology

Preliminary investigations had been done in the site. Borehole data, geological data, geomorphological data, survey data, rainfall data as well as socio–economic data

of the residents in the area were already available from the preliminary investigations conducted. Some instrumentation inclusive of; water level meters, piezometers, extensiometers and pipe strain gauges were installed at the site and the monitoring programme was in progress. More information on the site conditions were collected based on the visual observations.

Shear box test samples were collected from shallower depths, in undisturbed form, so as to determine the shear strength properties and other necessary unsaturated soil parameters which are essential for the analysis. The required parameters were then determined from the laboratory tests.

The most critical cross sections were selected from the survey data. Existing stability conditions of the slope was analyzed for those cross sections, incorporating the soil properties obtained from laboratory experiments. The same sections were then modified for the simulation of the effect of sub-horizontal drains. The response of the slope to a critical rainfall after improving drainage measures was also evaluated.

The effect of vegetation in reducing the risk of progressive shallow failures was then modelled with modified shear strength parameters. The effective stress shear strength parameters obtained from the laboratory tests were revised to account for the effect of vegetation. Root tensile strength tests were conducted on the selected plants to obtain the tensile strength of the roots. Empirical correlations available in the literature, which provide the relationship between root tensile strength and soil cohesion, were then applied to modify the soil shear strength properties.

Finally, the impact of the hybrid solution on protecting the slope was assessed. The results obtained from the numerical analysis were validated against the available field monitoring data. Ground deformations, variation of the pore water pressure profile and other related parameters predicted using the numerical model were compared with actual data available. Parametric studies were conducted to evaluate the variations of factor of safety under different drainage and vegetation conditions.

1.5 Thesis outline

Chapter 2: **Review of studies on rain induced slope instability and stabilization methods**

This chapter discusses current state of the art evaluation of stability of slopes, modes of slope instability - especially in rain induced slope failures and stabilisation of slopes with drainage. The use of vegetation in stabilizing slopes are also discussed.

Chapter 3: **Description of the case history**

This chapter presents a concise description of the Badulusirigama site, geology, geomorphology, sub soil conditions and also the nature and the history of the failures. It further details the different driving forces that led to slope instability and the extent of the slide.

Chapter 4: **Development of the geotechnical model of the Badulusirigama site**

Chapter 4 presents the engineering properties of the sub soil at the site. Index properties of the soil in the slide area, shear strength parameters of the slope material and other essential unsaturated soil properties in response to infiltration of rainfall, which are vital in modelling slope stability, are presented in this chapter.

Chapter 5: **Two dimensional (2D) plain strain analysis of the stability of the slope**

This chapter presents the comprehensive study conducted using 2 dimensional plane strain analysis with limit equilibrium approach. Stability of the slope has been assessed before and after installation of subsurface drainage measures. Influence of the sequence of installation of drains on the enhancement of stability was also illustrated. Influence of surface vegetation on slope stability and response of the slope to different rainfall events were also presented in this chapter.

Chapter 6: **Developing a three dimensional (3D) finite element model of the Badulusirigama landslide**

This chapter describes the development of the 3D finite element model for Badulusirigama Landslide. Different sequences of subsurface drainage construction, response of the slope to infiltration events after drainage improvement have been analyzed and the results are presented.

Chapter 7 **Conclusions and Recommendations**

This chapter summarizes the key findings of current study. Further, it discusses how these hybrid solutions, comprise of both structural and nature based mitigation measures can be effectively implemented in the field.

Chapter 2

2 REVIEW OF STUDIES ON RAIN INDUCED SLOPE INSTABILITY AND STABILIZATION METHODS

2.1 Introduction

In this chapter, a review of studies on rain induced slope instability and methods of rectification will be presented. Methods of analysis performed under such conditions are also reviewed.

2.2 Stability of a slope

Stability of a slope can be defined as the ability to withstand alone despite of the forces driving towards different movements (Duncan et al. 1996). This is a function of different internal and external factors associated with the slope. Type of soil cover, thickness of the soil overburden, slope angle, cyclic changes of the pore water pressure regime within the slope and other geological factors are vital internal factors in maintaining the stability of a slope. Climatic conditions, vegetation, disturbance due to human intervention are main external factors critical in stability (Sidle et al. 1985; Huang 2014). These factors have direct and indirect impacts on the stability of a slope.

Stability of a slope is directly connected with thermo – hydro – mechanical processes taking place in the soil and the surrounding environment (Elia et al. 2017). The outcome of different interactions between these factors, alter the natural equilibrium condition of the slope. In Sri Lanka, excessive rainfall is the main triggering factor for slope instability. The net infiltration as a result of prolonged rainfalls into residual or colluvium top soil formations of the slopes, create near surface perched water table conditions (Sujeevan and Kulathilaka 2011). On the other hand, these progressing water fronts into the soil pores, deplete the Matric suction and hence reduce the apparent cohesion (Collins and Znidarcic 2004). This is also a major governing factor especially in shallow translational slides. Variation

of the pore water pressure profile due to infiltration could result in either variability in the available shear strength or overall changes in the available shear strength. In either way, it could bring about an onset or progression of a failure (Elia et al. 2017). Besides, these shallow seated slope failures deep seated larger scale slope failures are also found in hill terrains. Some of them are creep movements, occurring over longer time durations and sometimes expedited by heavy rains. The threshold rainfall value for failure would be site specific.

With a prolonged rainfall of significant intensity or intermittent rainfalls over a long period of time, the infiltrated water will travel deeper causing a rise in the groundwater table. If the slope is formed of slopes of contrasting permeability; a layer of much lower permeability underlain by a layer of greater permeability, a pore pressure built up would develop at the boundary of the two layers. The failure surface could develop at the said boundary. (Sujeewan and Kulathilaka 2011). This phenomenon was observed at some large landslides that occurred in Sri Lanka within the last decade. In the landslides at Aranayaka and Meeriyabedda it could be seen that all the overburden soil down to the rock has moved as a debris flow.

Natural vegetation cover that exists on a slope has a profound impact on the stability of the slope. Vegetation cover on the slope resists the velocity of raindrops by providing a canopy effect (Coppin and Richards 1990). Thereby reduces the impact of the raindrops falling directly on to the soil slope. Surface vegetation covers inhibits the surface erosion of the slope and makes sure that the top soil is kept intact even at the presence of heavy rains. Vegetation also takes part in complex slope atmosphere interactions. It acts as an evaporation agent during the processes of evapotranspiration, to regulate the ground water condition of the slope. At present, it is quite popular to incorporate bio engineering measures in rectifying failed slopes, in combination with structural measures to enhance the aesthetic appearance as well as to provide the aforementioned additional stability. Lack of satisfactory methods to incorporate the effect of bio – engineering methods into conventional slope stability analysis is a major consideration among the researchers. Compared to well established design and computational approaches for

conventional slope retaining systems such as retaining walls, soil nail designs etc., standard methods for quantification of bio – engineering approaches, to a level at which it can be competently integrated into slope rectification designs, is still under developed and remains a major challenge. (Gray and Barker 2004; Yildiz et al. 2018)

Ingress of water into the soil mass during heavy rainfall conditions lead to generation of excess pore water pressures inside the slope. This excess pore water pressure will cause reduction in effective stresses and lead to slope instability. Therefore, the role of surface and subsurface drainage systems are vital in minimizing the infiltration into the slope as well as maintaining a low ground water table allowing rapid escape routes for water entered into the slope. Hence, drainage measures play an important role in slope stability. Natural slopes have their own drainage paths through which the surface runoff easily drains out of the slope area. These natural surface flow paths also reduce stagnation of the water in the body of the slope and the ingress of water into the slope. However, when a disturbed slope or a man-made slope is considered, the natural flow paths can be interrupted or not available at all and hence, artificial application of subsurface drainage measures is essential in maintaining its stability. Effort of a subsurface drainage network is crucial to maintain the stability of a slope, when there is a high tendency of infiltration and rise of ground water table conditions.

Overall stability of a slope is an integrated effort of number of components, which can be considered interdependent. These components, as a whole, have different interactions with the atmosphere, climatic conditions, geological and geomorphological conditions to balance the negative impacts and ensure the equilibrium state of the slope.

2.3 Methods of slope stability assessment

Slope stability assessment is one of the most important aspects in the field of geotechnical engineering. Stability assessment methods provide the fundamentals to ensure the safe design and construction in grounds with significant elevation

differences. It comes in to place in many geotechnical applications such as modification of natural slopes, construction of embankments and landslide studies. Assessing the stability of a slope was a long being interest within the geotechnical community. Simple qualitative approaches of understanding the stability state of a slope were adequate in the past. However, with the development of infrastructure facilities, confronting with adverse climate changes, rectification of failed/cut slopes, engineers wanted to assess the stability of a slope in terms of quantitative approaches. Consequently, number of methods have been developed and been in practice up to date, pertaining to slope stability analysis. These concepts have been incorporated into computer programmes to make the analyses efficient and user friendly. In broader terms, most widely used slope stability analysis methods can be divided into three main categories; limit equilibrium methods, limit analysis methods and finite element methods.

2.3.1 Limit Equilibrium Method (LEM) of Slope Stability Analysis

This is the most common approach for analysing the stability of slopes. In the limit equilibrium approach the equilibrium of mass of soil bounded by a failure surface is considered. Most of the limit equilibrium approaches use the Mohr – Coulomb failure criteria to determine the shear strength along a potential sliding plane of a slope. A good knowledge of the geology of the slope is essential in making a reasonable assumption of the shape of the potential failure surface. It has been shown in both analytically and through case records that in the case of uniform sub soil conditions the failure surface is likely to be circular. But in the case of non-uniform sub soil conditions the failure would take place along weaker links avoiding stronger material and would be non-circular. If there are stronger layers, the failure surface will avoid them. Accordingly, the trial failure surface of appropriate shape should be assumed giving due consideration to; (Figure 2.1), different sub soil layers, their shear strength parameters and the location of the phreatic surface. Within this framework number of different potential failure surfaces must be tried out. Then the Factor of Safety (FoS) is calculated considering the equilibrium of the soil mass bounded by the failure surface and the ground

profile. The shear resistance to be developed to maintain equilibrium with forces causing instability is computed and compared with the shear strength. The ratio of the available shear strength to the mobilized shear stress is called the factor of safety (Equation 2.1).

$$Factor\ of\ Safety = \frac{s}{\tau} \ldots\ldots\ldots (2.1)$$

Where, s is the available shear strength and τ is the shear stress necessary to maintain equilibrium or the mobilized shear stress. The FoS should be evaluated on all potential trial failure surfaces and the minimum out of them should be taken. The corresponding failure surface is termed the critical failure surface. Factor of safety is an indication of degree of stability of a slope. Normally a constant FoS is assumed along the entire failure surface.

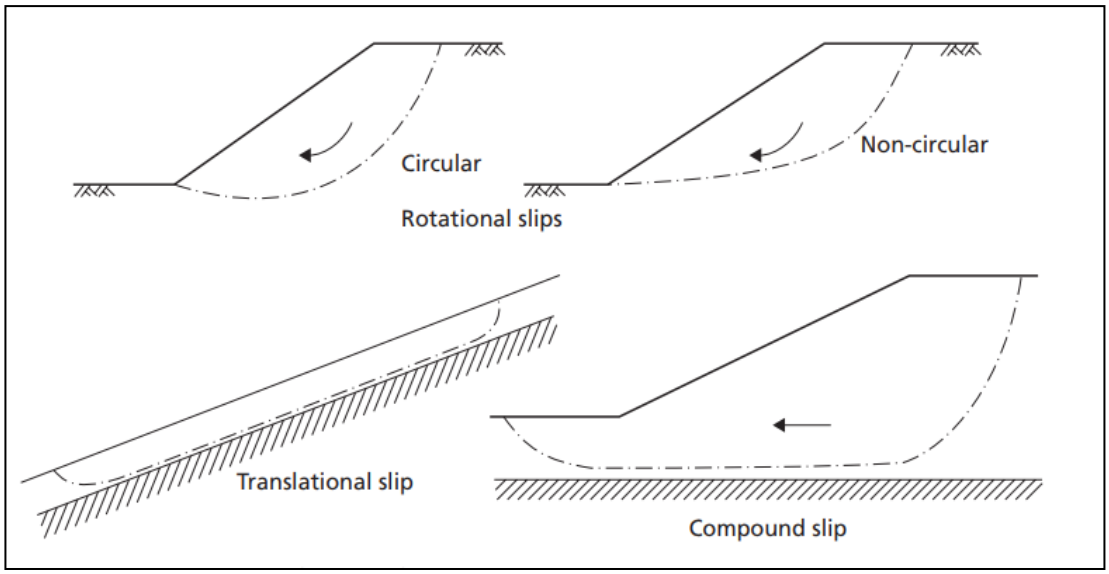

Figure 2.1: Types of slip surfaces (Knappett and Craig, 2012)

When the slope is made of the same material, the free body of the failure mass is drawn and all the forces are marked for the whole body and equilibrium equations are written for the entire mass (Figure 2.2). The problem was statically indeterminate and indeterminacy was eliminated by making assumptions on the distribution of the normal stress at the failure surface. Friction circle method is one such method applicable for solving the stability of slopes in a uniform soil masses.

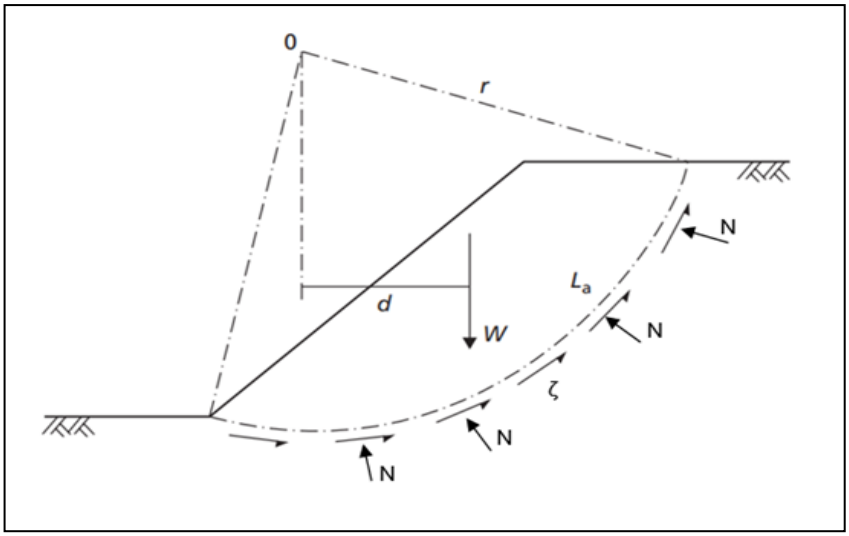

Figure 2.2 Free body diagram of the failure mass

When the slope is made of layers or zones of soils having different properties the failure mass cannot be treated as one uniform body. The shear stresses mobilized at different zone will differ and the mass has to be divided into zones. Methods of slices evolved under these conditions and the failure mass was divided into vertical slices accounting for the change of strength properties. The segment of the failure surface in one slice should be within the same zone of soil. It could change above the failure surface (Figure 2.3).

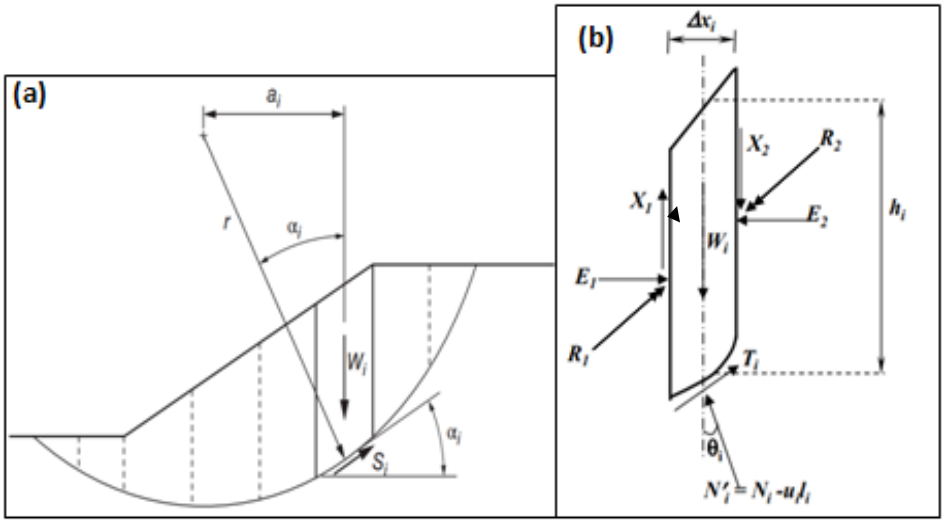

Figure 2.3: (a) Circular slip surface with overlying soil mass subdivided into slices (Duncan et al., 2012), (b) Forces acting on a slice

Number of different methods of slices were developed by researchers over the last few decades. These methods ended up with an expression for factor of Safety on the trial failure surface considered in the analysis. The problem of analysis of the stability of a soil mass divided into number of slices is statically indeterminate and it was made determinate by assumptions made on inter slice forces (Figure 2.3 (b)).

Ordinary Slices Method

The first method of slices, the Ordinary slices method or Swedish slices method (1937) was developed for circular failure surfaces and it assumes that the resultant force on the two vertical sides of the slice are parallel to the base. As such, the resultant forces in adjacent slides at a given boundary will not be in the same direction thus violating a basic requirement of force equilibrium (Newton's third law). The assumption results in a very simplified expression for factor of safety. The method yield FOS values that are smaller than those satisfying statics.

Bishop Simplified Method

This method assumes that interstice shear force is zero (forces X_1 and X_2 in Figure 2.3 (b)). This results in a nonlinear equation for FOS where an initial value has to be assumed to obtain the FOS. Iterations were done until the assumed value and computed values are sufficiently close. Usually it converges within 2 iterations. Wright et al., (1973) compared the answers obtained from Bishop's simplified method with those from further advanced methods developed subsequently and found that the answers are within 8%. This method is applicable only for circular failure surfaces.

Mogenstern and Price Method (1965), Spenser's method (1967) and Janbu's rigorous method (1967) developed subsequently consider both force and moment equilibrium and can be applied to both circular and non-circular failure surfaces. Different mathematical expressions were used for the ratio of vertical and horizontal inter slices surfaces. Iterations were done until the FOS on moment equilibrium and FOS on force equilibrium are sufficiently close. The FOS expressions for these methods are quite complex and this iterative procedures made

it necessary to use some computer program to arrive at an answer. Many commercial software currently available have incorporated these methods. The most appropriate method to be applied to a given problem should be decided exercising judgement based on the knowledge of fundamental geotechnical principles. Different limit equilibrium methods currently in use and their basic limitations/capabilities are summarized in Table 2.1.

Table 2.1 Comparison of factor of safety equations (Fredlund and Krahn 1977)

Method	Factor of safety based on	
	Moment equilibrium	Force Equilibrium
Ordinary Slice Method (1937)	Yes	No
Bishop Simplified Method (1955)	Yes	No
Janbu Simplified Method (1956)	No	Yes
Spencer's Method (1967)	Yes	Yes
Janbu Rigourous Method (1967)	No	Yes
Morgenstern and Price Method (1965)	Yes	Yes

With any of these limit equilibrium methods a large number of trial failure surfaces should be assumed and analysed to identify the most critical. There are various systematic methods such as; grid and radius method, block specified method built into commercial software in this context. In grid and radius method, which can be used for circular failure surfaces, number of grid points and set of tangential lines are defined covering the slope area (Figure 2.4). Alternate trial failure surfaces are obtained by drawing tangential circular surfaces from grid points. Once the FOS corresponding to these trail failure surfaces are computed the minimum FOS and the corresponding failure surface are identified. Block specified method uses two set of blocks defined as two grids to determine the critical slip surface (Figure 2.5).

As such failure surface would be non-circular. The location of the blocks should be carefully selected having considered the special geological features such as weak layers to capture the most critical failure surface. There was also an auto locate approach where the most critical failure surface was identified through an optimized search routine.

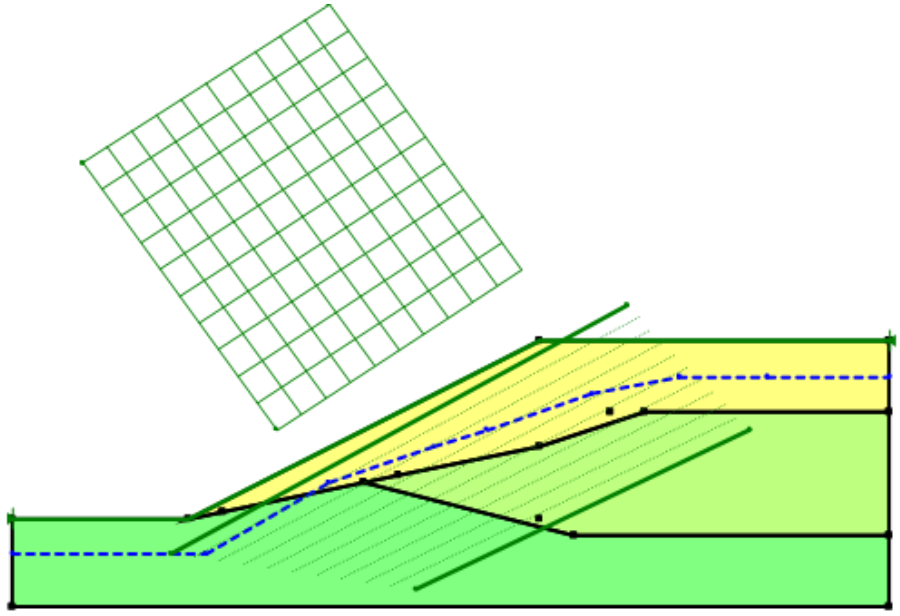

Figure 2.4 Definition of grid and radius method

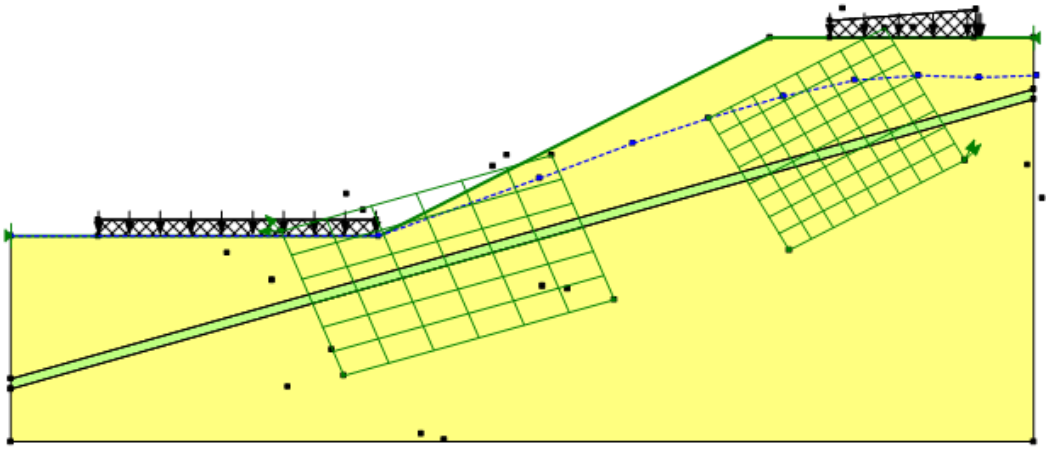

Figure 2.5 Definition of block specified method

2.3.2 Finite Element Method (FEM) to Assess the Stability of Slopes

Finite element method in geotechnical analysis gained more popularity over the limit equilibrium approaches since the development of advance computer programmes. Using finite element approach, the existing stress condition of a natural slope can be numerically simulated using the gravity turn on technique. In the FEM, slope is divided into number of elements which are connected at the nodes. Different zones of soil can be assigned appropriate characteristics. The soil is assumed to behave according to an appropriate constitutive model. The method satisfies the conditions of equilibrium, compatibility and constitutive relationship.

The method can be extended to account for; excavations in slopes, loading of slopes, construction of sloping ground in layers, seepage induced failures, brittle soil behaviours, and engineering interventions such as geo-textiles, soil nailing, drains and retaining walls (Swan et al., 1996).

In a finite element formulation; the loading of a slope or the excavation of a slope can be numerically simulated by applying the corresponding loading or unloading at the corresponding nodes. Deformations are computed at nodes and stresses are computed at Gauss points.

The response of a slope to; application of a surcharge load, excavation at the toe, can be estimated in the form of computed stresses and deformations. The infiltration of rainfall and the corresponding changes in the pore pressure regime could be estimated through a finite element formulation of seepage and incorporated into a stress analysis.

In the assessment of the stability of though the Finite Element Method there was no need to assume a trial failure surface initially. The potential failure surface is deduced through the results of the stress analysis. Displacement at critical points, displacement illustrated graphically in the form of displacement vectors, stress levels and stress level contours are different tools that can be used in this context. The Factor of Safety also emerges from the results of the stress analysis.

Factor of Safety based on stress level

Stress level or the amount of strength mobilized at a point can be defined as;

$$Stress\ level\ at\ a\ point\ = \frac{\left(\sigma_1^{/} - \sigma_3^{/}\right)}{\left(\sigma_1^{/} - \sigma_3^{/}\right)_f} \ldots\ldots\ldots\ldots\ldots\ldots \text{(2.2)}$$

The average stress level along the assume slip surface can be defined as;

$$Average\ stress\ level\ along\ the\ slip\ surface = \frac{1}{\sum \Delta l} \sum \frac{\left(\sigma_1^{/} - \sigma_3^{/}\right)}{\left(\sigma_1^{/} - \sigma_3^{/}\right)_f}\ \Delta l \ldots. \text{(2.3)}$$

This expression gives an indication about the mobilized stress level and the inverse of the same can be accepted as factor of safety.

Factor of safety based on shear stress

Factor of safety is defined as the ratio between the shear strength, τ_f, at a point, to the mobilized shear stress, τ_m, using the conventional definition.

$$Factor\ of\ safety = \frac{\tau_f}{\tau_m} = \frac{\sum (c^{/} + \sigma^{/} \tan \Phi^{/}) \Delta l}{\sum \tau_m \Delta l} \ldots\ldots\ldots\ldots \text{(2.4)}$$

Factor of safety based on nodal displacement technique

This method was first introduced by Donald (1986) and Donald and Tan (1986). In this method, separate finite element analyses are performed by incrementally modifying the modulus and shear strength parameters of the material by a factor, N. The displacements of a selected critical point is plotted against 1/N (Figure 2.6). The value of 1/N at which the displacement shows a sharp increase is considered as the factor of safety.

The nodal displacement method for factor of safety has now been embedded in the commercially available FEM software PLAXIS in the c, phi reduction approach.

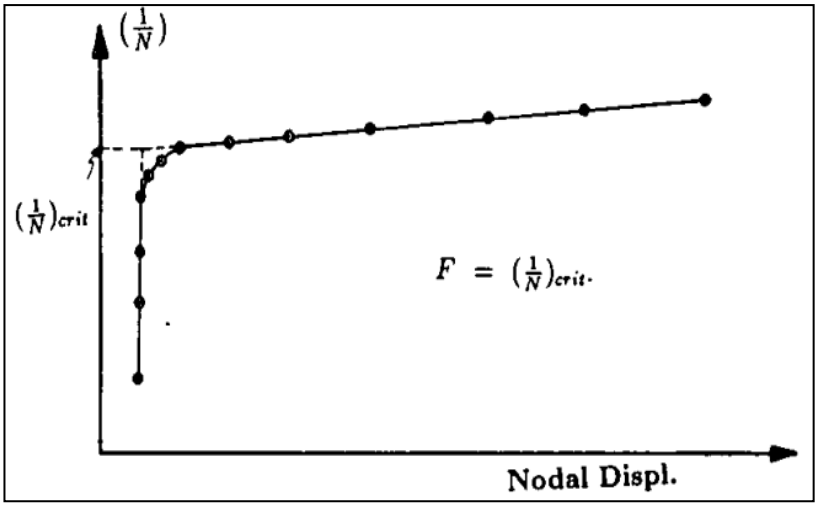

Figure 2.6: Typical nodal displacement curve (Donald and Giam 1988)

Use of displacement vectors

The displacement vector plots could be used to locate the critical slip surface. Figure 2.7 (a) shows a homogeneous slope with two soil layers. The nodal displacement plot obtained for the slope at nodes 18 and 19 shown in Figure 2.7 (b); according to which the critical factor of safety of the slope is 1.34. Figure 2.8 (a) illustrates the development of the failure surface and where displacement vectors of lager magnitude (Figure 2.8(b)) have clearly identified a failure surface at the said critical factor of safety.

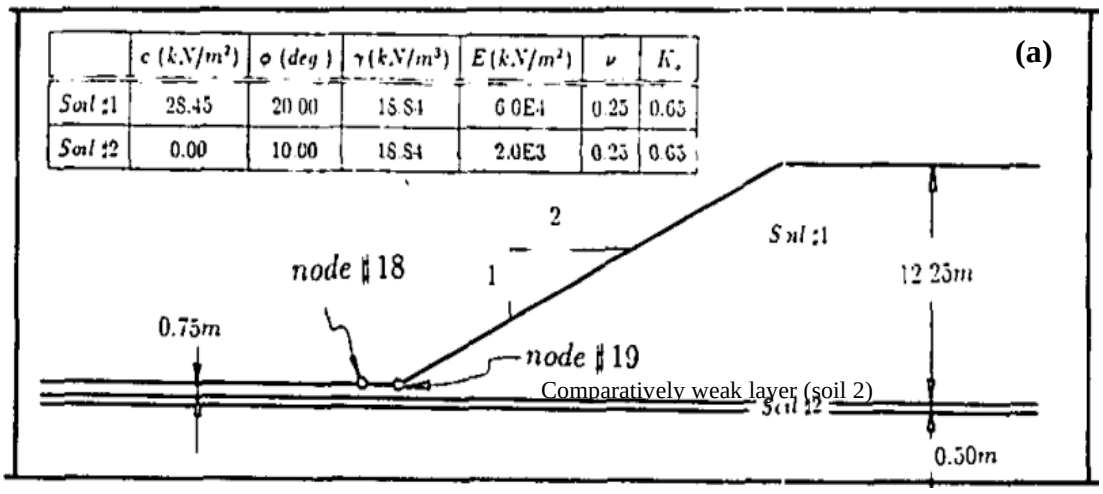

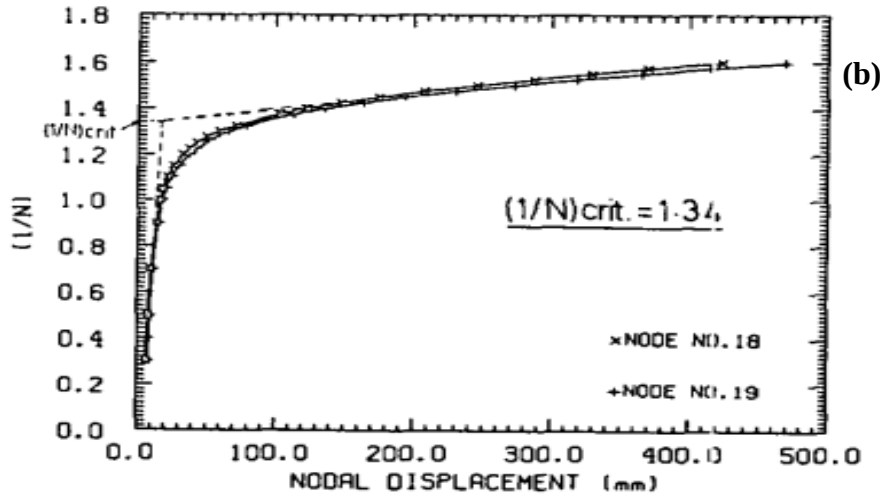

Figure 2.7 (a): A homogeneous simple slope composed of two soil layers (b): Nodal displacement curves obtained for the slope at Nodes 18 and 19 (Donald and Giam 1988)

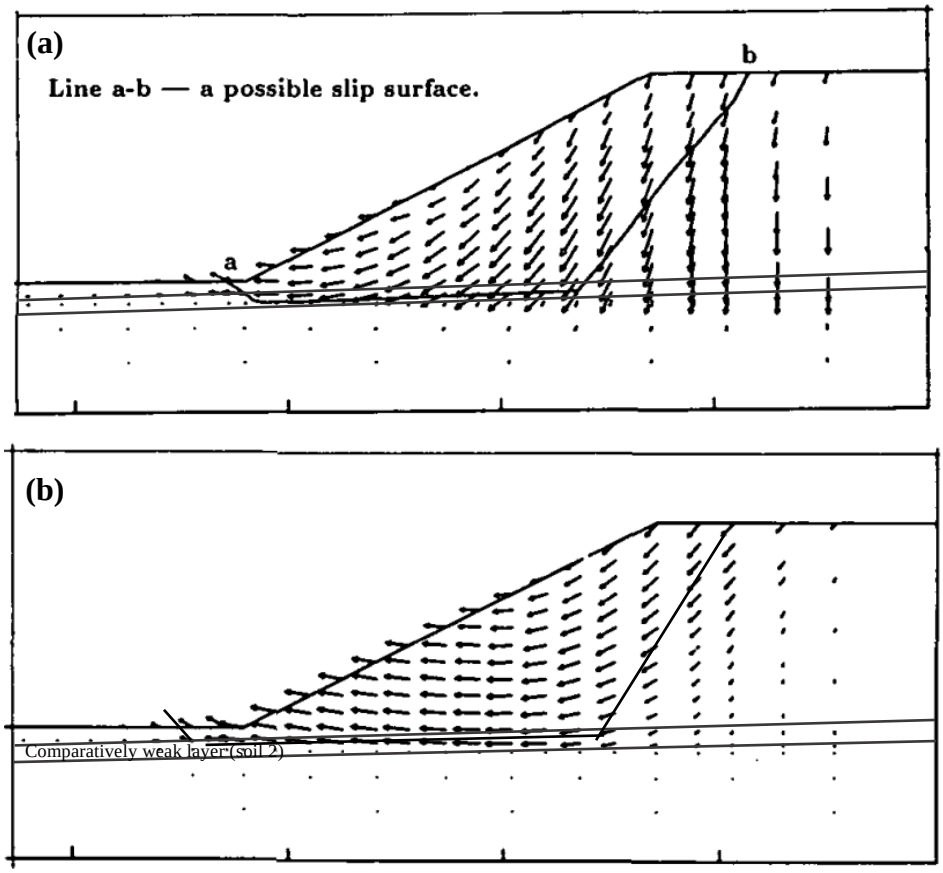

Figure 2.8: (a) Total displacement vectors (b) Incremental displacement vectors at critical nodal factor (Donald and Giam 1988)

The figure also illustrates that with the presence of a weak layer the failure is non-circular.

2.4 Slope Stabilization Techniques

When the safety margin of a slope is not adequate, appropriate methods should be applied to enhance the stability. As mentioned by Terzaghi, the methods of rectification should address the main reasons for slope instability. The various methods that can be adopted can be listed as;

- Modification of slope geometry
- Improvement of surface drainage
- Improvement of sub-surface drainage
- Provision of gravity support at toe
- Reinforcement with soil nails and anchors
- Provision of piles extending beyond the failure surface

The most appropriate technique is site specific and most often a combination of several methods will be necessary.

2.4.1 Surface Drainage Measures

Most of the Sri Lankan soil slopes are composed of residual soils, formed of in- situ weathering of parent metamorphic rock. The low phreatic surface is a characteristic feature in these slopes and the unsaturated zone above the phreatic surface is dominated by matric suction or the negative pore water pressure. This matric suction result in providing and additional shear strength to the soil mass above the water table, which indeed improve the safety margins of the slope. However, during the periods of prolong rainfall, water ingress into these slopes. Consequently, matric suction diminishes and additional shear strength due to suction will be lost. In addition, perched water table conditions are created. Loss of matric suction, increase of weight of the soil mass due to infiltration of water, formation of positive pore water pressures and thereby reduction of effective stress would cause slope instability, during the periods of prolong rainfalls. In Sri Lanka, all slope failures

are triggered by excessive rainfall. As such, minimisation of rain water infiltration into the slope, providing pathways to direct the surface water flow and providing subsurface drainage networks to intercept the rising ground water tables, are vital in maintaining slope stability.

2.4.2 Sub Surface Drainage in Slope stability

Most of the slope movements are caused by the action of increasing ground water pressures. Hence, removal of excess or additional ground water pressures from the slopes has become the most popular economic and efficient measures of slope rectification or stabilization (Cook et al. 2007). The main objective of using sub surface drains is the lowering of ground water table. Subsurface drains are also used in emergency situations occurred in highways where local instabilities are occurred due to the effect of excessive rainfalls (Conforth 2005). Design of proper sub surface drainage systems require an adequate knowledge in ground water conditions, aquifer types, geology and geomorphology, existing surface drainage network, soil parameters and potential failure type (Lau and Kenny 1984; Kleppe and Denby 1984).

Sub surface drains are drilled into the rock or soil mass with a slightly positive inclination to the horizontal plains. The drilled holes are then installed with perforated polyvinyl pipes so that water comes out under gravity (Santi et al. 2003; Cornforth 2005).

Sub surface drains should be located appropriately identifying the critical soil layers facilitating the rapid outward movement of water trapped inside. The length and the spacing should be decided on these factors.

Shallow translational slides are possible due to the water level increase and development of perched water table conditions caused by infiltration, in the upper slope. In contrast, rising of pore water pressures in the lower slope region could initiate rotational failures in the toe region of a slope. Therefore, type, length and density of the drainage network should be decided after a thorough investigation of

slope profile and other hydrological properties of soil such as conductivity and water storage capacity.

When designing the sub surface drains, main focus is to lower the water table. Use of sub surface drains to eliminate the formation of perched water table conditions in the upper regions of the slope alone, sometimes may not be effective in long term (Rahardjo 2012).

2.4.2.1 Location of Sub Surface Drains

Sub surface drains should be located after a thorough investigation on geological profile of the slope, possible failure mechanisms as well as possible failure surfaces. An idea about the variation of initial pore water pressure profile in the slope and thickness of the unsaturated soil profile are essential in designing horizontal drains. Hence, adequate number of piezometers should be installed at identified locations to obtain information pertaining to the changes of the pore water pressure regime, before the design of sub surface drains (Cornforth 2005). Meantime, continuous monitoring data obtained from piezometers after installation of sub surface drains could be used to assess the effectiveness of the system in drawing down the water table.

2.4.2.2 Zones of Penetration

Sub surface drains are functioning most effectively when they intercept the ground water table below the zone of instability. Properties of the slope material, directions of the ground water flow, critical water bearing layers of low permeability, presence of discontinuities, fissures in clayey soils and perched water table conditions should be precisely identified when designing sub surface drains (Figure 2.9), (Cook et al. 2007).

Drain 1 in Figure 2.9 crosses only three discontinuities whereas drain 2 crosses five discontinuities. Drains intersecting the maximum number of discontinuities are the most efficient when transporting water out. The method developed by Zhou and Maerz (2002), to identify the optimum drilling direction in jointed rocks is also

suitable for soils with stratigraphic layering, fissures and presence of such relatively high permeable zones (Cook et al. 2007; Pathmanathan 2009).

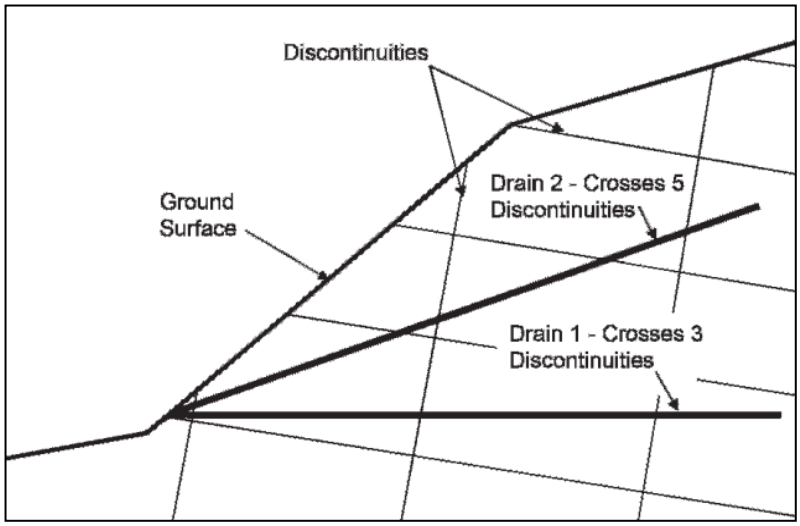

Figure 2.9 Variation of number of discontinuities crosses by the drain depending on rain inclination (Cook et al. 2007)

Anisotropic ratio of permeability is also considered important in installing sub surface drains for slope stabilization (Pathmanathan 2009). The anisotropic ratio changes the profile of the phreatic surface rapidly (Figure 2.10).

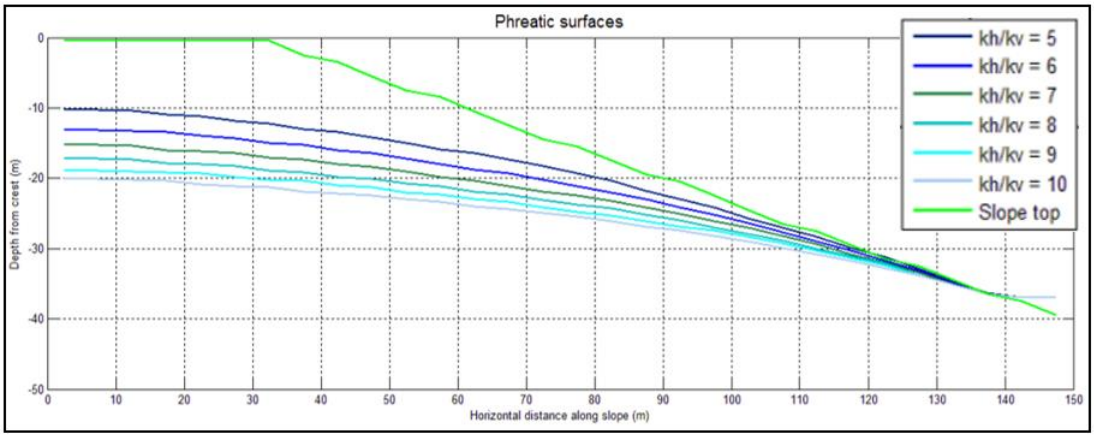

Figure 2.10 Modelled phreatic surfaces for a slope with no drains with different anisotropic ratios of permeability (Pathmanathan 2009)

The figure illustrates that slopes with higher ratios of horizontal permeability to vertical permeability stabilize quicker than those with low ratios of anisotropic permeability. Hence, the presence of layers with various permeability as well as their orientations should also be accounted in designing sub surface drains with the maximum efficiency.

2.4.2.3 Maintaining a Constant Matric Suction Profile

Rahardjo et al. (2012) have carried out comprehensive studies on the location of the sub surface drains for most efficient functioning. A parametric study has been carried out using the typical properties for Singapore soils on a slope with a typical geometry. During this study, sub surface drains have been introduced at three different locations of the slope and slope is subjected to a continuous rainfall. The analysis shows that the drains installed at the toe area of the slope are the most effective in improving the stability of the slope (Figure 2.11). The drains at upper levels have not contributed much to maintenance of stability.

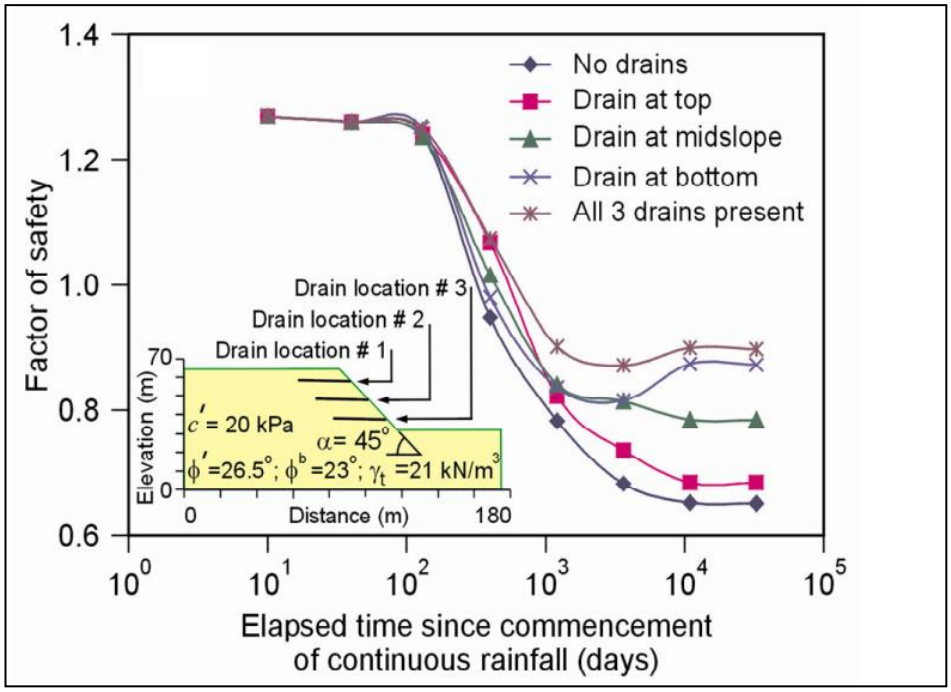

Figure 2.11 Theoretical effectiveness of horizontal drains in terms of flux with respect to drain position (Rahardjo et al. 2012)

Monitoring results obtained from different field studies have also confirmed this finding (Rahardjo et al. 2003).

The zone between the lowered water table and the influence depth of the rainfall (Figure 2.12) maintains a constant matric suction profile and thus improve the factor of safety of the slope due to the contribution of additional shear strength. When deciding the orientation or the inclination of sub surface drains, it is important to pay attention on optimizing the thickness of this unsaturated zone of the slope.

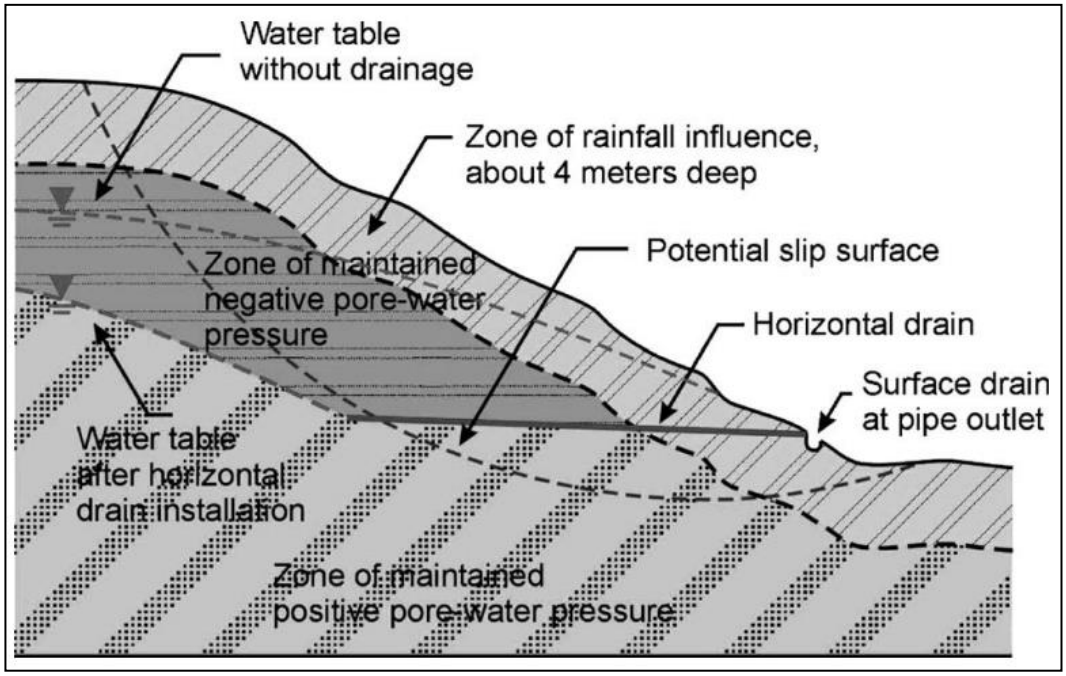

Figure 2.12 Conceptual design for subsurface drains (Rahardjo et al., 2003)

Besides, studies conducted by Rahardjo et al. (2003) have also shown that the installation of sub surface drains within the unsaturated soil zone is not that effective. Because the water will tend to move downward the slope direction creating near surface saturated conditions within the slope.

2.4.2.4 Length of Sub Surface Drains

The length of the sub surface drains has a great impact on the effectiveness of the drain system (Rahardjo 2012). Santoso et al. (2009) investigated the effect of drains

of different lengths on the stability of the slope. Two slopes (Sedimentary Juromg formation and Bukit Timah Granite) of different geological formations have been modelled, using SEEP/W finite element software, to study the impact of the length of the drain on the stability. Slopes have modelled under different circumstances as listed below.

- Without drainage measures
- Drains extended to the middle of the slope
- Drains extended to the critical slip surface
- Drains extended beyond the critical slip surface (to a distance below the crest of the slope)

During modelling, all the other factors such as slope height, slope angle and the rainfall intensity had kept constant. Location of the critical slip surface has been obtained from the analysis conducted with no drainage condition. In the initial stage of the modelling, different drain configurations have been allowed to come to an equilibrium state. During the next stage of modelling, slopes have been exposed to a rainfall intensity of 22 mm/hour, for 24 hours and then allowed to come to a state of equilibrium. Figure 2.13 shows the variation of factor of safety with the ratio of the drain length to drain spacing.

It is evident that the factor of safety tends to increase with the drain length and gradually becomes constant. The improvement of factor of safety in Sedimentary Jurong Formation with the drain at the middle of the slope is around 13%. The same for drains extended to the critical slip surface and for the drains extended a distance below the crest of the slope are around 15% and 15.4 % respectively. A similar behaviour is observed with regard to the Bukit Timah Granite slope, where, drains extended to the middle of the slope improved the factor of safety by 10.5%, drains extended to the critical surface improved FoS by 12% and the drains extended to the point below the crest of the slope improved FoS by 12.5%. This indicates the optimum length of the sub surface drain is limited by the location of the critical slip

surface (Rahardjo et al. 2012). These findings further confirm the works of previous researchers (Lau and Kenny 1984; Nakamura 1988; Cai et al. 1998) which also showed that the maximum reduction of subsurface water is limited by the drain length extended to the slip surface. In addition, drain diameter, drain inclination, drain spacing as well as the soil properties of the slope too are vital in maintaining the stability of a slope (Rahardjo et al. 2012).

Cai et al. (1998) has conducted similar studies to assess the impact of sub surface drains in slope stability. In their study, a rainfall has been simulated on a three dimensional slope and the effect on stability is evaluated using an elasto-plastic shear strength reduction finite element method. These results also have proven that the rate of increase of factor of safety reduces when the drains are extended beyond the critical slip surface. In addition, the analysis also showed that lengthening of drains is more effective than reducing the spacing between the drains and increasing the number of drains. This study also concluded that the effect of drains is mainly influenced by the ratio of rainfall intensity to saturated hydraulic conductivity.

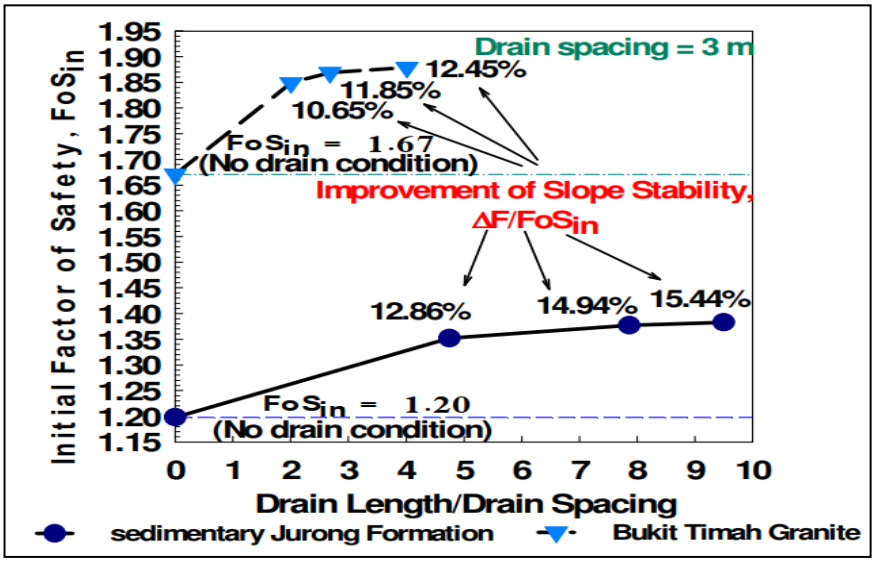

Figure 2.13 Influence of drain length on stabilizing effect of horizontal drains (Santoso et al., 2009)

2.4.2.5 Inclination of the Sub Surface Drains

Drains are inclined upwards in view of maintaining a positive hydraulic gradient throughout the drain (Cornforth 2005). The nominal inclination of horizontal drains is between $2^0 – 10^0$ from the horizontal. However, installation of drains with angles of almost 25^0 or more is possible depending on the subsurface profile (Conforth 2005). Lower angles are much preferred as they are in lower elevations at the back end of the drain and induce more drawdown in the ground water table (Santi et al. 2001). Even the drains installed horizontally would function properly as long as a positive hydraulic gradient exists within the slope (Cook et al. 2007).

2.4.2.6 Configuration of Sub Surface Drains

Conforth (2005) describes that subsurface drains can be installed either parallel to each other or in a fan shaped orientation. The parallel configuration is more common and used in road cuts, railway roads and canals. In the parallel orientation, drains are spaced normally 1.0 – 3.0 m apart.

Fan type drains are widely used in landslides. It makes easier to collect the ground water, causes minimum disturbance to the ground during installation and requires minimum movements of the drill rig. Figure 2.14 shows two arrays of fan type drainage networks used to stabilize a landslide in Oregon State in USA. The first array of the drains (indicated by A) has been installed to avoid the water feeding from the upper hillside area to landslide area. The second array of drains has been installed to intercept the ground water table before reaching the failure surface of the landslide. Along with the drainage measures, a shear key and some surface drains have also been introduced to ensure the slope stability and restrict any further movements.

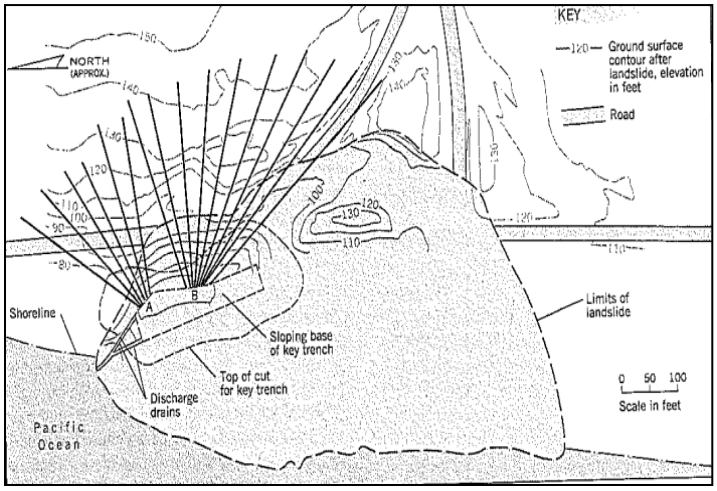

Figure 2.14 Two arrays of horizontal drains used to lower the ground water table at Sandlake roadside, Oregon (Conforth 2005)

Kleppe and Denby (1984) have also presented a similar case study on use of radial drainage network as a long term measure for stabilizing a highway embankment in Seattle. Two sets of fan shaped sub surface drainage systems have been installed at two different elevations of the slope (Figure 2.15). The construction of drainage has been done in two phases. However, it is recommended to install appropriate number of drains in the fan type configuration to ensure the total spacing covered by the drains, equal to that of the parallel drains (Cook et al. 2007).

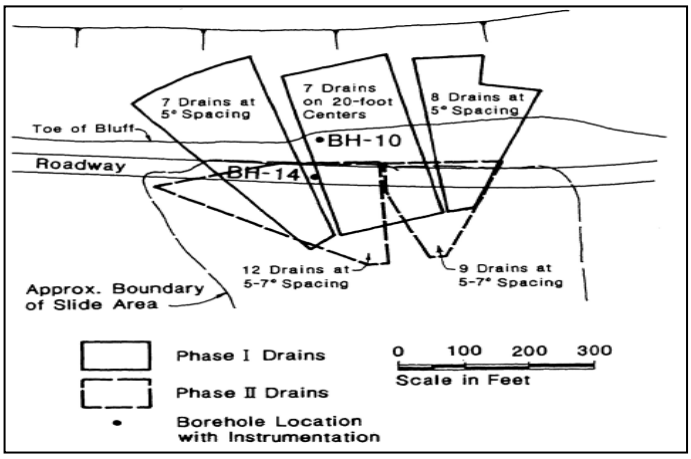

Figure 2.15 Plan view of the horizontal drains installed in the slope (Kleppe and Denby, 1984)

2.4.3 Landslide Mitigation using Sub Surface Drainage Improvements in Sri Lanka

2.4.3.1 Rectification of Watawala Landslide (Chandler and Broise, 2000)

Watawala is located about 160 km by rail from Colombo in the central highlands of Sri Lanka. The average annual rainfall of the area is about 5500 mm. The slide area is situated in an abandoned tea plantation. Considerable movements had been occurred since 1957. After a major movement occurred in 1992, Sri Lanka Railway decided to stabilise the slide. In June 1992, the track moved down with a locomotive of 97 tons, after a rainfall of 200 mm. Some further movements of 8 m has occurred in the same month. At the time the decision was taken to rectify the slide, it had extended to a length of about 500 m with a width of 60 m (Figure 2.16). The depth to the failure surface is around 30 m (Figure 2.17).

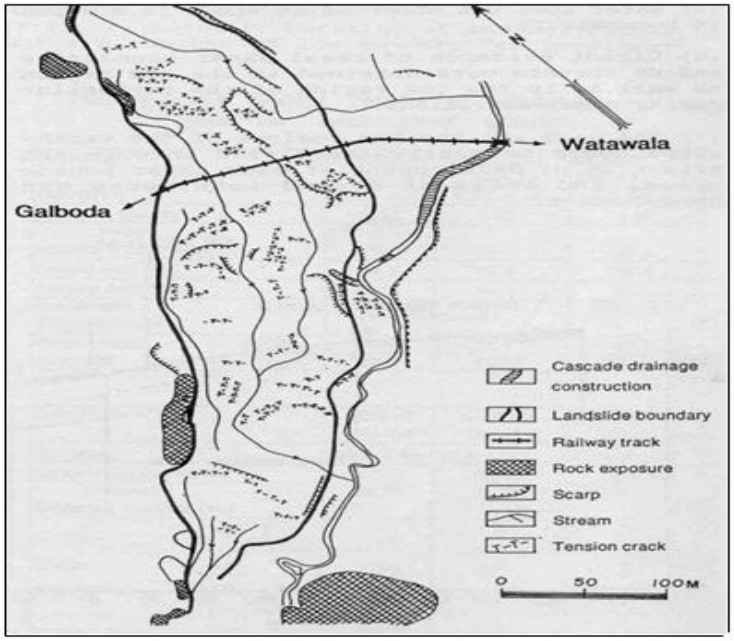

Figure 2.16: Plan view of the landslide area

The slide is situated in a “v” shaped valley area formed of high grade metamorphic rocks which are highly fractured and faulted. Right beneath the slide a highly weathered fault zone is located, which is overlaid by colluvium deposits of sandy

silts and some zones of clay. Owing to this formation, permeability of the subsurface ground was relatively high in the area.

The major issues to be addressed in rectifying the slide is the deeper slip surface and substantially larger areal extent. It was difficult to reach the deep failure surface along the full length of the slide with uni – directional drains. Therefore, it had been decided to permanently lower the water table using directional drilling technique, beneath the slide. In addition to drainage measures, deep wells and eductor system too has been installed for rapid draw down and dewatering. Also this is the first application of directional drilling technique to landslide mitigation. The system of directional drains which was just under the identified potential failure surface would be able to relieve the pore water pressure building up there quickly. With the large movements taken place along this failure surface over a long period, shear strength has reduced to residual values.

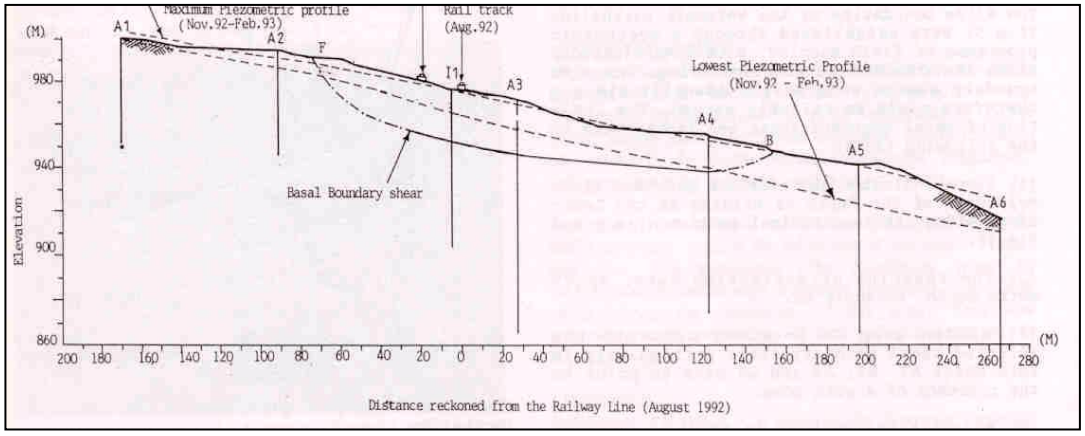

Figure 2.17: Cross section along the shear plane

Subsurface drainage network

Eleven sub surface drains have been installed in the upper weathered zone of the rock, a few meters below the base of the colluvium (Figure 2.18). The interface between the weathered rock and the colluvium deposit had been estimated by computer interpolation using borehole data. Each and every drain has been designed independently in accordance with the subsurface profile. Therefore, drains have their own unique three dimensional outfit (Figure 2.19). The drain material is high

density polythene (HDPE) pipe, which is capable of withstanding strains of 800 % before failure. It ensures the ability to withstand further moments during and after the construction phase. In addition to main eleven drains, another four short drains have been installed to drain the area just about the toe of the slide.

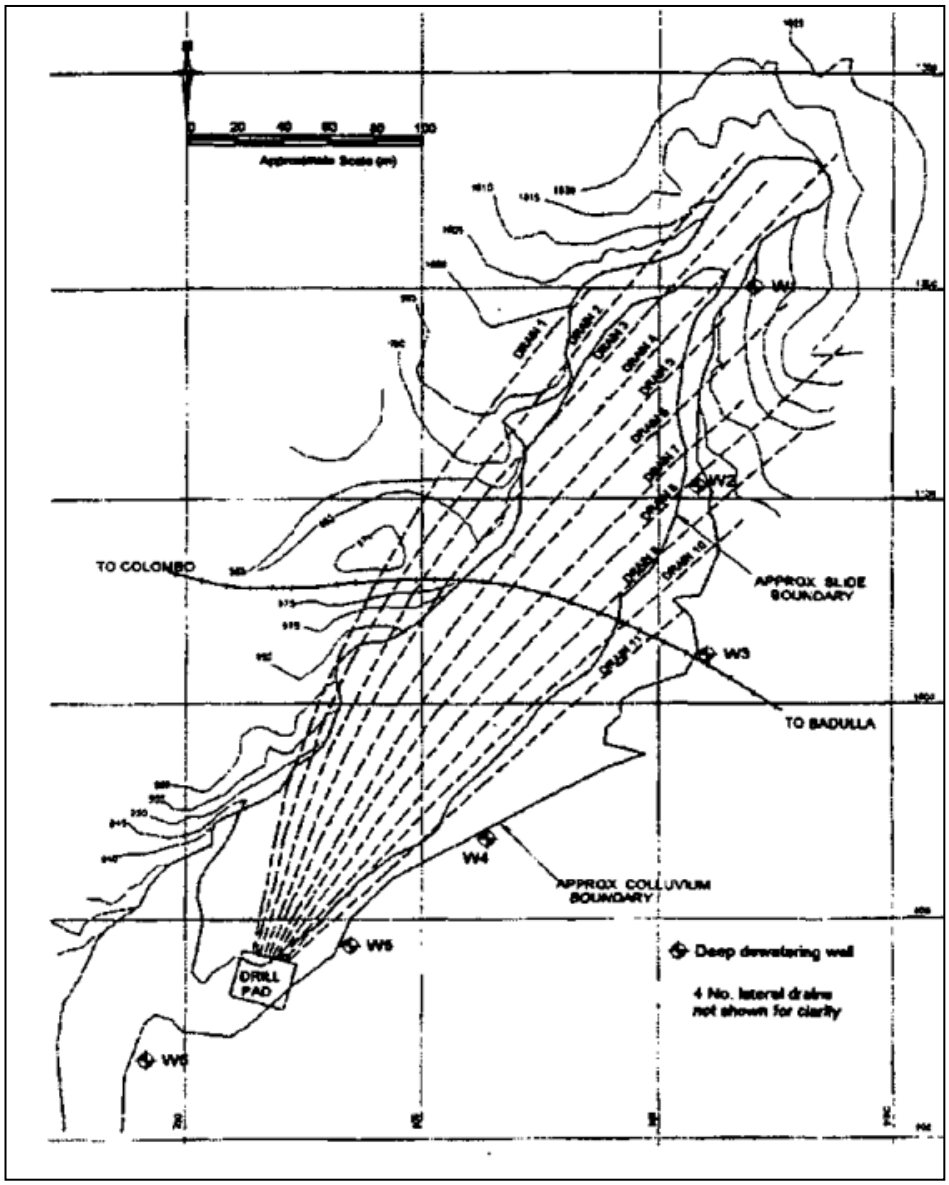

Figure 2.18 Layout of subsurface drains and deep wells at Watawala landslide (Chandler and Broise, 2000)

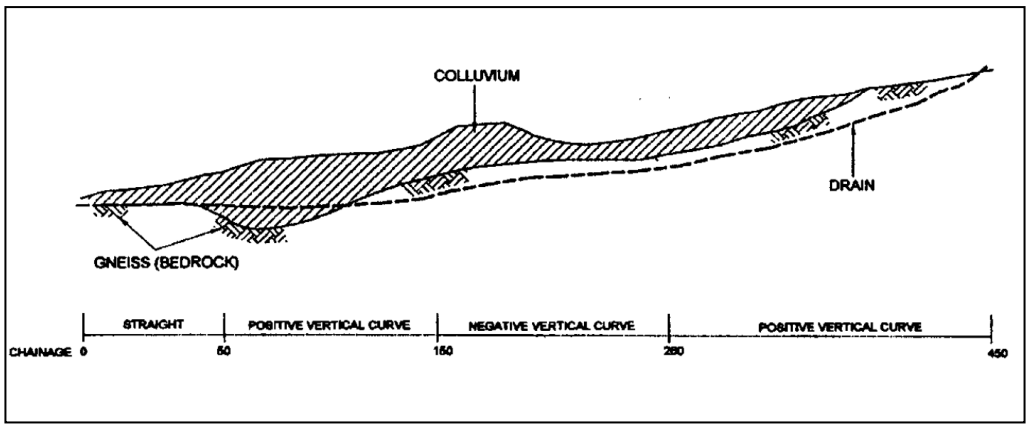

Figure 2.19 Typical sub surface drain profile (Chandler and Broise, 2000)

In order to install the drains, drill holes have been drilled from a drilling pad located near the toe of the slide (Figure 2.18). The diameter of the drill hole is 215 mm, which is drilled with a 130 mm diameter drill pipe. The holes are daylight at the upper part of the slope (Figure 2.19). The drain pipe which is of 63 mm diameter was pulled through the drilled pipe and the drilled pipe was then withdrawn over the top of the drain. The drain pipes possess filtered openings at each 1 m interval to facilitate water entry into the drain.

Post construction monitoring of the site rainfall and sub-surface drainage discharge has indicated that the peak flow rates coincide with heavy rains of several days (Figure 2.20). It further shows that the effect of isolated storms are less likely to influence overall flow rates. Also the quick response time of the subsurface drains to rainfall events indicates the relatively high permeability of the subsurface zone. Pizometric levels measured after the construction of drains indicates that the ground water table in the colluvium in the middle is maintained at a depth of 15 m or greater and the same in the toe region 3 – 5 m from the ground level, even in the presence of peak rainfall events. The readings obtained from surface movement monitoring monuments have indicated total cumulative horizontal slope movements in the range of 10- 50 mm, since the commencement of monitoring (during the first nine months of the year 1995). The vertical movements were in the range of 15 – 55 mm. This is directly related to stabilization work, resulting from consolidation settlements due to lowering of the ground water tale. In addition, stability

calculations performed using 3D CLARA programme has indicated a maximum theoretical factor of safety value of 1.8, assuming the fully efficiency of sub surface drains (Chandler and Broise, 2000).

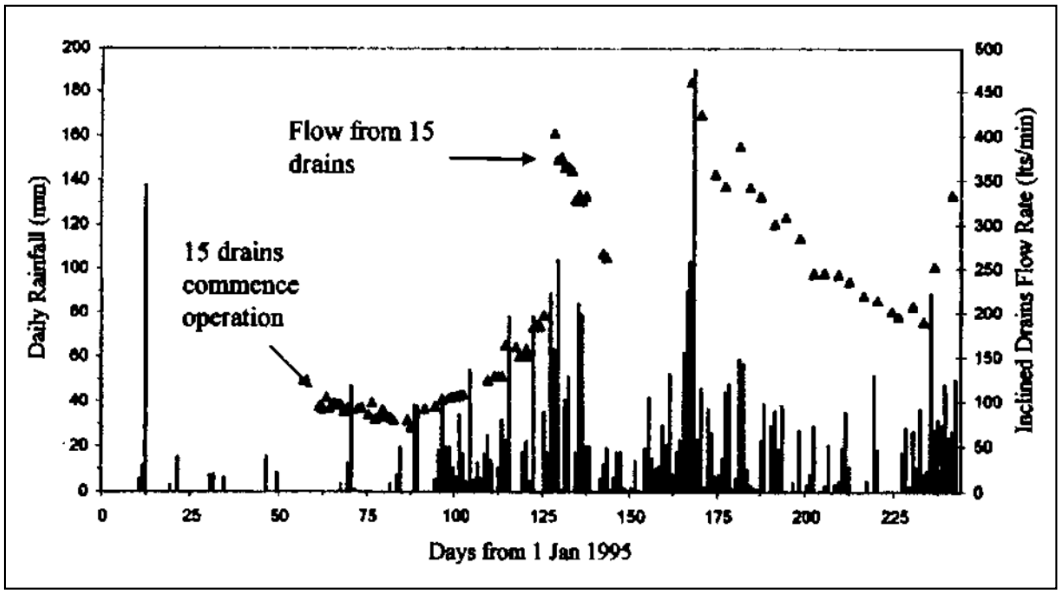

Figure 2.20 Rainfall and discharges from the sub surface drains (Chandler and Broise, 2000)

The case study has shown the effective use of long subsurface drains as a drainage blanket beneath the slide to stabilize the slide. Adoption of directional drilling technique has enabled the installation of long drains in compatible with subsurface conditions so as to attain the maximum efficiency. Apart from that, rectification of Watawala landslide is a good example which illustrates the effective use of sub surface geological, hydrological and geomorphological conditions along with the structural measures of slope stabilization. The system of drains function even today although there are some reports of blockages (Figure 2.21).

Figure 2.21: Photograph taken at Watawala in June 2018

2.4.3.2 Rectification of Ihalakotte Earth Slip (NBRO Report 30/25273)

A subsidence occurred on 17th May 2016, at 59¾ Milepost in the Main Railway Line in between Ihalakotte and Balana Railway stations. Tension cracks have appeared on the railway track as well as on the down slope. The incident happened after the area experienced heavy rains that continued for couple of days. The extent of the slide area was around 80 m to 100 m along the railway track.

Field investigation programme was conducted to detail the subsurface conditions as well as the depth of the slip surface.

Borehole investigation data revealed that the top most soil layers consists of relatively high permeable gravelly and sandy soils. This subsurface condition encourages the deeper infiltration of water during rainfall events. In addition, water seeping from highly fractured rock above the railway track also ingress into the slope area through the top soil layer, causing the ground water table to rise. As per the analysis conducted, the subsidence is due to development of a shallow slip surface resulting from build-up of positive pore water pressures.

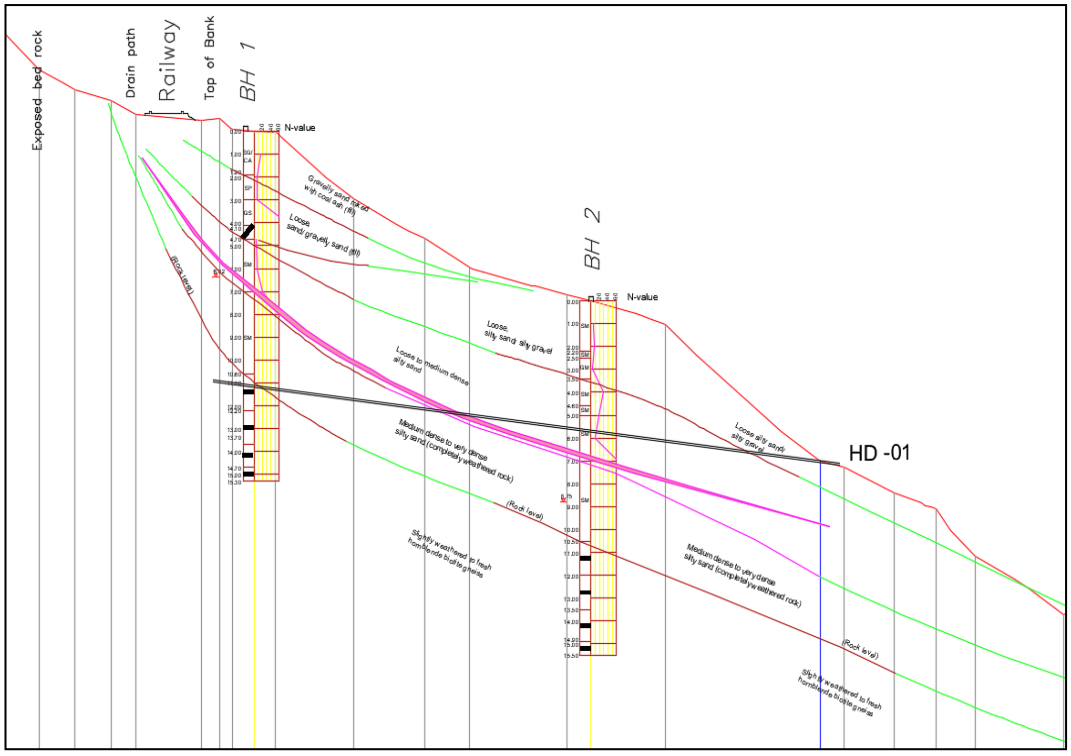

Figure 2.22: Subsurface profile and the failure surface established through BH investigation and proposed alignment of the sub surface drain

In view of mitigating the failure, improvement of surface drainage measures, sealing of cracks and subsurface drains were introduced. Surface drainage was improved by construction of cut off drains and cascade drains to prevent stagnation and improve runoff of water minimizing infiltration. Surface drainage was improved by construction of cut off drains and cascade drains to prevent stagnation and improve runoff of rainwater minimizing infiltration. Four long sub-horizontal drains were done to facilitate the rapid outward movement of water inside the slope, so that the pore water pressures developed during the rainy season will be dissipated quickly. The location, directions and the length/s of the sub horizontal drains were decided based on the results of the geotechnical investigations conducted by drilling four numbers of boreholes (Figure 2.22).

Observations from the piezometers installed in the boreholes were also considered when designing the subsurface drains. Figure 2.23 shows outlet of a subsurface drain installed at the site

Figure 2.23 Outlet of a subsurface drain installed at the site

Post construction monitoring carried out in the site indicated that no development of excessive pore water pressures encountered after installation of sub surface drains. Accordingly, the rail track was re- opened for after 14 days.

The two case studies provides a glimpse of utilization of sub surface drains in landslide rectification in the Sri Lankan context. It highlights the effective use of local terrain conditions in designing and implementing drainage measures. Further, the extent and the momentousness of the two cases described above, manifest that the sub surface drainage measures are applicable in landslide rectification even under the most critical circumstances.

2.4.4 Modelling the Effects of Sub Surface Drains in a Plain Strain Formulation

It is always important to evaluate the performance of a proposed sub surface drainage system in stabilizing a slope, before the installation in the site. There are different methods available to simulate the effect of a horizontal drain in slope stability analysis. SEEP/W by Geoslope International, a finite element software used for seepage analysis, proposes two methods to simulate the drains. First method is modelling the drain as a circular opening in the soil region. Then the perimeter of the opening is assigned with potential seepage review boundary

condition. The second method is to specify a pressure or head type boundary condition at the location of the drain. In this method, it is assumed that the drain can handle the inflow into it and no excess pore water pressures are developed. However, when modelling drains, it is vital to pay attention on adjusting the drain size of the model in accordance with the size of the domain. SEEP/W requires the Soil Water Characteristic Curve (SWCC) and the Hydraulic Conductivity Function (HFC) in modelling unsaturated flow problems.

Gjetvaj et al. (2009) has conducted a comparative study to assess the applicability of 2D models in place of 3D models to evaluate the performance of horizontal drains in improving slope stability. The results obtained by Nonveiller (1981) for 3D seepage analysis has been compared with the results obtained from the 2D seepage analysis conducted for the same slope. In the 3D analysis, drains have been installed at a spacing of *S* (Figure 2.24). In order to represent the effect of this 3D installation, Gjetvaj et al. (2009) has calculated an equivalent hydraulic conductivity, k_d, so that the distribution of heads in the 2D case is similar to the distribution of the heads in the 3D slope. This equivalent hydraulic conductivity for drain material has been obtained by comparing and adjusting the head distribution in 2D seepage analysis (Figure 2.25) with 3D hydraulic heads from Nonveiller (1981).

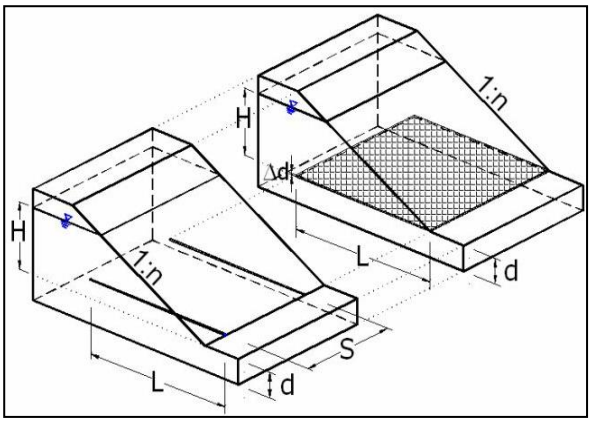

Figure 2.24 The slope models with drains installed at a spacing of S and simulated blanket drain Gjetvaj et al., (2009)

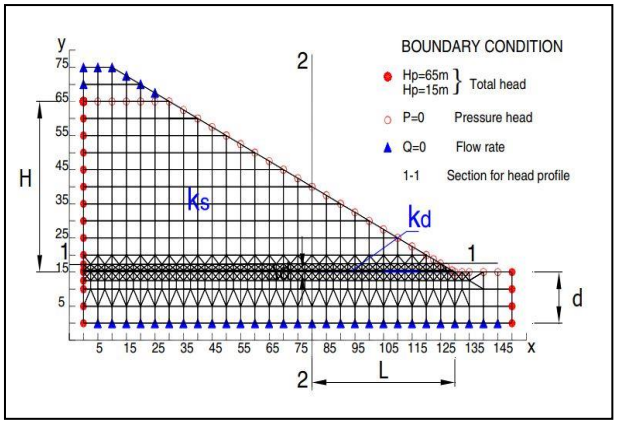

Figure 2.25 Slope model for SEEP /W analysis (Gjetvaj et al., 2009)

Based on the analysis conducted, a relationship has been established between the hydraulic conductivity of the drain material, k_d, and the hydraulic conductivity of the soil, k_t, in terms of the thickness of the drain, ΔD, total head, H, drain length, L, and the drain spacing, S.

$$\frac{k_d}{k_t}.\frac{\Delta D}{H} = 1.2\left(\frac{L}{S}\right)6.09X10^{-15} \ldots..(2.4)$$

An approximation for hydraulic conductivity of the drain material, k_d, from the Equation 2.4:

$$k_d = 1.2\,.\,kt.\frac{H}{\Delta D}.\left(\frac{L}{S}\right) \ldots\ldots\ldots..(2.5)$$

The Equation 2.5 can be used to estimate the equivalent hydraulic conductivity of the drain material to be used in the 2D seepage analysis. Using this relationship an equivalent hydraulic conductivity for drain material, for a specific drain length, spacing and soil hydraulic conductivity can be obtained. The results of the analysis conducted varying the parameters have shown that they are in a good agreement with the results obtained from the 3D analysis Nonveiller (1981) (Figure 2.26).

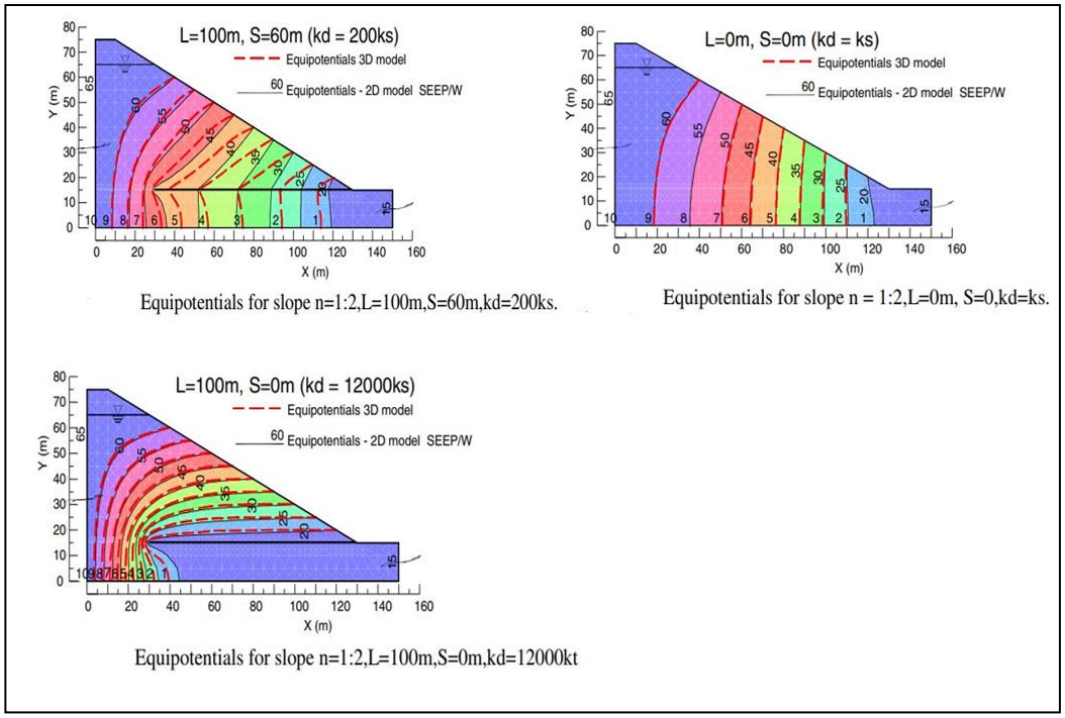

Figure 2.26 Equipotential lines obtained from 2D and 3D seepage analysis for different drain lengths and spacing (Gjetvaj et al. 2009)

The results further validate the use of 2D seepage analysis for real world scenarios, with a simple but realistic approach. Besides, this methodology is more advantageous as it required less time and input parameters compared to a 3D analysis (Gjetvaj et al. 2009).

2.5 Effect of Vegetation on Stability of Slopes

Vegetation is the natural blessing from the nature on slopes, in maintaining the stability. Trees, shrubs, grasses and such various kinds of vegetation have been contributing in stabilizing slopes for years. However, the initial attempts on accounting the effect of vegetation on stabilizing the slopes were made on 1960's (Chock 2008). Most of the initial attempts on assessing the effect of vegetation on slopes were based on field observations and qualitative approaches. Studies of Banthlahmy (1962), Bishop and Stevens (1964) and Endo and Tsuruta (1969) opened up the pathway for more quantitative approaches. Figure 2.27 illustrates the general effects of vegetation on a slope.

Vegetation is an essential part of the ecosystem, has a key role in maintaining the stability of a slope. The main functions of vegetation in reducing landslide risk of a slope can be attributed to hydrological and mechanical effects (Morgan and Rickson ,1995). Figure 2.27 summarizes the hydrological and mechanical effects of vegetation on slope stability.

Hydrological effects of vegetation are (Figure 2.27);

1. Foliage intercept rainfall, causing absorptive and evaporative losses reducing infiltration
2. Roots and stems increase the roughness of the ground and permeability increasing infiltration
3. Roots extract moisture which is lost to atmosphere by transpiration – reduce pore water pressure
4. Cracking in soil due to drying out may increase infiltration

Mechanical effects of vegetation include (Figure 2.27);

5. Roots reinforce the soil increasing shear strength
6. Tree roots may anchor into firm strata providing a buttressing or arching effect
7. Weight of tress increasing the normal and downhill forces
8. Vegetation transmitting dynamic forces
9. Roots binding soil particles reducing susceptibility to erosion

Bio engineering concepts of slope stabilization are becoming popular due to number of advantages. Roots improve slopes by both mechanically and hydrologically by means of different soil vegetation interaction process (Gray and Sotir 1995; Yildiz et al. 2018). Roots systems penetrate the potential failure surface and act as reinforcing agents as well as anchor the soil layers within the shallow depths. Although the physical interpretations of these effects are simple and straight forward, incorporating these concepts into stability analysis is still a major challenge (Yildiz et al. 2018).

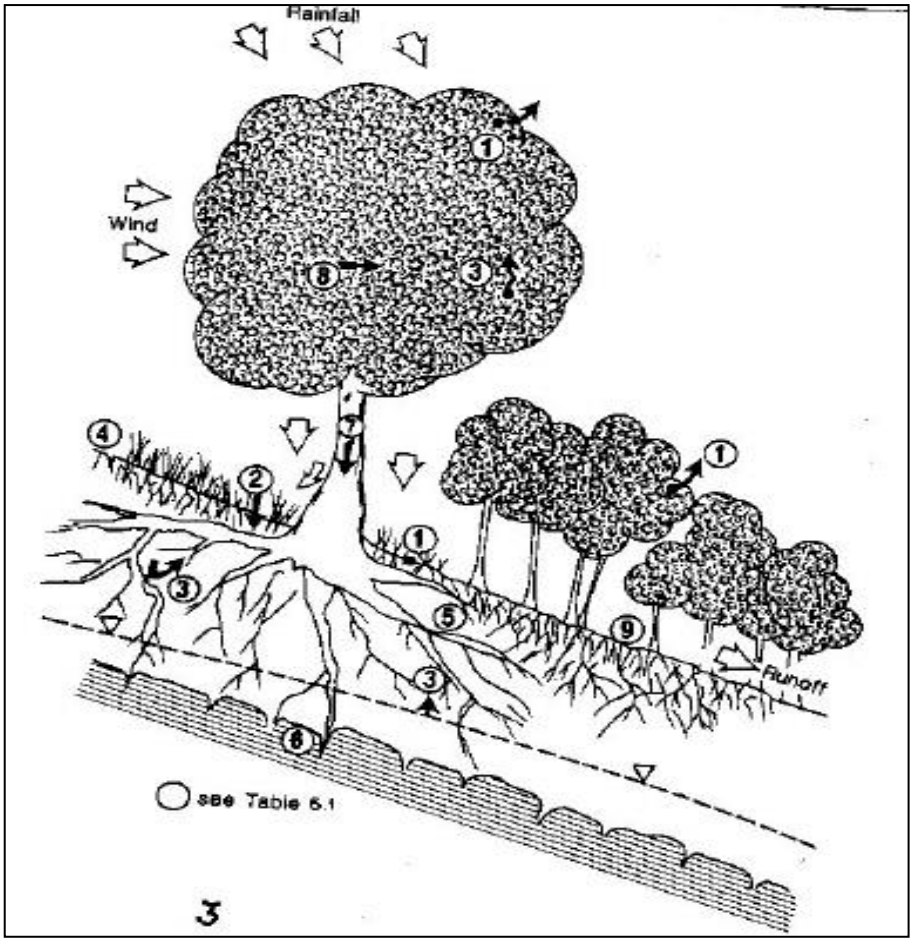

Figure 2.27 Effects of vegetation on slopes (Morgan and Rikson, 1995)

The stability of a slope is a function of hydro – thermo – mechanical process within the soil mass of the slope. In this process, vegetation together with climatic conditions (rainfall, temperature, wind speed, relative humidity) determines the top boundary condition of the slope (Figure 2.28). The amount of rainfall infiltration into the slope depends on the behaviour of the top boundary condition (Elia et al. 2017). In addition to this, the functions of vegetation include providing root cohesion, controlling surface erosion and controlling infiltration of a slope (Morgan and Rickson 1995).

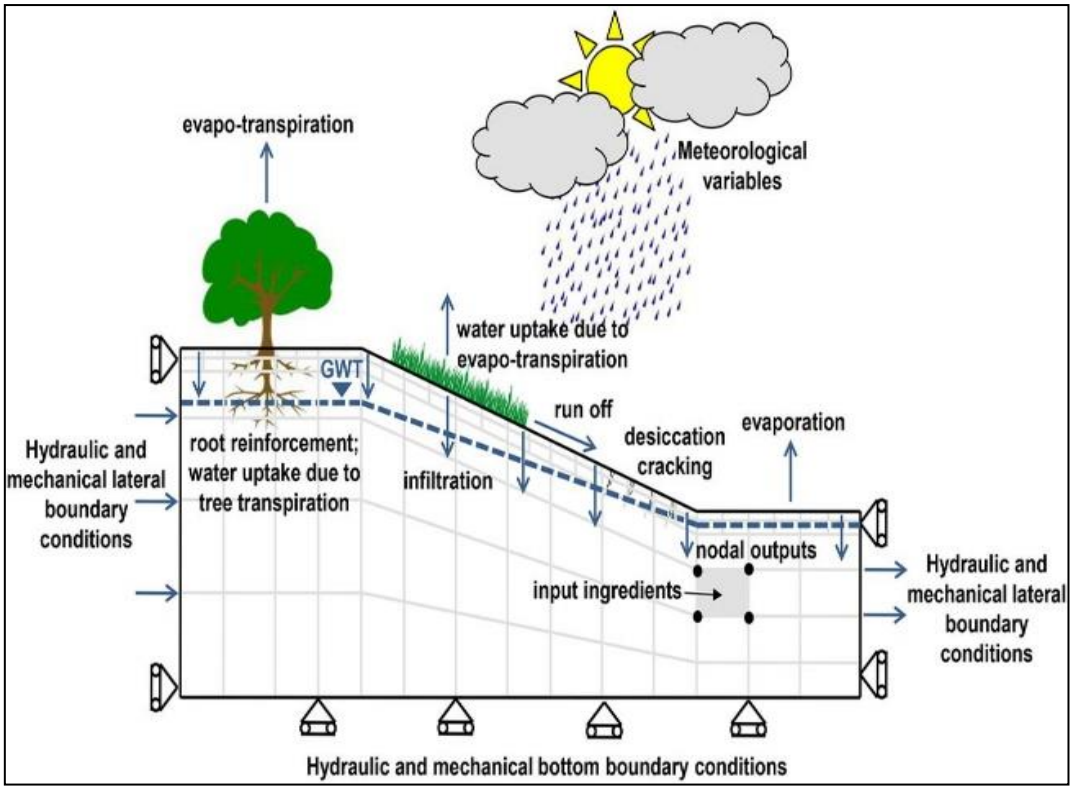

Figure 2.28 Schematic slope model showing slope – vegetation – atmosphere interacting phenomena (Elia et al. 2017)

Use of these positive aspects of vegetation in slope stabilization is no more seldom all over the world. Due to its low cost, aesthetic and environmental value and sustainability, it has gained a great attention among the researchers as well as practitioners (Gray and Sotir 1996; Rahardjo et al. 2012; Jotisankasa et al. 2014).

2.5.1 Mechanical Effects of Vegetation

Vegetation has number of mechanical effects on slopes. Plant roots reinforce the soil due to their tensile strength and adhesion properties (Chock 2008). The reinforcement effect is considered one of the most significant effects of the vegetation on the stability of slopes (Greenwood et al. 2006). Root matrix also binds the soil mass together and result in increasing confining stress within the soil – root system (Chock et al. 2008).

2.5.1.1 Effect on Shear Strength of Soil

Presence of plant roots in the soil is identical to the effect of reinforcement in a concrete element. In the same way, steel bars enhance the tensile and shear capacity of the concrete, plant roots tend to increase the shear and tensile capacity of the composite plant-soil system. This effect of root reinforcement on the soil is treated as an increment in the apparent cohesion (Chock et al. 2008; Morgan and Rickson 1995). It is generally said that the roots have no effect on the friction angle, due to their random orientation (Gray and Leiser 1982). Tenbeh (1989) found that the friction angle of sandy soils are slightly increased by plant roots, whereas no such effect on clayey soils were found. Hence, the strength contribution from the plant roots by the soil is treated as an increase in the cohesion component of the soil.

Deeper the roots penetrate in the soil, thicker the zone of enhanced cohesion (Chock et al. 2015). The depth of penetration of the root system depends on type of species, soil type and condition of the growing environment (Greenwood et al. 2006). Kozlowski (1971) reports 1 – 3 m depth of root zone, for trees and shrubs, as the most widely reported range. Root morphology and architectural traits too have a direct impact on the additional shear resistance provided to soil (Nilaweera et al. 1999; Ghestem et al. 2013). The study reveals that the number of roots presents and branching is more significant in enhancing the soil shear resistance than the effective area of the root. When different root architectures are present, their combined effect is greater than the individual effect of each architecture. However, it is strenuous to determine the individual effect of each and every root architecture. Hence, it is more reasonable to consider the global effect of the root system on the stability of a slope.

Waldron et al., (1977), Wu et al. (1979), extensively analysed the root breakage during a shear failure. The roots within the shear zone are elongated and subjected to tensile stresses (Figure 2.29). These mobilized tensile stresses in the roots act as stabilizing forces on the soil. The normal component, t_n, result in increasing the confining stress of the soil mass and thereby mobilizes the additional shear

resistance. The tangential component, t_t, directly acts against the driving shear force acting on the soil mass.

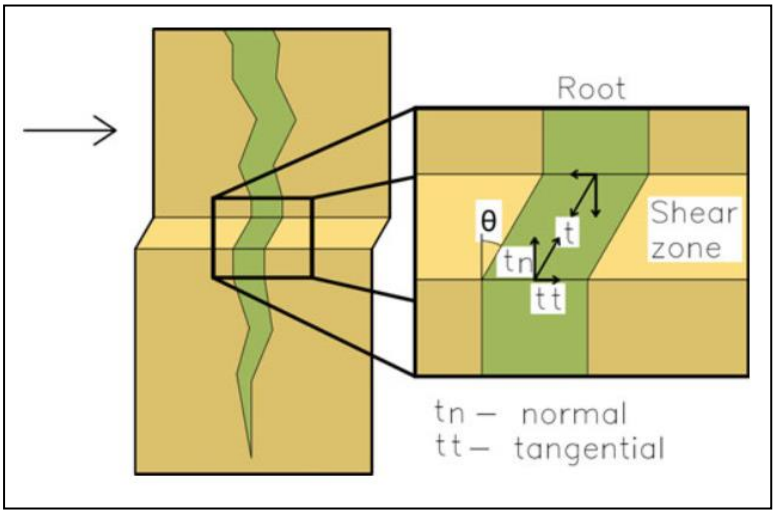

Figure 2.29 : Schematic diagram of the stresses in the root during shear (Dias et al., 2017)

Based on number of assumptions Wu et al., (1979) and Waldron (1981) proposed that the shear strength contribution from the roots can be treated as an increase in cohesion and consequently can be added to the Mohr – Coulomb equation. The following expression was developed to represent the shear strength,τ , of root-permeated soil.

$$\tau = c + \Delta S + \sigma_n \tan \Phi \ldots\ldots\ldots (2.5)$$

where, c = cohesion of the soil: Φ = friction angle of the soil and σ_n= normal stress acting on the shear plane.

Quantitative analyses on the impact of root density on shear strength were further studied by different researchers (Ziemer 1981; Coppin and Richards 1990). Coppin and Richards (1990) proposed the term Root Area Ratio to account for the root density within a considered soil mass. The root area ratio is calculated counting the number of roots within a size class in a given area of soil mass.

$$Root\ Aria\ Ratio\ (RAR) = \frac{A_r}{A} = \sum \frac{n_i a_i}{A} \ldots\ldots. (2.6)$$

where; n_i = number of roots within the size class : a_i = mean cross – sectional area of a root in size class I : A = area of the soil mass considered

Depending on these studies, the following expression has been developed to evaluate C_r, the additional cohesion provided to the soil mass by the root system due to the effect of reinforcement.

$$C_r = \sigma_t \frac{A_r}{A} (\sin\theta + \cos\theta \tan\Phi) \ldots\ldots (2.7)$$

Where; σ_t = the mobilized tensile stress of the root fiber at the failure plane: θ = the angle of the shear distortion in the shear zone.

$(\sin\theta + \cos\theta \tan\Phi)$ is relatively insensitive to the angles θ, Φ and is close to 1.2 (Wu et al. 1979; Gray and Sotir 1996). Hence, the Equation 2.7 is modified:

$$C_r = 1.2\sigma_t \frac{A_r}{A} \ldots\ldots\ldots (2.8)$$

Schwarzả et al. (2010) conducted further studies on root tensile strength. Based on their studies, it was found that the roots are progressively failed at different strains and stresses and these stresses are less than the tensile strength of the roots, T_R. The mobilized tensile strength at the time of failure is around 40% of T_R. The equation 2.8 was further modified using the average tensile strength of the root, $\bar{T}_R$.

$$C_r = 0.4\bar{T}_R \left(\frac{A_r}{A}\right) \ldots\ldots\ldots\ldots (2.9)$$

There are other models developed assuming different root orientations (Gray and Leiser 1982; Wu et al. 1988b). However, Gray and Ohashi (1983) showed that the perpendicular orientation of roots provides the comparable reinforcement to randomly oriented roots. Therefore, the perpendicular root model is still used widely due to its simplicity as well as acceptability of results.

Based on the results of these studies, Coppin and Richards (1995) modified the Mohr – Coulomb equation to account for the shear failure of vegetated soils, treating enhanced soil strength as an increased in the apparent cohesion, C_r.

$$S = C' + C_r + (\sigma_n - u)\tan\Phi' \ldots\ldots\ldots\ldots (2.10)$$

Where; S = shear strength of the soil: C' = effective cohesion of the soil: σ_n = normal stress: U = pore water pressure: Φ' = effective friction angel of the soil.

Figure 2.30 indicates the comparison of shear strength of a rooted soil and a root free soil.

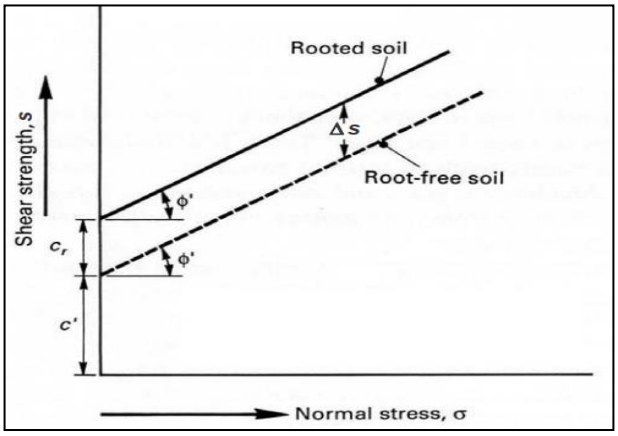

Figure 2.30: Increase of soil shear strength due to the effects of roots (Copping and Richards, 1995)

2.5.1.2 Effect of Root Suction on shear strength

The additional stability effect provided by the root reinforcement is considered as a constant apparent cohesion increase, in performing conventional slope stability analysis. However, it has been found that the fundamental mechanical properties such as root tensile strength, root pull out resistance and tensile modulus are suction dependent (Jotisankasa et al. 2018). A model has been proposed to predict the changes in root cohesion corresponding to the changes in suction. The study further reveals that the effect of suction on root tensile stress and root tensile modulus can be either positive or negative. It depends on the suction level and the plant species. Mahannopkul and Jotisankasa (2019) showed that the rate of increase of root cohesion with increasing root concentration is higher around the suction values of 10 – 30 kPa. Mahannopkul and Jotisankasa (2018) have carried out extensive

studies to investigate the effect of root and soil suction on vetiver grass. The results of the study have been used to estimate the suction effect on hypothetical root reinforced slope. Tensile strength of the roots of which had a diameter of about 0.2 mm, has been found decreasing with increasing root suction. For larger diameter roots of around 1.0 mm diameter and above, tensile strength remains unaffected by the variation of root suction. The lowest shear strength is expected when the root suction increased and the soil suction decreased. The outcome of these studies shows that the contribution of root cohesion is no more a constant parameter and subjected to change with soil moisture variation.

Pallewatta et al., (2018) proposed a mathematical model to incorporate both root reinforcement and soil suction in calculating shear strength. The experiments conducted at various suction levels including null suction, have clearly demonstrated the inter dependency between the root reinforcement and the suction surrounding the soil. Under the saturated conditions, root reinforced soils have shown a shear strength improvement of 5 -8 kPa and when tested under suction levels of 50 - 100 kPa, the shear strength improvement of the soil is around 10 – 15 kPa. Based on the results of the study, a mathematical model has been formulated incorporating root geometry, root mapping and failure pattern observed during shearing. The predictions done using the model were in good agreement with experimental results (Figure 2.31).

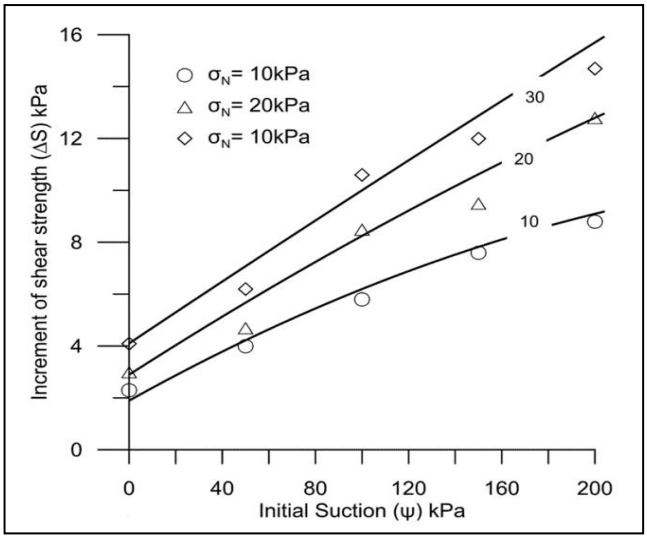

Figure 2.31 Comparison of model predicted and experimental values (experimental values are represented by open symbols and predicted values by continuous line, Pallewatta et al., 2018)

2.5.1.3 Effects of Root System on Soil Water Characteristics curve and Permeability

Jotisankasa and Sirirattanachat (2017) have conducted studies to assess the impact of grass roots on soil water retention curve (SWRC), saturated permeability, k, and permeability function of two soil types: low plasticity silt and clayey sand. The findings of the study reveal that the hydraulic behaviour of the soil has been affected by the grass root in the range of pore size greater than 1.5 mm, for suction less than 1 kPa. Within the lower range of threshold root bio mass, saturated permeability has increased and air entry value has reduced. Beyond the threshold value of the soil bio mass, saturated permeability has reduced and air entry value has slightly increased for low plasticity silt. However, no such significant variations of the hydraulic parameters have been observed in the clayey sand.

Leung and Ng (2013) and Leung et al., (2015) have done comprehensive studies to investigate the effect of plant evapotranspiration on soil suction. Leung and Ng (2013) has shown that the depth of influence of root suction during evapotranspiration process is shallower than 200 % of the root depth (i.e. for root

zone with a depth of 1.2 m the influence area is around 2.0 m). The outcome of the study further shows that the process of root water uptake is more or less governed by climatic variations than the root suction.

Ni et al., (2019) has proposed a model to account for possible influences of root growth and decaying, on hydraulic conductivity of coarse-grained soil. The model captures the variation of void ratio of the soil with respect to root growth and decaying. This relationship has been incorporated into a void ratio dependent SWRC model.

2.5.1.4 Experimental Studies on Root Reinforcement

Ali and Osman (2008) have carried out experimental studies to assess contribution of plant roots to improve the cohesion. Set of large scale direct shear tests have been carried to study the reinforcement effects of different plant species on soils. Four different type of species (*Vertiveria zizanoides, Bauhinia purpures, Leucaena leucocephala* and *Bixa orellana*) were allowed to grow for 6 to 12 months, in specially fabricated boxes, in which the soil collected from a slope area was compacted (Figure 2.32). Then the samples were tested in an especially fabricated large direct shear box (Figure 2.33) along with some control samples (samples with no vegetation). All the samples were fully saturated in a specially designed saturation box prior to conduct the direct shear tests in order to remove the effect soil suction.

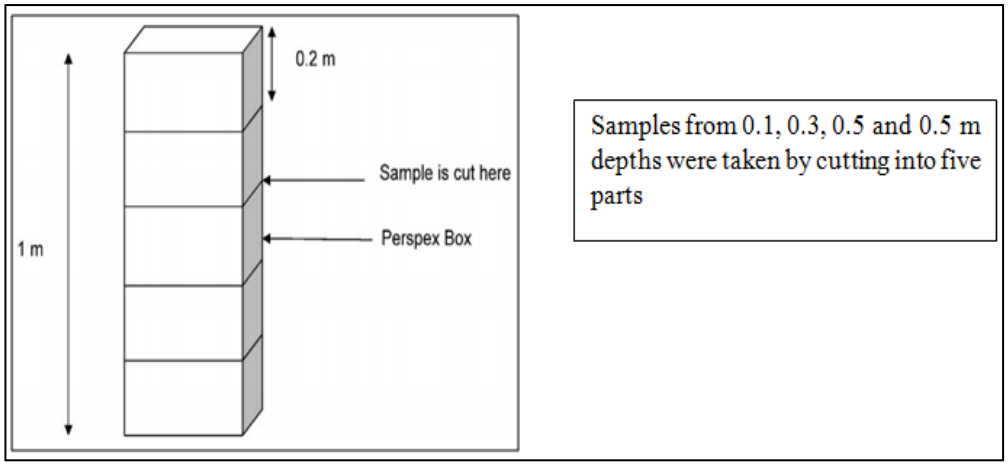

Figure 2.32 Perspex boxes for preparation of samples (Ali and Osman 2008)

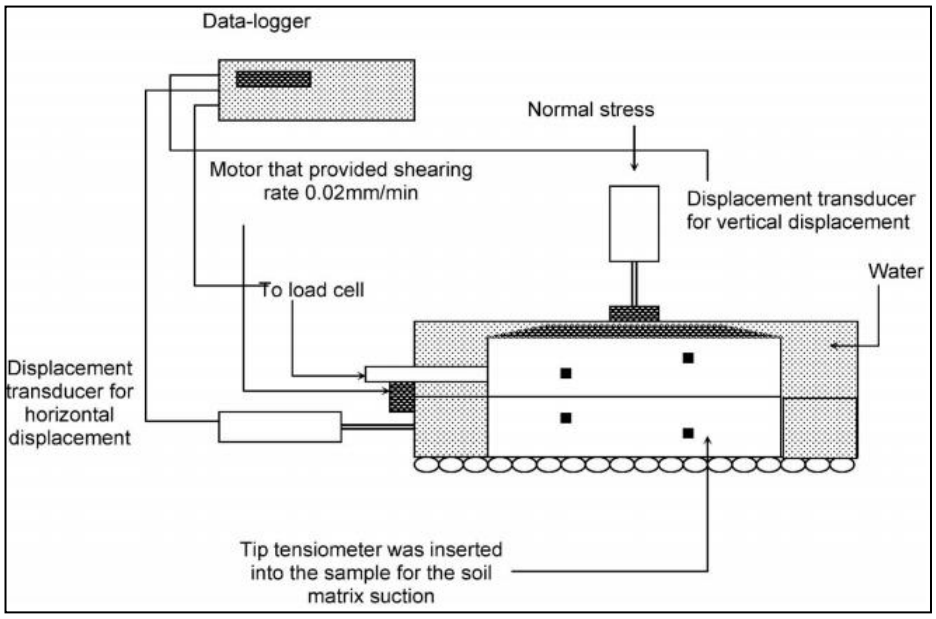

Figure 2.33 specially fabricated large shear box (Ali and Osman 2008)

The direct shear box is fixed with tip tensiometers to monitor the suction during shearing. Different normal loads (10 kPa, 20 kPa, and 30 kPa) have been applied using a hydraulic pressure system.

Results have shown that the roots of all the plants studied, have significantly contributed to improve the shear strength of the soil (Figures 2.34 and 2.35). Results also confirmed that the cohesion rapidly increases when the length of the root

system increases. This is evident by the significant improvement in the cohesion from six months to twelve months (Figure 2.34).

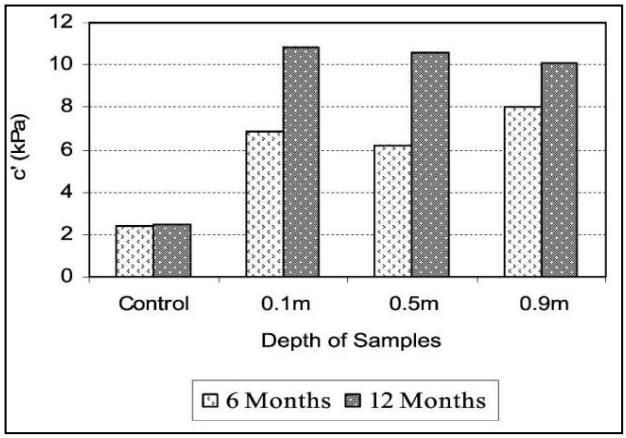

Figure 2.34 Values of cohesion for Vetiver at various sample depths (Ali and Osman 2008)

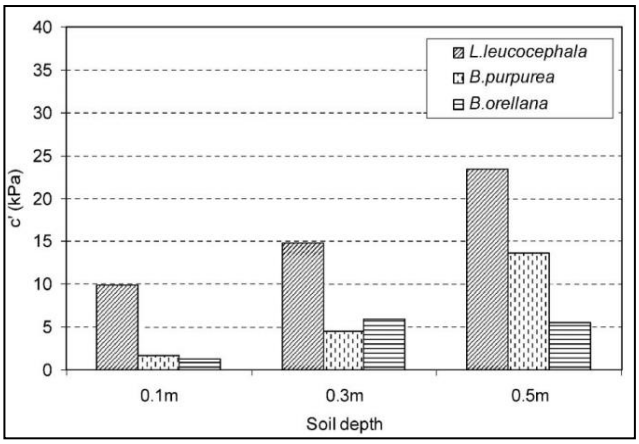

Figure 2.35 Values of cohesion at various sample depths for different plants (Ali and Osman 2008)

Yildiz et al. (2018) has conducted studies to investigate the behavior of root – permeated soils exhibiting dilative characteristics. The studies have shown that the peak shear stress of a root reinforced soil depends on the dilatancy, voids ratio, biological parameters of the roots and other soil related mechanics. However, extensive research in this area still needed to quantify the findings.

2.5.1.5 Numerical Studies on Root Reinforcement

Chok et al. (2015) has carried out extensive studies to analyze the effect of vegetation in enhancing the effective cohesion of the soil. The effect of increased apparent cohesion, due to the presence of plant roots has been assessed using *slope64*, a finite element method developed by Griffith and Lane 1999. The finite element model is based on elasto–plastic, stress–strain Mohr–Coulomb failure criteria. Factor of safety is defined as the parameter, by which the original shear strength should be divided to bring the slope to instability (Griffith and Lane 1999).

$$C_f' = \frac{C'}{FOS} \dots\dots\dots\dots (2.11)$$

$$\Phi_f' = \tan^{-1}\left(\frac{\Phi'}{FOS}\right) \dots\dots\dots\dots (2.12)$$

where; C_f'= effective cohesion at failure : C'= effective cohesion : Φ_f'= effective friction angle at failure : Φ'= effective friction angle

The effect of root reinforcement is taken into analysis using the Equation 2.13, where total cohesion, C_T, which is the summation of root cohesion, C_r, and effective soil cohesion C'.

$$C_T = C' + C_r \dots\dots\dots (2.13)$$

Two separate analyses have been performed to assess the effect of spatial variability of vegetation as well as effect of root cohesion, on the stability of a soil slope. To assess the different consequences of the spatial variability of vegetation a homogeneous slope of 2H: 1V with homogeneous conditions of γ_t = 20 kN/m^3, C'= 1 kPa and Φ'= 25^0 has been assumed (Figure 2.36). Analyses have been conducted for different cases (Figure 2.37). Root zones have been defined at different locations of the slope. Influence zone of the root cohesion, h_r, is 2 m and the root cohesion value is selected as 10 kPa. The shaded zones in Figure 2.37 (root zones) are assigned with total cohesion, C_T, and the bare slope areas are assigned with the effective cohesion C'. The only parameter that is changed during the analysis is the

location of the root zone. Results of the stability analysis performed varying the location of the root zone, are presented in Table 2.2.

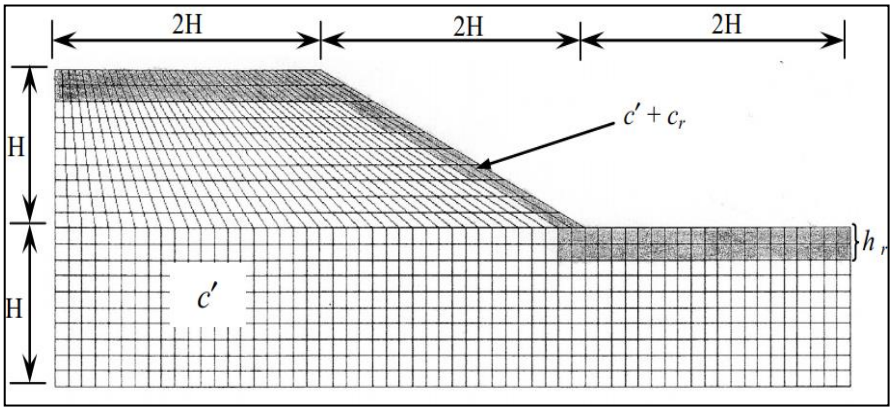

Figure 2.36 Typical finite element mesh assumed for analysis (Chok et al. 2015)

Table 2.2 FoS variation with the location of root zone (Chock et al. 2015)

Case	**Description**	**FOS**	**Increase (%)**
1	Bare slope	1.05	-
2	Vegetation grows on the slope surface	1.08	3.0
3	Vegetation grows on the slope toe	1.05	0.0
4	Vegetation grows on the slope surface and toe	1.20	15.0
5	Vegetation grows on the upper slope region	1.08	3.0
6	Vegetation grows on the lower slope	1.05	0.0
7	Vegetation grows on the upper and lower slope region	1.08	3.0
8	Vegetation grows on the entire ground surface	1.25	19.0

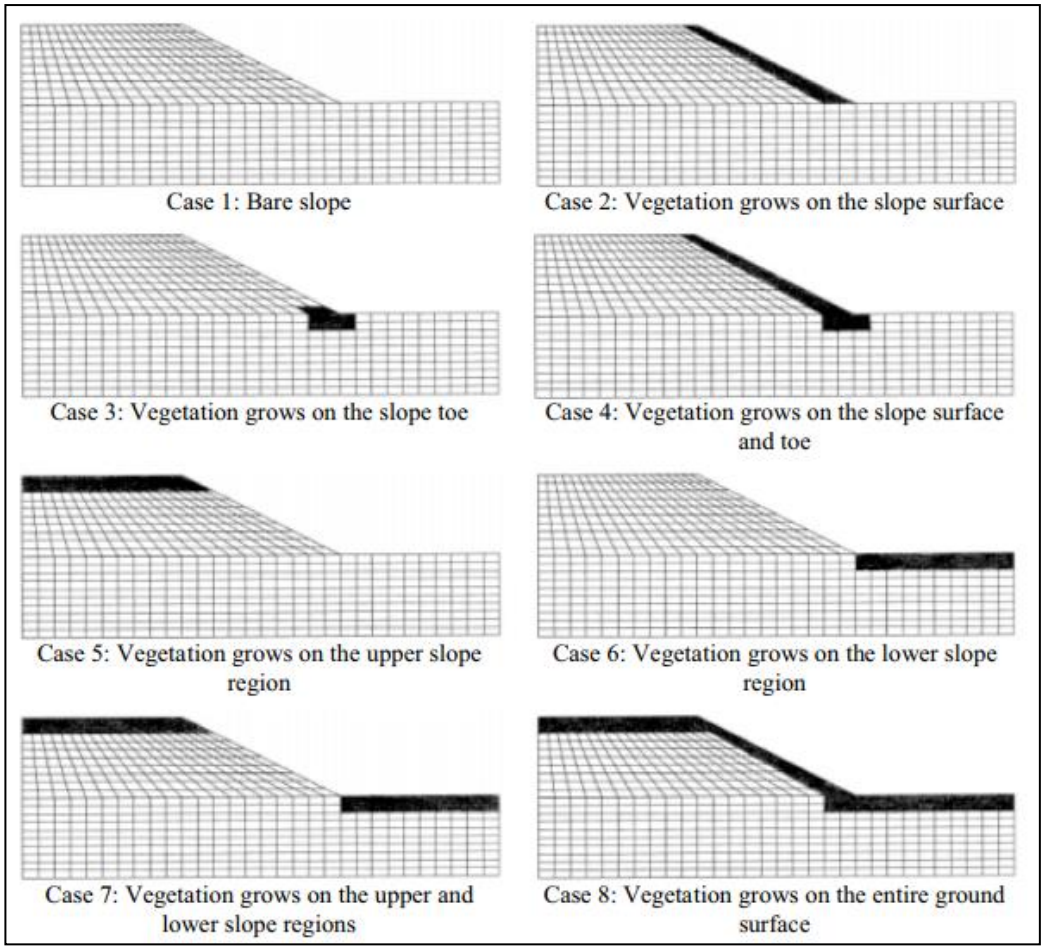

Figure 2.37: Slope with the vegetation at different locations (Chok et al. 2015)

The results suggest that the vegetation growth on the entire ground surface of the slope has the most positive impact on the stability of the slope. To get the maximum benefit of vegetation on the stability of the slope, it should be grown on the entire slope area or at least covering the slope surface and toe (Case 4 and 8, Figure 2.37).

The other analysis investigates the effect of root cohesion on slope stability. During this analysis, vegetation was assumed to grow on the entire slope surface. The same slope has been modeled with C_r between 1 kPa and 20 kPa, while varying h_r between 1 m and 2 m. All the other parameters have been kept constant. Results are shown in Figure 2.38. Figure 2.39 shows the effect of root cohesion on slope stability for slopes consists of soils with different effective cohesion, C'.

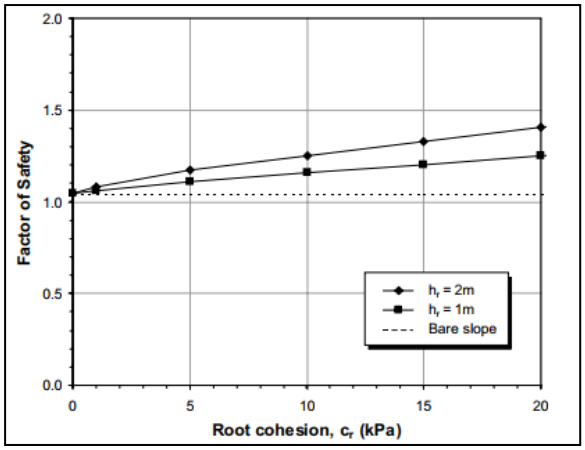

Figure 2.38: Variation of FoS with the depth of root zone (Chok et al. 2015)

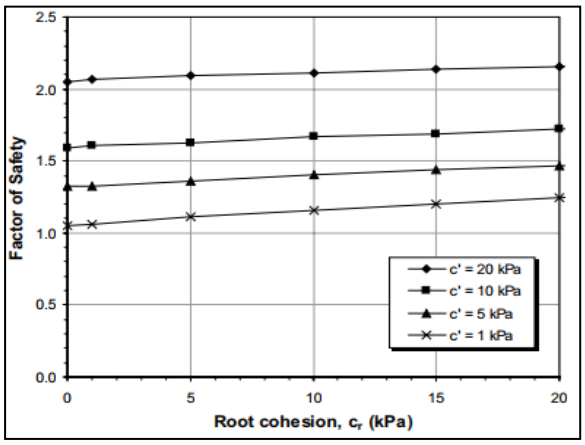

Figure 2.39: Variation of FoS with root cohesion for different effective cohesion (Chok et al. 2015)

According to the results of the analysis, it is evident that the FOS increases with the increasing depth of the root zone (Figure 2.38). Figure 2.39 shows that the slope with the least effective soil cohesion has gained the maximum improvement in the stability, after introducing vegetation. In other words, root reinforcement provides a higher improvement in the stability in a slope with lower FoS than a slope with a higher FoS. Analysis conducted varying the friction angle of the soil slope, while keeping other parameters constant (γ_t= 20 kN/m^3, C'= 1 kPa and h_r =1 m) also produces similar results to the previous analysis, confirming that the root reinforcement provides an improvement of factor of safety for all friction angles considered (Figure 2.40).

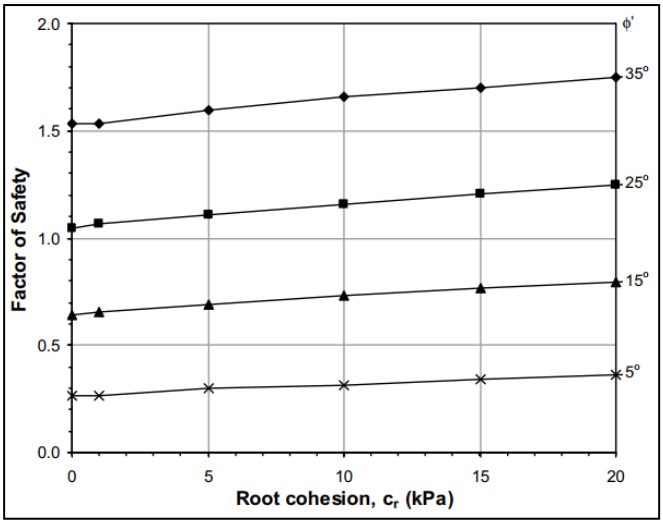

Figure 2.40 Variation of FoS of the vegetated slopes with different effective friction angle (Chok et al. 2015)

2.5.1.6 Anchoring Effect of the Roots

Soil roots aid in anchoring and reinforcing the soil structure (Tsokamoto and Kusakabe 1984). Hence unstable soil stratums are joined to competent soil layers by means of reinforcement piles (Cebada 2017). The amount of the anchoring effect provides by the roots depend on the profile of the slope and the composition of the sub soil properties. Cebada (2017) explains that the anchoring could either be between different soil layers or between the soil layers and highly weathered jointed rock stratums (Figure 2.41).

Nilaweera and Nutalaya (1994) shows the importance of determining the pull out resistance of tree roots in evaluating the effect of root anchoring on a slope. Pull out resistance of a root system is a function of root strength and root morphology and it is increased with root length distribution and depth of root penetration (Nilaweera and Nutalaya 1994). Greenwood (2006) shows that the roots with multiple number of branches have a higher pull out resistance than the roots with minimal branches. This study further suggests that root tensile strength values are reasonable indicators of pull out resistance. Therefore, in the absence of pull out resistance data, tensile strength values could be used in place of pull out resistance values, with a reasonable safety factor (Greenwood 2006).

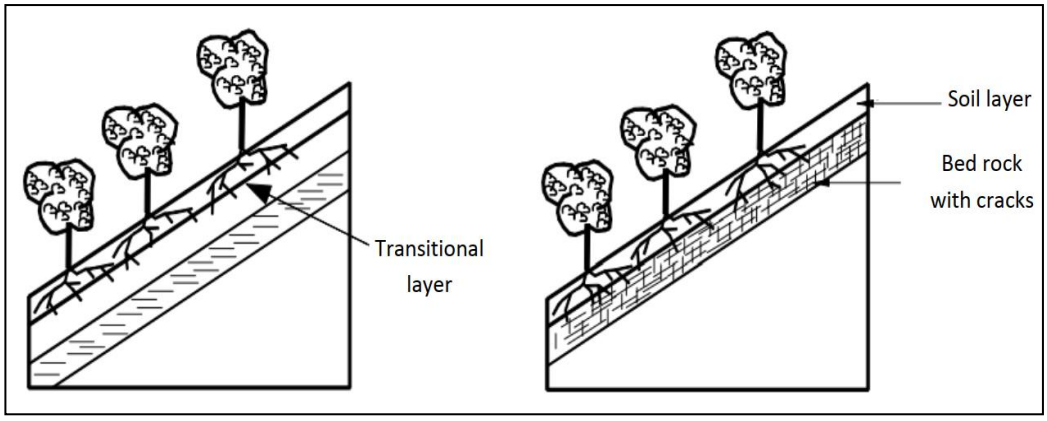

Figure 2.41 Root anchoring in two different soil profiles (Cebada 2017)

Index of Root Anchoring (IRA), provides an idea about the effect of root anchoring in terms of some quantitative forms. IRA is the ratio between square of the diameter of the vertical roots to square of the tree diameter at breast height (DBH). Studies have been conducted by Hairaih et al. (2006), to investigate impact of plant tree species in anchoring a river bank subjected to erosion. The study has shown that the unpruned coffee trees are more effective in providing a good anchoring force which is indicated by an IRA value of 7.7. Other species have indicated low IRA values denoting low efforts of soil anchoring. The results of the study also reveals that frequent pruning of the above ground regimes stimulate the growth of near surface roots, which are more effective in controlling the surface erosion. The study further concludes that planting a mix of species of trees is an ideal option to protect both the surface erosion and provide anchoring effects. Another study conducted by Rienternberg (1994) shows that the presence of tap roots which are able to penetrate greater depths are effective in anchoring the shear zones.

2.5.1.7 Wind Load

Effect of wind depends on the type of vegetation covering the slope (Coppin and Richards 1995). Wind throw forces are less significant in slope stability as it represents a smaller proportion of the potential disturbing force (Greenwood et al. 2004). When cluster of tress are present at a slope, trees in the middle are sheltered by the tress at the edges, hence less exposed to wind throw forces.

Impacts of wind throw forces are significant to some extent when the wind velocity exceeds 11 m/s. The resulting forces on the trees in a slope, could cause topple over of trees especially when they have shallow root systems. Consequently, shallow soil mass is disturbed and creates water ingress paths towards the slope. This can have a negative impact on the stability of the slope (Morgan and Rickson 1995).

2.5.1.8 Surcharge

Surcharging of the slope by the weight exerts by the vegetation has both positive and negative effects on the stability of the slope. The component of the weight parallel to the slope direction could have a negative effect on the slope stability while the perpendicular component could have a positive impact on the frictional resistance of soil (Morgan and Rikson 1995). The surcharging effect is significant only from larger trees whereas grass and shrubs do not provide such additional weights on the slope (Morgan and Rikson 1995).

Diameter at the breast height (DBH) provides an indication of amount of surcharge on the slope by a tree. Greenwood et al. (2004) suggests that the surcharging from trees becomes critical only when DBH is greater than 0.3 m. For an example, a 30 m tree having a DBH of 0.8 m is likely to induce a weight of around 100 – 120 kN. If such tree is located near the toe of a potential slip, factor of safety could be increased by around 10%. Meantime, if the same tree was located at the top of the potential slip plane, then the factor of safety could be reduced by around 10% (Coppin and Richards 1990; Greenwood et al. 2004). Stokes et al. (2008) showed that the increment of surcharge due to vegetation is negligible when compared with soil mass and it has very little or no effect on the stability of the slope.

2.5.2 Hydrological Effects of Vegetation

Hydrological effects of vegetation are important in modifying the ground water table condition of the slope. Evaporation and evapotranspiration might bring the changes in the pore water pressure regime of a slope and hence the stress – strain condition is subjected to vary. When the stability condition of the slope is marginal,

these minor changes (i.e. reduction in pore water pressures due to the effect of evaporation and evapotranspiration) in the pore water pressure regime would result in maintaining the stability of the slope (Elia et al. 2017). Vegetation in the sense act as a media, facilitating slope atmosphere interactions. Nature of the vegetation by which the slope is covered, has a direct influence on these processes.

2.5.2.1 Evapotranspiration

The combined process of removing water from earth's surface is termed as evapotranspiration (Morgan and Rickson. 1995). Plant roots carry the soil moisture from the soil to the pores underneath the leaves of the plant which is known as transpiration. Evaporation is the direct vaporization of the water into the atmosphere. This results in reducing the pore water pressure conditions in saturated slopes as well as increasing the soil suction in unsaturated soil slopes. Both the phenomenon has positive impact on enhancing the stability of a slope. However, the quantitative effect of evapotranspiration is difficult to separate. Fatahi et al. (2004) has developed a model to account for the rate of root water uptake. Three independent features are considered in this model, namely, soil suction, root distribution and potential transpiration. The model has been validated by conducting set of field measurements. Predicted data using the model is in good agreement with the observed field data.

2.5.2.2 Infiltration

Reduction of the effective stress arising from increase of pore water pressures due to infiltration is the main driving force behind most of the slope failures in tropical regions (Hidalgo et al. 2017). Vegetation plays a key role in controlling the infiltration into soil slopes. Presence of soil roots, organic matter within the shallow depths of the slope help to maintain a continuous pore system (Cepeda 2017). Plant roots penetrating into the shallow soils create flow paths and increase the permeability of the soil. Consequently runoff is reduced and rate of infiltration is increased (Zhan et al. 2007). They have further compared the rate of infiltration into a bare slope and a vegetated slope. Figure 2.42 indicates that the more

infiltration is allowed when vegetation is present in the slope. Also when a rainfall event occurs in a bare area of the slope, soil particles are easily detached and prone to wash off causing surface erosion.

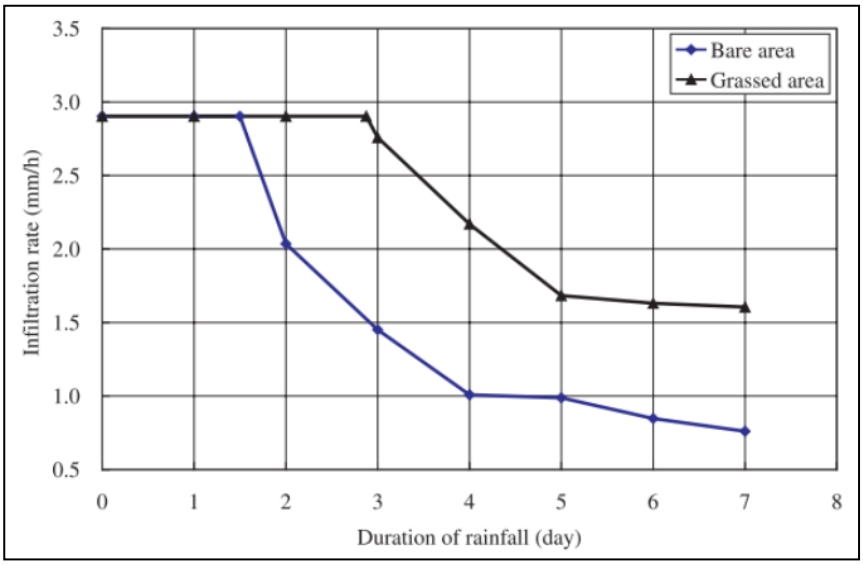

Figure 2.42 Rate of infiltration into a bare area and a vegetated area of slope (Zhan et al. 2007)

This increase of infiltration due to the presence of vegetation has its adverse too, on the stability of the slope. Jotisankasa et al. (2014) showed that the factor of safety of a slope could be decreased due to increase infiltration resulting from vegetation. The study further reveals that the variation of factor of safety also depends on the depth of root penetration as well as angle of the slope.

Rahardjo et al., 2014 has done extensive studies to find out the effect of shrubs and deep rooted grass on the soil. The study has proven the contribution of different selected vegetation, reducing the rainwater infiltration into the slope and thereby maintaining the negative pore water pressures within the slope, during rainfall conditions. Figure 2.43 illustrates the response of the pore water pressure regime and FoS variation of the bare slope and vegetated slopes, with different rainfall intensities. It is evident from the results that the formation positive pore water pressures, even under very high rainfall intensities, is minimal in vegetated slopes. Consequently, a higher factor of safety is maintained in the slope. The effect is more

prominent at the presence of Vetiver grass. Figure 2.44 shows the variation of factor of safety of the slope under different vegetation conditions studied, for a one day rainfall intensity of 22 mm/ hour. The results also demonstrate the applicability of vegetation as a surface cover on the slope.

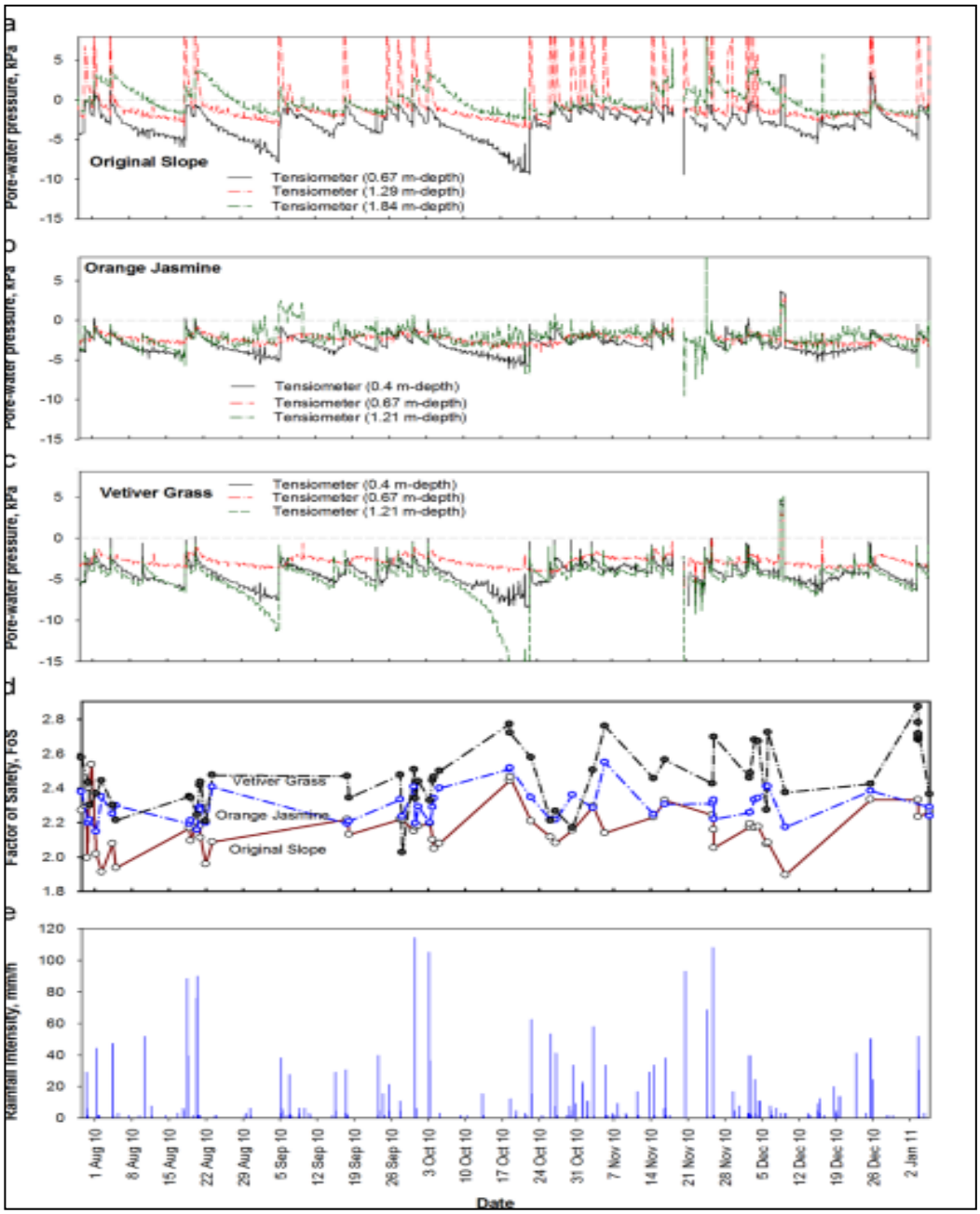

Figure 2.43 Pore water pressure variations with rainfall at different depths for (a) bare slope, (b) Slope with Orange and Jasmine, (c) Slope with Vetiver grass, (d) FoS variation and (e) Rainfall intensity (Rahardjo et al., 2014)

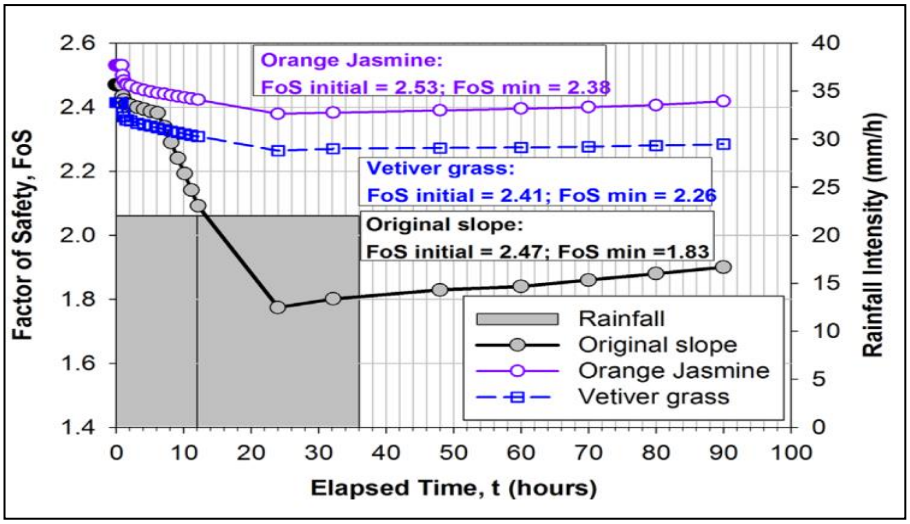

Figure 2.44 Variation of factor of safety variation for different slope for one day rainfall intensity of 22 mm/hour (Rahardjo et al., 2014)

2.5.2.3 Canopy Interception

Rainfall which is in contact with the vegetation cover has two components; 1) through fall, which reaches the ground after passing the gaps in the canopy and 2) interception, which strikes the vegetation cover and subsequently result in stem flow, interception storage or leaf drainage (Morgan and Rickson. 1995). The hydrological effect of the canopy interception on a slope is attributed to the nature of the vegetation covering the slope as well as the intensity of the rainfall. This is because, the canopy rainfall storage capacity can directly influence the amount of water retained by the canopy and the balance is discharged to the ground surface, which ultimately affect in modifying ground water conditions (Yu et al. 2011).

2.5.3 Modelling the Effects of Vegetation on Slope Stability

After quantifying the contribution of vegetation to stabilise the slopes, the next challenge is to incorporate this contribution into conventional slope stability analysis methods. Mainly two different types of slope failures are widely considered in the literature; shallow translational failures and deep–seated rotational failures (Chok 2008).

When the length of the moving mass is very high compared to its depth, the failure mechanism is shallow translational. These slopes are analysed using the infinite slope models. Wu et al. (1979) modified the traditional factor of safety expression for infinite slope model, to account for the contribution from vegetation.

$$FOS = \frac{(C' + C_r)l + [(W + S_w)\cos\beta - ul\ ]\tan\Phi'}{(W + S_w)\sin\beta + D} \quad \ldots\ldots\ldots\ldots (2.14)$$

where: C'= effective cohesion; C_r= root cohesion; l= length of the slice; W= total weight of the slice; S_w = surcharge due to vegetation; β = slope angle; u = pore water pressure; Φ'= effective friction angle of soil; D= wind loading.

Wu et al. (1979) has conducted a comprehensive case study to assess the effect of vegetation on slope stability, using the proposed Equation 2.14. A failed slope in Alaska region in USA, has been investigated, before and after removal of vegetation. The assumed average root cohesion to represent the effect of vegetation was 5.9 kPa and the surcharge from the trees was 3.8 kPa. The results of the study indicated that the initially unstable slopes have become stable after introducing the effect of root cohesion. Consequently, removal of forest in the slope region had led to slope instability. The results predicted based on the proposed model were in good agreement with the observed behaviour of the slope.

The initial concepts proposed by Wu et al. (1979), Waldron (1981), have been further developed by succeeding researchers considering various other factors (Sidle 1992; Wu and Sidle 1995). Wu and Sidle (1995) shows that the accuracy of the results obtained from the proposed models are highly dependent on the spatial variability of some parameters (e.g. cohesion, friction angle, saturated hydraulic conductivity, soil depth).

However, use of conventional limit equilibrium models to analyse the effect of root cohesion on slopes may not always produce agreeable results. Predefinition of the critical slip surface would not be valid due to the complex behaviour of the root zone. Chock et al., (2004), Chock et al., (2015), have develop finite element approach to model the effect of root reinforcement on slopes. Root cohesion is

integrated into the analysis and the FoS is determined based on the concept explained in Griffith and Lane (1999).

Dharmasena and Kulathilaka (2015) have modelled the root system using reinforcing elements of appropriate length and direction in the form of soil nails. In the plane strain analysis this root system was assumed to exist at 3m intervals. The roots were modelled as nails of drill hole diameter 50 mm and tensile strength of 200 kN (Figure2.45).

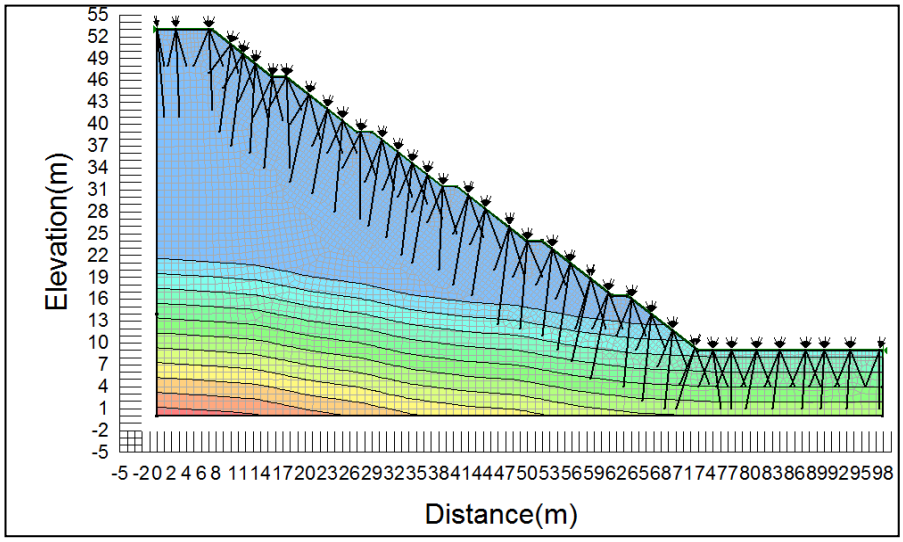

Figure 2.45 Root configuration used in the analysis (Dharmasena and Kuathilaka , 2015)

The results of the analysis conducted shows that roots need to grow deeper and should present in close spacing in order to provide a similar effect that of soil nailing. In a prolonged rainfall where shallow failures would occur due to complete loss of suction or perched water table condition the simulated system of roots were effective in maintaining a reasonable safety margin.

In tropical humid climatic conditions, the soil profiles extend to greater depths of around 30 m (Collison and Anderson 1996). The failure mechanisms of these slopes are rotational or circular and the failure plane is encountered well below the root zone (Chock et al. 2008). Also the ground water table in these regions are very deep. Hence, the effect of Matric Suction plays a vital role in maintaining the

stability of the slope. In such cases, the use of infinite slope model is inappropriate to assess the stability of the slope. In analysing deep seated failures, methods proposed by Greenwood (1983) based on the ordinary method of slices or the SLIP4EX, the excel programme developed by Greenwood (2006), can be utilized. This programme also inclusive of provisions for consequences of hydrological changes, wind loading and surcharging on slope stability.

2.6 Summary

Number of studies that have been carried out by various researchers to evaluate the stability of slopes with the installation of sub surface drains (Lau and Kenny 1983; Rahardjo et al. 2002; Rahardjo et al. 2012). Most of the early analyses have been conducted using limit equilibrium approaches. Attempts have been made to integrate finite element approaches to model the effects of horizontal drains in improving slope stability (Cai et al. 1998; Gjetvaj et al. 2009). However, the majority of the studies conducted are based on 2D theories based on plane strain formulations. Comprehensive 3D modelling of the effect of horizontal drains in improving the slope stability seldom exist. A numerical 3D model validated with a real case study has not yet been conducted up to date.

Quantification of the effect of vegetation in slope stability is a topic of interest among the researchers over the past three to four decades (Wu et al. 1979; Coppin and Richards 1990; Morgan and Rikson 1995; Greenwood et al. 2006). Various empirical and mathematical models have been developed up to date to account for the contribution of vegetation in enhancing shear strength of soil (Waldron 1977; Wu et al. 1979; Pallewatta et al., 2018). Number of attempts have been taken to incorporate the increased shear capacity of the soil root system, in slope stability analysis, using both limit equilibrium and finite element approaches (Wu et al., 1977; Greenwood 2006; Chok et al., 2004, Chok et al., 2015, Kulathilaka and Dharmasena 2015). The results of these studies have proven the existence of positive effects of vegetation in enhancing the safety margins of both man–made and natural slopes.

The combined effect of vegetation and horizontal drains in improving slope stability has not yet been extensively presented in literature. The study presented in the forthcoming chapters is aimed to model the combined effort of vegetation and sub surface drainage measures in landslide mitigation. The results obtained from the model will be compared and validated with a real case study.

Chapter 3

3 DESCRIPTION OF THE CASE HISTORY

3.1 Background

Badulusirigama landslide is a slow moving landslide which may get accelerated during heavy rainfall events. Noticeable movements in this landslide were observed after major rainfall events in 2007, 2011 and 2012. Consequently, this was identified as a high-risk landslide which requires immediate rectifications by the government of Sri Lanka,. Following the government's decision, this landslide was included in the "Landslide Disaster Protection Project of the National Road Network (LDPP), funded by the Government of Japan, which commenced in March 2013. The main rectification measure used in this landslide is long subsurface drains arranged in fan-like groups. Remediation of Badulusirigama landslide is remarkable due to the usage of longer subsurface drains of about 40 - 60 m in length as opposed to typically applied lengths of 15 to 30 m in parallel orientation. Badulusirigama landslide was also equipped with different monitoring instruments which are functioning since 2014 to date. Thus, this landslide is a resourceful case history to improve our understanding on the behaviour of rain induced landslides in the region. This chapter provides detailed information about the landslide area, history of the landslide, geotechnical investigations conducted including monitoring programmes and design of countermeasures to rectify the landslide.

3.2 Geomorphology and Geology of the area

3.2.1 Geomorphology of the area

The landslide is located on a gentle valley type slope. The slope angle is around 10 – 15 degrees. Top most soil cover consists of gravelly and sandy soils. Colluvium deposits could also be observed in the body of the landslide. The area is covered by a mixed vegetation. Shrubs, bushes and some varieties of herbal plants are

common in the area. Isolated larger trees are also present at some locations. Residential buildings are concentrated into the toe area of the slope (Figure 3.2).

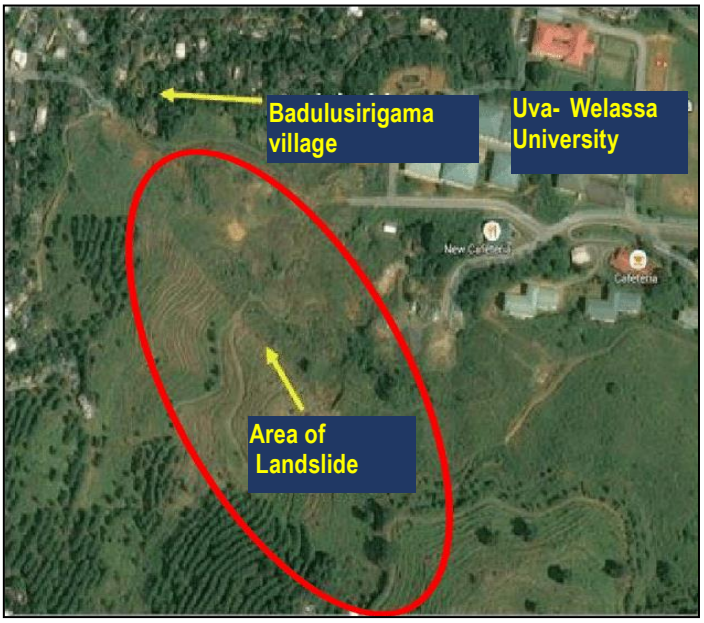

Figure 3.1 Location of the landslide (Balasuriya and Nishikawa, 2016)

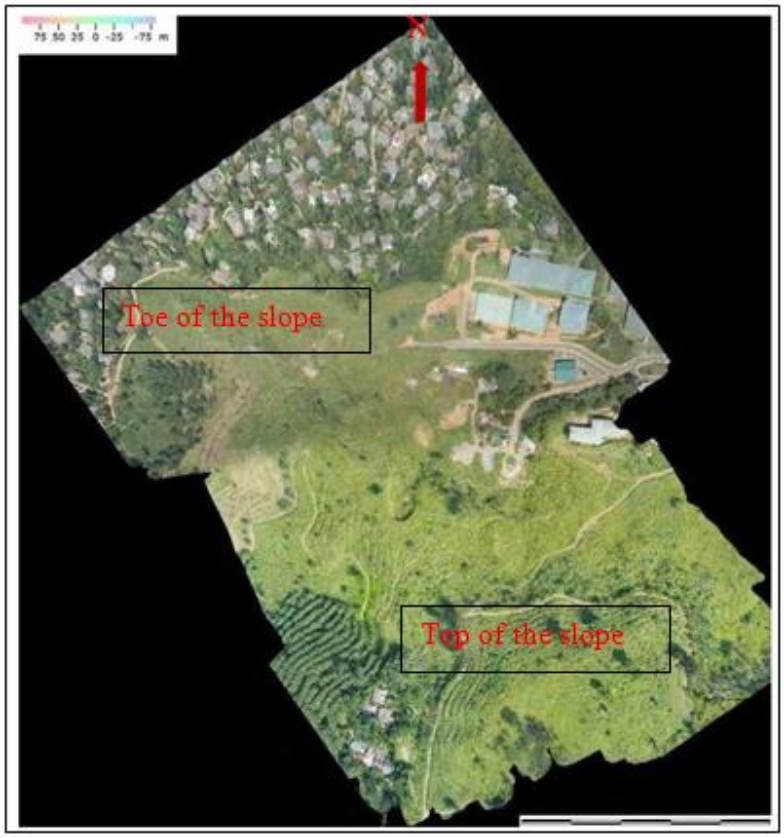

Figure 3.2 Aerial Photograph of Badulusirigama area (JICA Report, September 2015)

3.2.2 Geology of the area

3.2.2.1 Regional Geology of Sri Lanka

Approximately, 90% of the basement rocks of Sri Lanka are composed of highly crystalline, non-fossiliferous rocks. Based on the rock types, metamorphic grade and isotopic characteristics, the crystalline crust of Sri Lanka has been subdivided in to four main Lithotechtonic units namely Highland Complex (HC), Vijayan Complex (VC), Wanni Complex (WC) and Kadugannawa Complex (KC). Figure 3.3 shows the different geological complexes of Sri Lanka and the location of the Badulusirigama area within the zone of Highland Complex on the map.

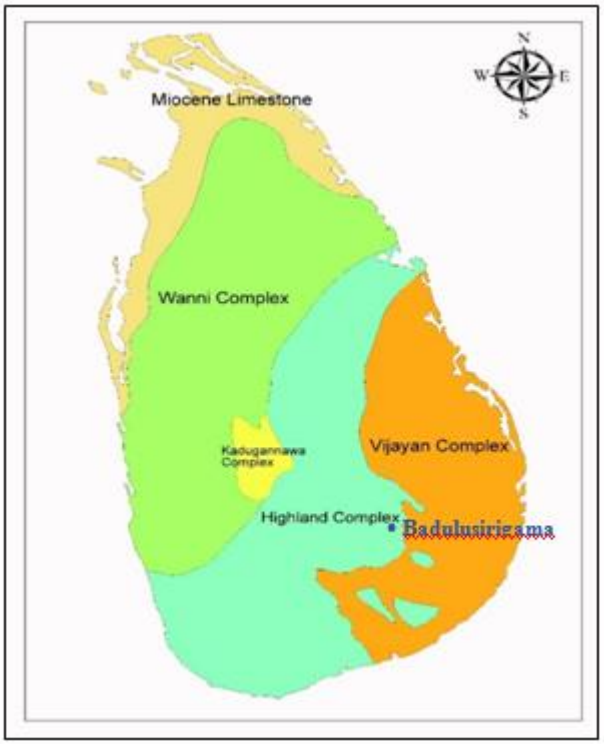

Figure 3.3 Geological complexes of Sri Lanka and location of Badulusirigama site

3.2.2.2 Local Geology of the area

Landslide area of Badulusirigama lies within the Eastern part of Highland Complex. This complex is composed of two main types of rocks, namely meta-sedimentary and meta-igneous (Cooray, 1984). In addition to that, Garnet Biotite Gneiss and Hornblende Biotite Gneiss are common rock types.

Badulusirigama area is located adjacent to the Uwa Wellassa University from east. The geology map (Figure 3.4) affirms that the location is bounded by two prominent shear zones where the rock can be structurally weakened and hence, more susceptible to the weathering process. According to the literature, Charnockitic Gneiss rock is abundant in the region.

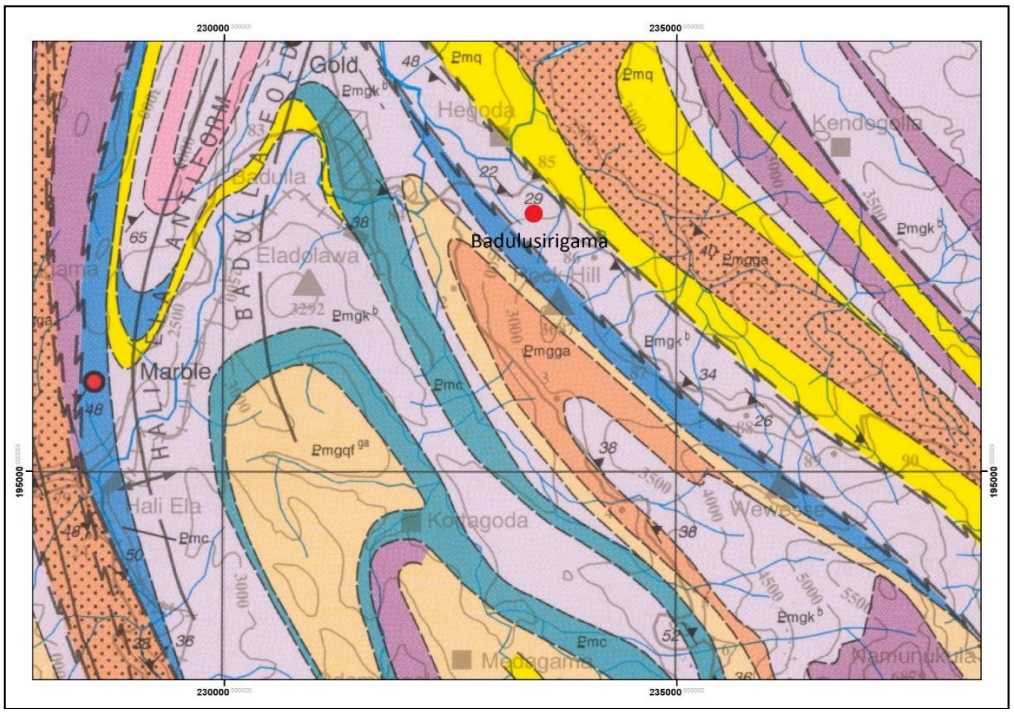

Figure 3.4 Geology map of the area

Overburden Soil

Overburden soil of the area comprises with both colluvium and residual soils. In general, top layers of northern part of the site were formed with paleo landslide debris. This colluvium soil deposits contain - some boulders. Reddish brown

residual soil is a prominent feature with weathered quartzitic bands. It is commonly observed that the weathering product of quartzite is reddish brown in colour. Borehole data indicate that the bedrock of this area is variably weathered and thick layer of completely weathered rock was encountered in several borehole locations. It can be described as weathered granular or cohesive soil in a friable condition with only fragments of rock texture and structure preserved. General gneissic rock appearance of multicolored interbedded texture is dominant with reddish brown, orangish brown, grayish white colours.

Bed Rock

Generally, the rock level is encountered around at depth of 18 m - 20 m . Rock planes are oriented to North West direction with south west dipping. According to the investigation data, Calc Gneiss rock is identified along the area.

3.3 Description of the Landslide

The landslide area comprised of multiple stances of slopes along the slopping direction. The ground surface was highly deformed and consisted of water stagnating areas, streams as well as depressions. Remittance of former landslide debris were also observed.

3.3.1 Failure mechanism

Rupture surfaces had been formed in layers composed of low strength material. The continuous creep movement of the mass had further decreased the shear capacity of the rupture zone. In addition, presence of deeper cracks have promoted deeper infiltration of water into the mass and water accumulated in those cracks had resulted in generating positive pore water pressures, encouraging the slope instability.

3.3.2 Historic Events

Badulusirigama landslide is a slow moving landslide, accelerated by heavy rainfall events. Some movements had occurred during the rainy seasons of 2007, 2011 and

2012. However, the movement pattern was irregular. Some local failures occurred in the retrogressive manner were also visible within the landslide. Excessive rainfall is the main triggering factor behind the failure mechanism. During the heavy rainy season in 2012 landslide was reactivated causing subsidence in the road and structural damages to the houses within the area.

3.4 Implementation of Mitigation measures

The government of Sri Lanka identified the necessity of applying immediate counter measures to rectify the slope movements at Badulusirigama. In view of this, site was included under "Landslide Disaster Protection Project of the National Road Network (LDPP), which was funded by the Government of Japan. This project was initiated with the purview of rectifying selected landslides associated with major national roads in seven districts of Sri Lanka.

3.5 Site Investigation Programme at Badulusirigama

Site investigation comprised of a series of surveys to collect information of the landslide. The information is gathered through field visits, geomorphological survey, borehole survey and geophysical survey. Figure 3.5 shows the site investigation plan with selected locations for borehole survey and section lines along which the geophysical surveys had been carried out.

Geomorphological Survey

This comprised of topographic survey, cross sectional survey and an Unmanned Aerial Vehicle (UAV) analysis. The UAV survey data had been used to develop the Digital Elevation Model (DEM) of the site.

Borehole Survey

Five boreholes had been drilled at selected locations (Figure 3.5) in order to identify the subsurface conditions as well as to grasp an idea about the location of the slip surface. Standard Penetration Tests (SPT) had been carried out at 1.0 m intervals to determine the formation of geological structure and presence of weak planes in

terms of strength. These drill-holes were then utilized to install other different monitoring instruments for further monitoring purposes. The instrumentation includes inclinometer guide pipes, pipe strain gauges and water level sensors. The predicted subsurface conditions at the site along with the possible failure planes are shown in Figure 3.6 and Figure 3.7. The selected cross sections are indicated in Figure 3.5.

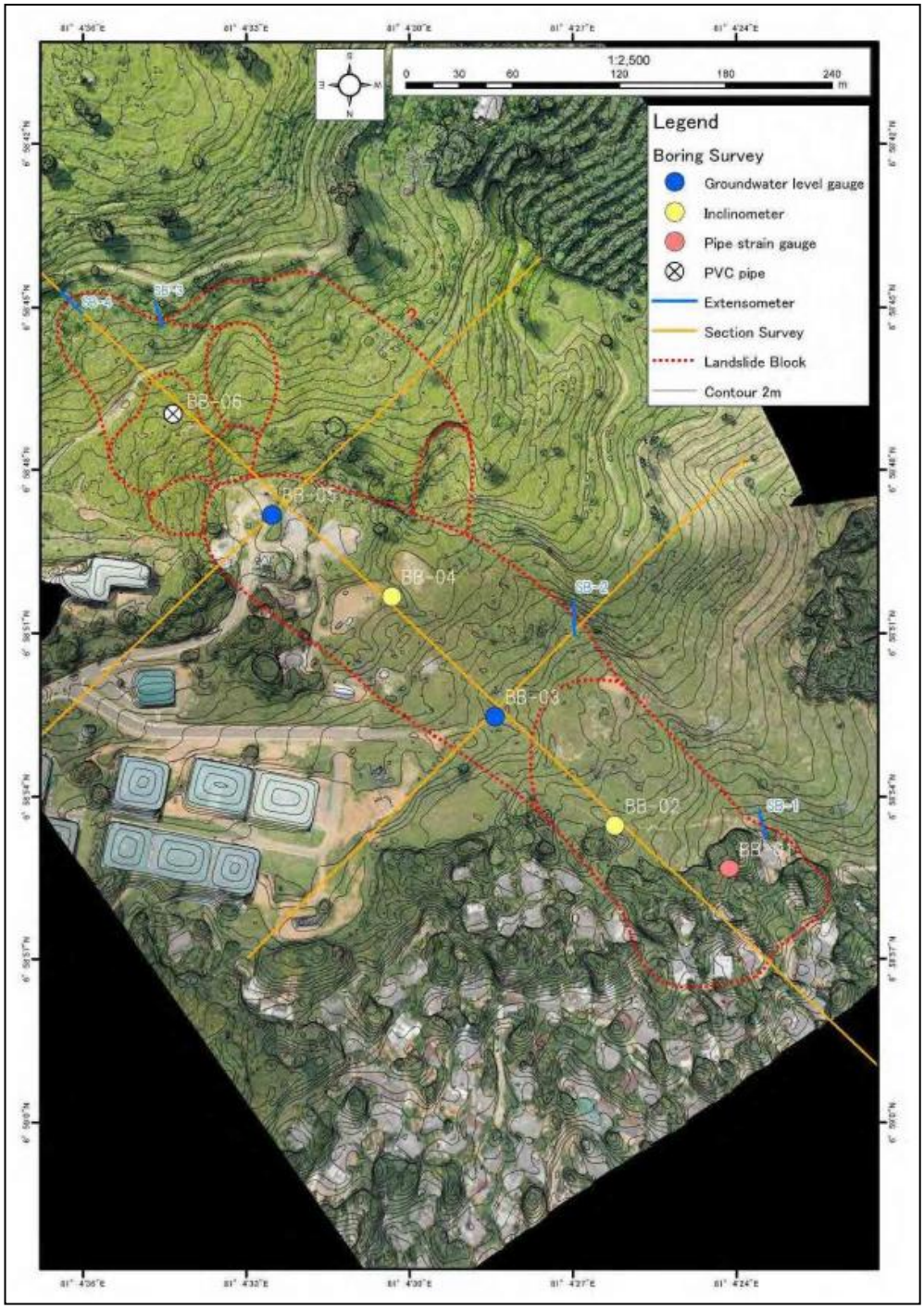

Figure 3.5 Selected investigation locations and survey lines (JICA Report, September 2015)

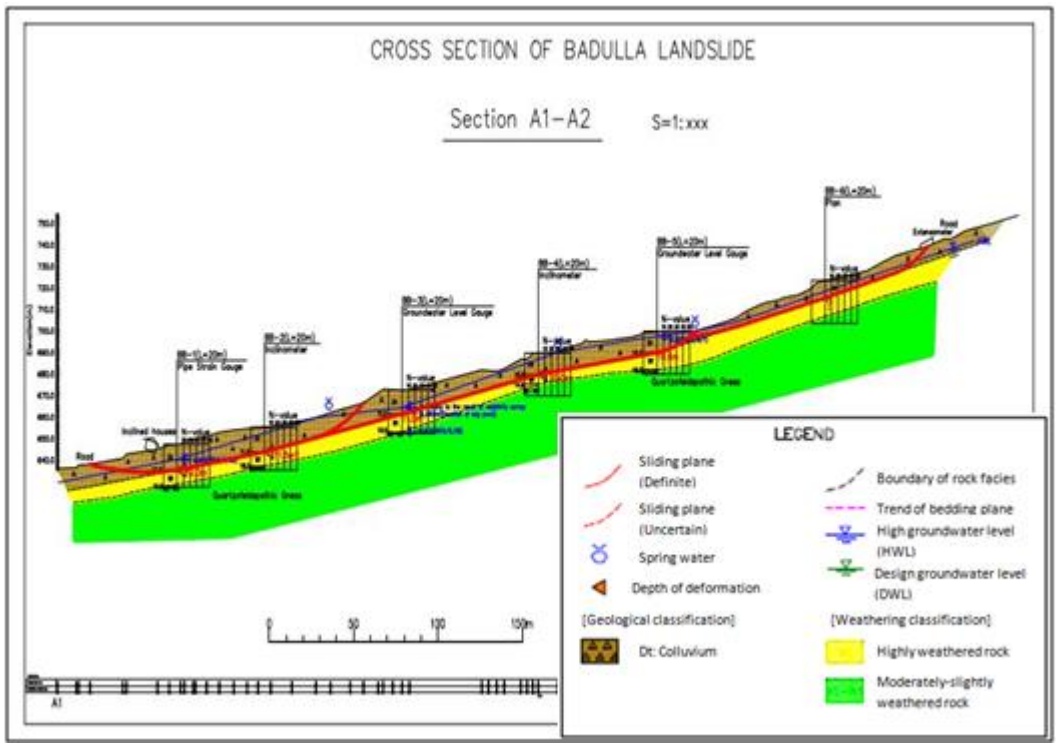

Figure 3.6 Cross section along A1- A2 (JICA Report, September 2015)

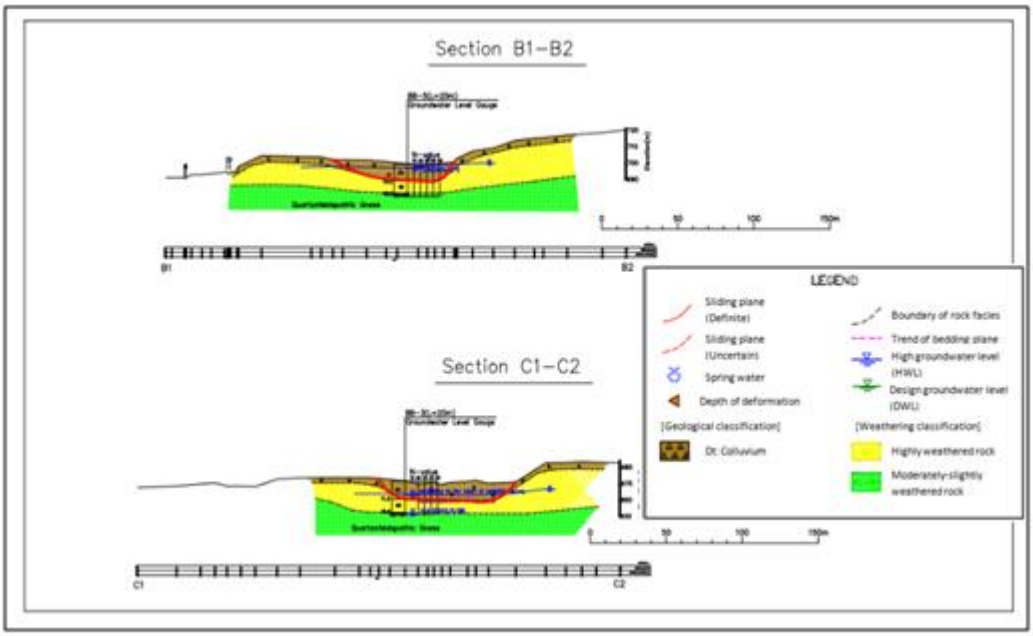

Figure 3.7 Cross sections along B1-B2 and C1-C2 (JICA Report, September 2015)

Geophysical Survey

Seismic Refraction Surveys and Resistivity Surveys had also been conducted along the selected sections of the site (Figure 3.5). Results of the electrical survey data were mainly utilized to investigate the ground water conditions including the locations of aquifers and to confirm the information gathered by the geological surveys. Figure 3.8 shows the results of a resistivity survey conducted along a selected cross section.

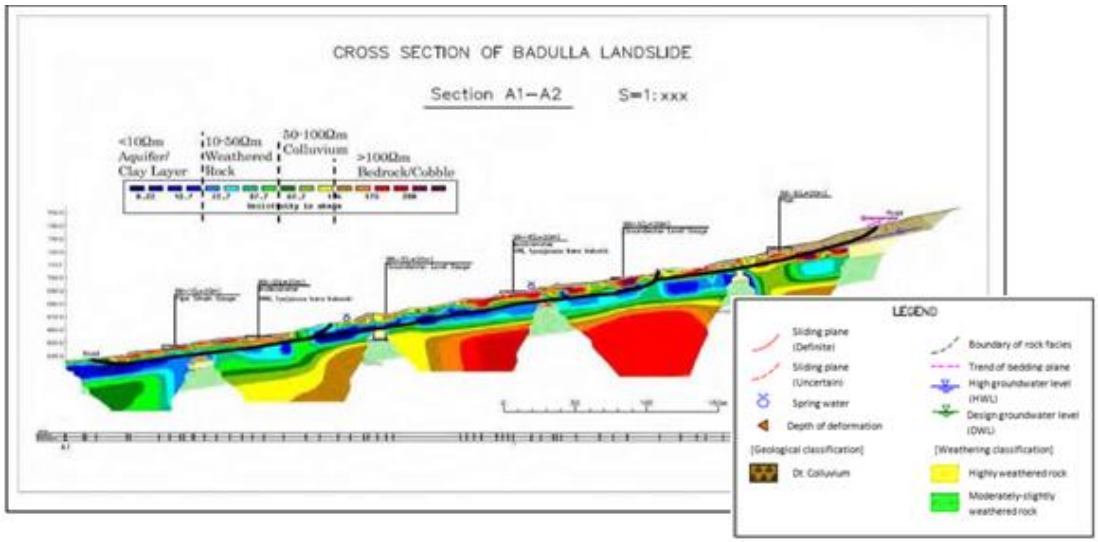

Figure 3.8 Resistivity contours on a long section along the landslide (JICA Report, September 2015)

3.6 Monitoring programme Conducted at the site

A comprehensive monitoring programme was conducted at the site to discern the movements of the soil mass. In this regard, different monitoring instruments had been set up at the site to measure the daily rainfall, mass movements as well as the water table variation within the sliding mass. The following monitoring instruments were installed at the site.

Table 3:1 Instrumentation at the site

Monitoring instrument	Description
Rain Gauge	A rain gauge has been installed to measure the daily rainfall record.
Ground Water level meter	Ground water level meters were installed in boreholes (BB) 3 and 5 (Figure 3.5).
Extensometers	Extensometers were used to monitor the relative displacement of the slide. At Badulusirigama four extensometers had been set up in a direction parallel to the slide. The locations of the four extensometers are indicated as SB 01, SB 02, SB 03 and SB 04. (Figure 3.5).
Inclinometers	Borehole inclinometer had been installed at BB 04 (Figure 3.5). The lower end of the grooved casing had ben grouted to the bed rock to ensure the rigid contact with the bed rock.
Pipe Strain Gauges	Pipe strain gauge had been installed at BB 01 (Figure 3.5). Changes of the strain of the pipes were used to detect the movement.

3.7 Interpretation of the Investigation Results

Direct and indirect geo surveys conducted at the site reveals that the Badulusirigama landslide covers a relatively large land area. The width of the slide is about 120 m, length is around 500 – 600 m and the depth of the failure plane varies in between 10- 20 m. The whole moving mass was divided to three blocks namely upper slide middle slide and lower slide (Figure 3.6). This was based on the tension cracks which were observed in the ground surface and findings of the geophysical investigations. The top most soil layer at the site is formed of colluvium materials and has a thickness of around 10 – 15 m. The colluvium layer is followed by a completely to highly weathered rock layer and the thickness of this layer is

around 15 – 25 m. Highly to moderately weathered rock layer encountered at a depth of around 25 – 30 m at the site according to the investigation results. The interpreted sub soil profile based on the geological survey data is shown in Figure 3.6.

The ground water table had been encountered at an average depth of around 6 – 7 m at the investigated locations and confirmed by geophysical survey results. However, presence of shallow water table conditions and stagnant ditches have also been observed at some locations (Figure 3.6 and 3.7). Existence of local unconfined aquifers are perceptible from the results of the resistivity survey (Figure 3.8). in addition BB 05 had indicated a ground water level 2.5 m below the ground level during significant precipitation events.

Results of the monitoring programme indicate slight movements of the landslide when excessive rainfall events were present. The extensometers installed at the upper slope area (SB 03 and SB 04) had indicated that the slide was actively moving during the heavy rainfall in December 2014 (total cumulative rainfall of 622 mm during 18 days). Meanwhile, extensometers at the bottom of the slope (SB 01 and SB 02) had indicated compression displacements which denoted that the slide was rotational in nature. In addition to this, inclinometer and the pipe strain gauge which were installed at BB 04 and BB 01 respectively had shown some displacements corresponding to rainfall events. The inclinometer data showed some relative displacements at a depth of around 9 – 10 m from the ground surface and strain gauge indicated displacements at a depth of 12- 13 m from the existing ground level. These evidences confirm the occurrence of active movements of the landslide in response to excessive rainfall events along the potential failure plane.

3.8 Stability Assessment Conducted

Based on the information obtained in terms of different investigations, an initial stability assessment had been conducted. A summary of the stability assessment conducted by the LDPP design team is shown in the Table 3.2.

Table 3:2 Summary of the initial stability assessment (JICA Report, September 2015)

Stability Analysis for Landslide

Item		Unit	Lower Slide	Middle Slide	Upper Slide
Formula	-	-	Modified Fellenius Method		
Factor of Safety	Fs	-	0.98	0.98	
Proposed Factor of Safety	P·Fs	-	1.20	1.20	
Length of slip surface	L	m	184.092	402.094	Under
Area	A	m^2	1714.96	3879.11	Investigation
Normal Force	N	kN/m	30251.4	68746.6	
Pore pressure	U	kN/m	9762.2	23641.6	
Pore pressure(drainage)	Up	kN/m	1819.6	7574.7	
Resistance force	S	kN/m	4496.732	10737.346	
Resistance force(drainage)	Sp	kN/m	5526.178	13129.725	
Tangential force	T	kN/m	4588.502	10956.471	
Cohesion	C	kN/m	10.0	10.0	
Shear resistance angle	Φ	degree	7.39	8.47	
Wet weight	Γt	kN/m^3	18.0	18.0	

It is evident from the results that the upper and middle blocks of the landslide have factor of safety values of 0.98 each. However, it seems that the cohesion and friction angle values used to define the shear behaviour of colluvium, in the LDPP design, differ from the nominal values generally obtained for colluvium found in Sri Lanka. In general, Sri Lankan colluvium soils possess a slightly high friction angles and lower cohesion values even in the residual state.

3.9 Design of Mitigation Measures

According to the information obtained from the filed investigation surveys and monitoring programme it was apparent that the Badulusirigama landslide was a slow moving (creep) deep seated landslide in which the movements were accelerated during the periods of heavy rainfall. The main triggering factor is the prolong rainfall and consequent rise of the phreatic surface. Apart from this

development of perched water table conditions, increase of loading above the failure surface as a result of stagnant water bodies, were the main causative factors leading to slope movements. Therefore, the foremost focus when designing mitigation measures was to control the rise of ground water table during heavy precipitation events and direct the surface water paths away from the slope.

Subsurface Drainage Measures

The main objective of introducing subsurface drainage was to lower the rising ground water table during infiltration events. In this context, altogether fifty one (51) number of subsurface drains have been installed at the site. The drains have been grouped in fans named from A to F. The first three fans (i.e. A, B and C) composed of eight (8) drains and the rest has nine (9) drains each. The drains are about 10 degrees inclined to the horizontal plane. Figure 3.9 gives a plan view of the subsurface drainage arrangement. Figure 3.10 shows the elevation of each drainage fan in relation to section A1- A2.

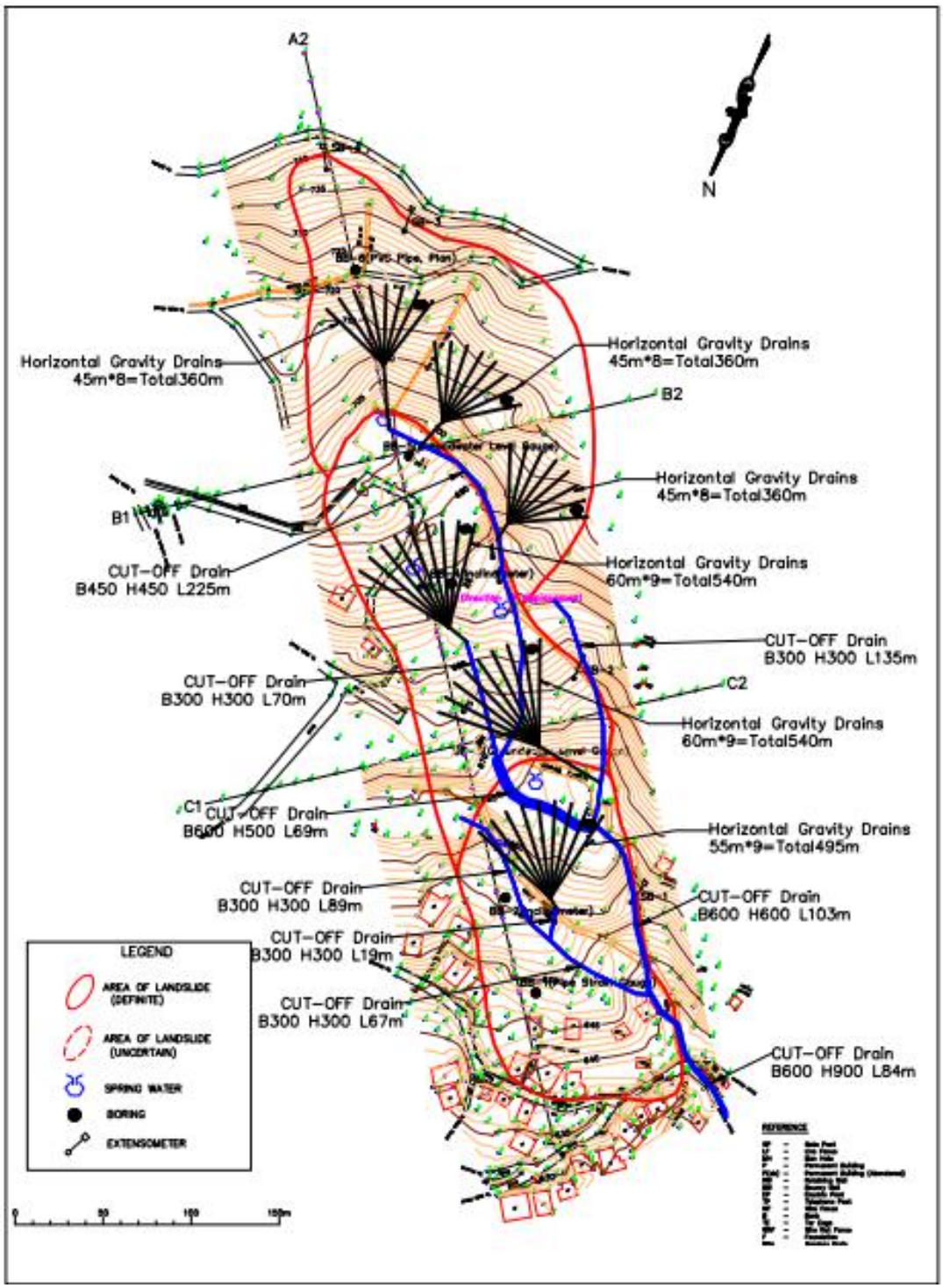

Figure 3.9 Plan View of the subsurface drainage improvement (JICA Report, September 2015)

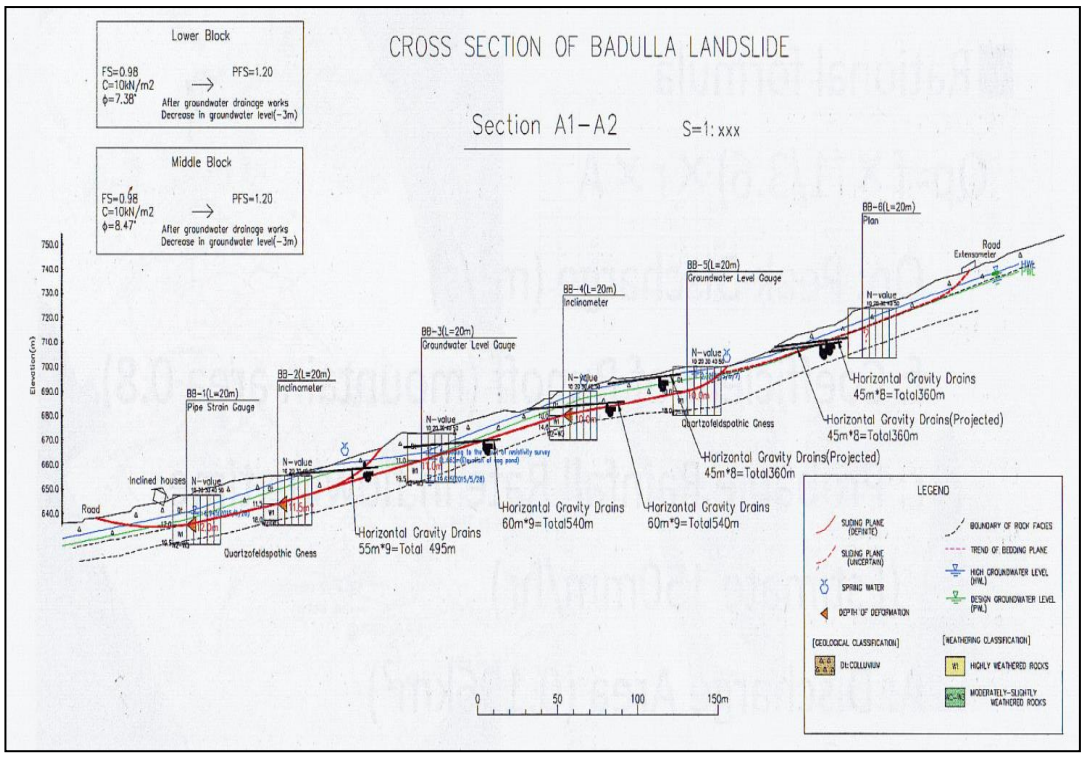

Figure 3.10 Sectional view of subsurface drains (JICA Report, September 2015)

The length of the subsurface drains are being varied in between 45 to 60 m. Drains are designed to outbreak the potential slip surface by 5 to 10 m distance. The tip interval of individual drains of the fan varies from 5 to 10 m. Each fan (drainage group) has a footprint of approximately 1800 m^2.

Surface Drainage Measures

The surface drainage ditches have been designed in align with natural channels to eliminate the infiltration and spring flow. The total length of the surface drainage ditches are 861 m. A summary of design countermeasures is shown in Table 3.3.

Table 3:3: Summary of design countermeasure (JICA Report, September 2015)

Pilot Area	Type of rmeasure works	Details	Priority	Quantity	Unit	Remarks ex.concrete type
Badulu sirigama	Ditch	Type1	A	256	m	600 × 900 600 × 600 600 × 500
		Type2	A	225	m	450 × 450
		Type3	A	380	m	300 × 300
	Horizontal Drilling	Upper slope	A	1080	m	45m × 8nos × 3area
		Upper slope	A	1575	m	(55～60)m × 9nos × 3area

3.10 Future studies

Badulusirigama landslide mitigation project is an exemplary case for implementation of new mitigation measures along with comprehensive monitoring approaches. Though the rectification measures (i.e. improvement of surface and subsurface drainage) look very straight forward, it unfolds how the same has been used effectively and efficiently to rectify a large scale landslide.

In this study, almost all the analysis have been conducted using two dimensional plain strain conditions. However, a three dimensional analysis will give much insight to the effects of non-symmetrical arrangement of subsurface drains which are meant to address localized variations of ground terrain. Using the Finite Element model results, the current stability level of the drains, threshold rainfall that existing drains can handle, consequences of failure (clogging, malfunctioning) of some drains over time (this also gives an understanding on the maintenance requirements),could be understood. It would also provide some idea about the allowance of any excavations/constructions on and near the site and would help to develop risk management and evacuation processes for the village and roads at the downstream of the landslide in severe weather conditions.

3.11 Summary

Badulusirigama landslide located in central highlands of Sri Lanka, has been identified as a critical landslide that needs immediate rectifications. The

rectification activities of the landslide were undertaken in 2016 under LDPP in collaboration with JICA. Prior to the design of remediation measures, a comprehensive investigation programme was conducted at the site. This enabled engineers to gather information required for design of countermeasures and also to comprehend the long term behaviour of the sliding mass corresponding to time and different climatic conditions. The investigation programme consisted of Geomorphological Survey, Borehole Survey and Geophysical Survey. The investigations revealed that the land slide area comprised of soft colluvium soil to about 15 m depth underlained by residual soil to about 15-20 m depth, then underlained by the bedrock. High ground water table as well as localized perched water conditions were also identified from the survey. These investigation results revealed that the main triggering factor behind the slope movement is the excessive rainfall and consequent rise of ground water table. The raised ground water can induce additional water pressure loads on the soil body, increase soil weight and reduce soil strength, triggering the slope movements. Hence, improvement of both surface and subsurface drainage measures have been proposed as the main rectification method to mitigate the slope movements. For the subsurface drainage, six fan type subsurface horizontal drainage structures were introduced to lower the ground water table. The surface runoff and the drainage from subsurface drains were diverted to lower elevations using concrete ditches.

This chapter presents the initial survey results of the land slide along with an evaluation of the information and the mitigation measures designed and implemented by LDPP. The chapter provides a broader understanding on the general setting of Badulusirigama village and the landslide, site geology, current knowledge on the site behavior and opportunity to further the knowledge on the rain induced landslides in Sri Lanka.

The parameters used by the JICA study were different that used by the analyses and designs done in Sri Lanka, but the report has presented facts to prove that the safety margins of the slide area had been improved from an initial value given by a FOS of 0.98 to a state with a FOS of 1.2.

Chapter 4

4 DEVELOPMENT OF THE GEOTECHNICAL MODEL OF THE BADULUSIRIGAMA SITE

4.1 Background

Chapter 3 presented the available information from site investigation at the site of Badulusirigama landslide. In this chapter, the methodology followed in deriving the subsurface geotechnical model of the Badulusirigama landslide using the investigation data, is presented. The geotechnical model developed in this chapter will then be used in the succeeding chapters to simulate the behaviour of the landslide using two dimensional and three dimensional numerical models.

4.2 Assessment of investigation data

The investigation data gathered from contour survey, geotechnical and geophysical investigations were used to deduce a subsoil profile, soil strength parameters and potential slip surface at the site. An assessment of the data and basis for the development of the ground model is discussed in the following sections.

4.2.1 Contour Survey

A contour survey has been conducted at site (Figure 4.1) covering the impended landslide area. Elevation contours have been taken at every 1 m intervals along the slope. According to the survey, the toe area of the slope is at an elevation of around 625 m – 630 m above the mean sea level and the crest of the slope is at an elevation of 750 m above the mean sea level

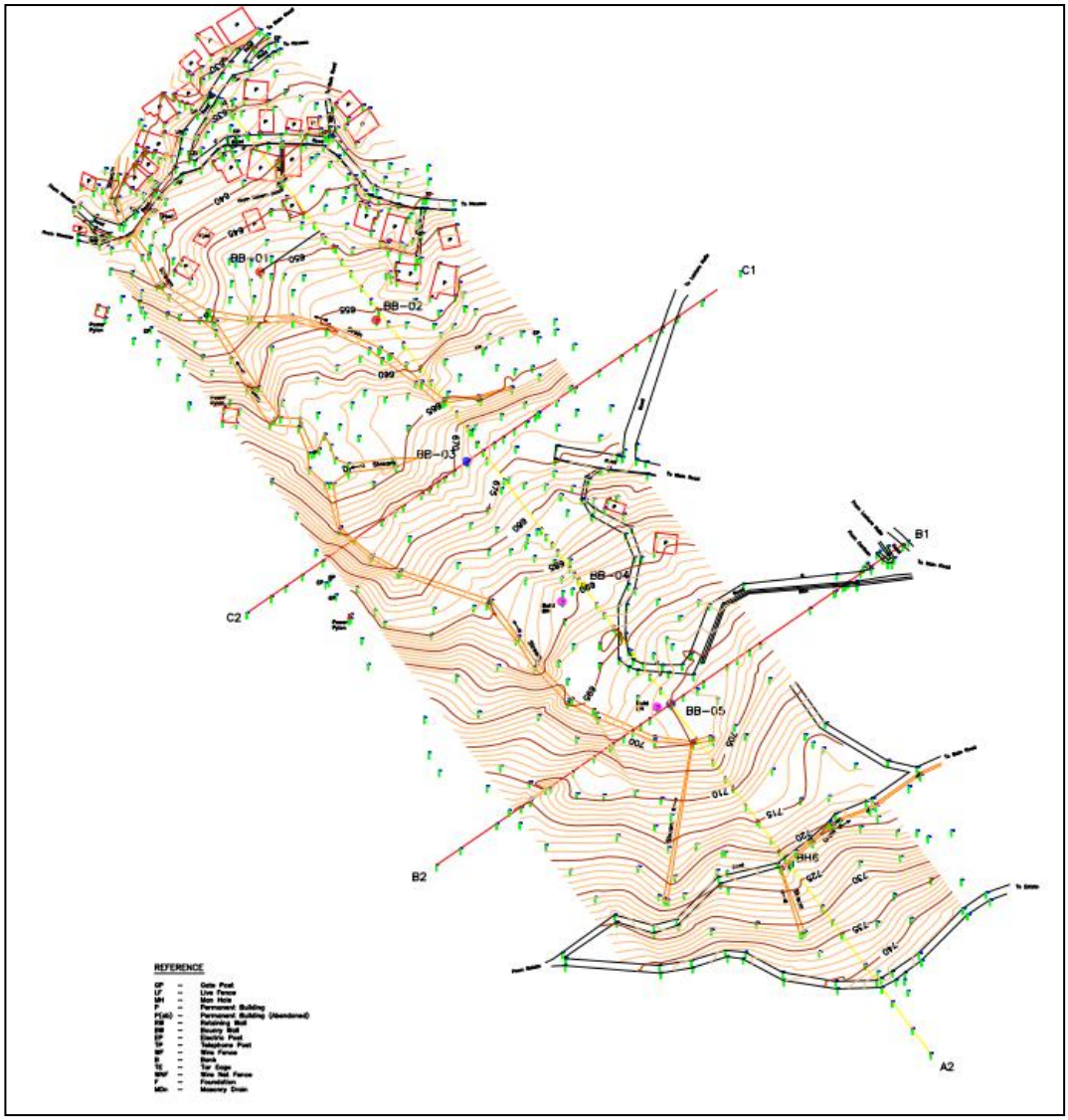

Figure 4.1: Contour survey plan of the area

Figure 4.1 presents a detailed contour pattern within the survey area. Along with the contour plan the cross sections, B1 – B2 and C1 –C2, and a long section along alignment A1 – A2, are also presented. . The ground profile along the long section A1 – A2 is shown in Figure 4.2. The contour map shown in Figure 4.1 was used in developing ground surface profile in both 2D and 3D models in this study.

4.2.2 Borehole Survey

Six number of boreholes have been advanced at selected locations of the landslide area, along the A1-A2 long section alignment, as indicated in Figure 4.1. Table 4.1 presents a summary of borehole logging information.

Relative compactness of the sub soil layers, changes of the soil layers with the depth and depth to the ground water table from the existing ground surface have been derived using the borehole investigation data. Variation of SPT "N" value, visual classification of the soil samples obtained from different depths and the rate of the drilling fluid returning from the drilled locations were closely examined in defining the subsoil / rock layers. Based on the information, three main subsoil layers have been identified.

Table 4.1 Details about the location, depth of termination and depth to the ground water table at borehole locations

Borehole number	**Co-ordinates**	**Depth to the ground water table (m)**	**Depth of termination (m)**
BB 01	06^0 59` 06.9``, $81^0$ 04`19.0``	11.8	20
BB 02	06^0 59` 06.9``, $81^0$ 04`21.1``	15.4	20
BB 03	06^0 59` 04.9``, $81^0$ 04`23.3``	19.8	20
BB 04	06^0 59` 02.7``, $81^0$ 04`25.2``	6.8	18.5
BB 05	06^0 59` 01.2``, $81^0$ 04`27.4``	7.6	20

4.2.3 Deduction of the subsurface profile

Subsurface information acquired though borehole investigation were compared with the data obtained from geophysical surveys. It enabled the prediction of subsurface profile with a substantial degree of accuracy. Relative thicknesses of the subsurface layers encountered at each drilled location are summarized in Table 4.2. Subsurface profiles at borehole locations were linked together with geophysical

survey data to procure the continuous subsurface profile of the site. Figure 4.2 presents the subsurface profile of the site along the long section A1 - A2.

Table 4.2: Interpreted subsurface soil profile of Badulusirigama landslide

Soil layer	Formation / weathering condition	Thickness (m)
1st layer (top layer)	colluvium deposits	vary from 10 m to 20 m
2nd layer (middle layer)	completely to highly weathered rock	vary from 10 m to 20 m
3rd layer (bottom layer)	highly to moderately weathered rock	Not confirmed due to borehole termination

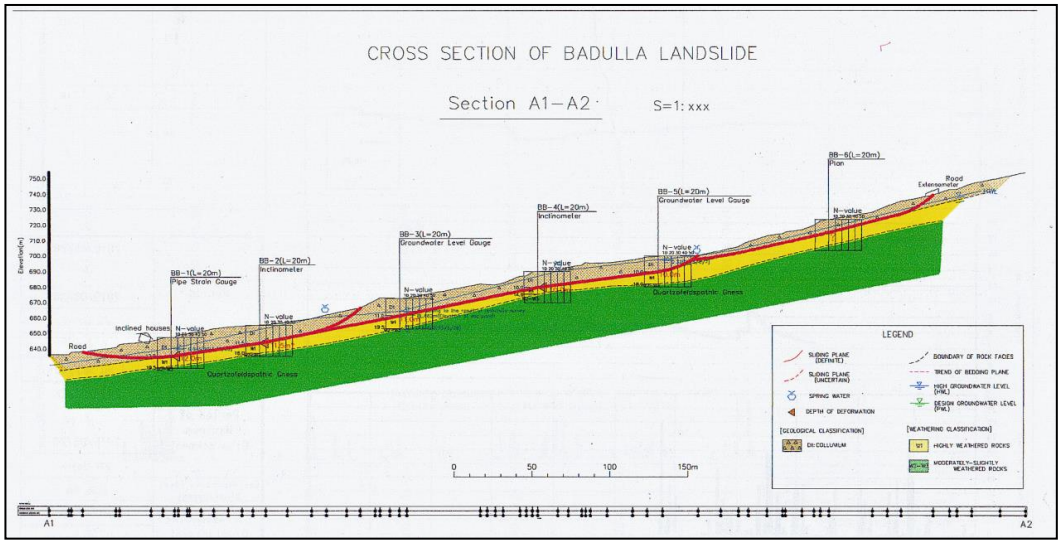

Figure 4.2: Subsurface profile through section A1- A2

4.2.4 Determination of the active slip surface

The information from different monitoring instruments, destructive surveys and non-destructive surveys were integrated with field observation data to locate the potential failure plane of the landslide. Extensive monitoring instrumentation done at the site (see Section 3.7) furnished wide range of data pertaining to the location and the behaviour of the slip plane. Besides, the tension cracks appeared in the

surface of the slope were also useful in determining the number of slip surfaces. Table 4.3 gives a summary of information obtained from field instruments. Position of the failure planes along the long section A1 - A2 is shown in Figure 4.2. Location of the failure surface in the cross sections B1 - B2 and C1 - C2 were shown in Figure 3.7 and Figure 3.8 in Chapter 03.

Table 4.3: Summary of information from monitoring instrumentation

Instrument	Location	Indication	Remarks
Pipe strain gauge	BB 01	Cumulative displacement at 12.0 – 13.0 m from the GL	Figure 4.3
Inclinometer	BB 04	Cumulative displacement at 9.5 – 10 m from the GL	Figure 4.4
Inclinometer	BB 02	Cumulative displacement at the 9.5 – 11.5 m from the GL	Figure 4.5
Extensometers	(SB 03 SB 04)	Active movements in the upper slope during rainy period in December 2014	Figure 4.6
Extensometers	(SB 01 and 02)	Compression displacements	Indicate the rotational type sliding

(Source: Japanese International Cooperation Agency (JICA), 2015, "Proposal for rectification on landslide, slope failure and rock fall in pilot sites".)

Figure 4.3 shows the cumulative displacement of the sliding mass captured by the pipe strain gauge installed at BB 01. During the monitoring period (from 06th of June 2015 to 27th August 2015), the total strain recorded is 58 µ, with a daily average of 0.71 µ. Maximum displacement has been recorded from 09th to 10th of June, which is around 7.5 µ. This value is well above the average daily figures recorded. Figures 4.5 and 4.6 indicate the relative displacement of the sliding mass

monitored from two inclinometers at BB 04 and BB05, respectively. It further indicates that the maximum movements have occurred after the periods of significant rainfalls. Figure 4.6 shows the graphs derived from the readings obtained from the four extensometers installed at the site. In conclusion, the slip surface is identified to be around a depth of 10 – 15 m from the existing ground level. Figure 4.6 also indicates the variation of ground water levels in BB 01, BB 03 and BB 05 of which BB 03 and BB 05 are with automated ground water level sensors.

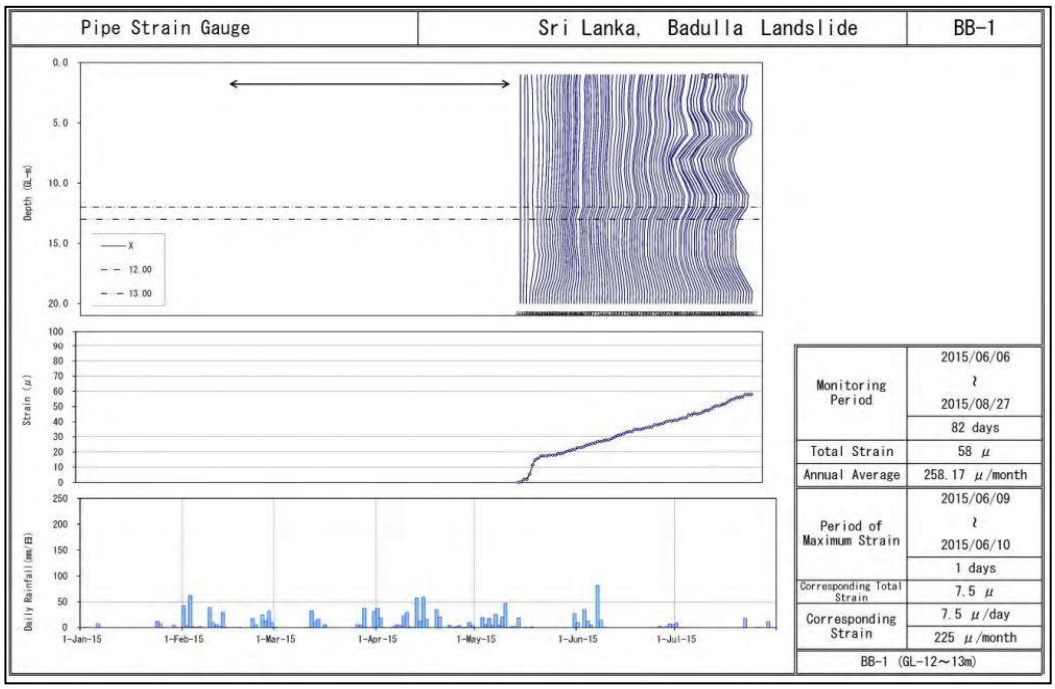

Figure 4.3 Graph pertaining to pipe strain gauge at BB 01

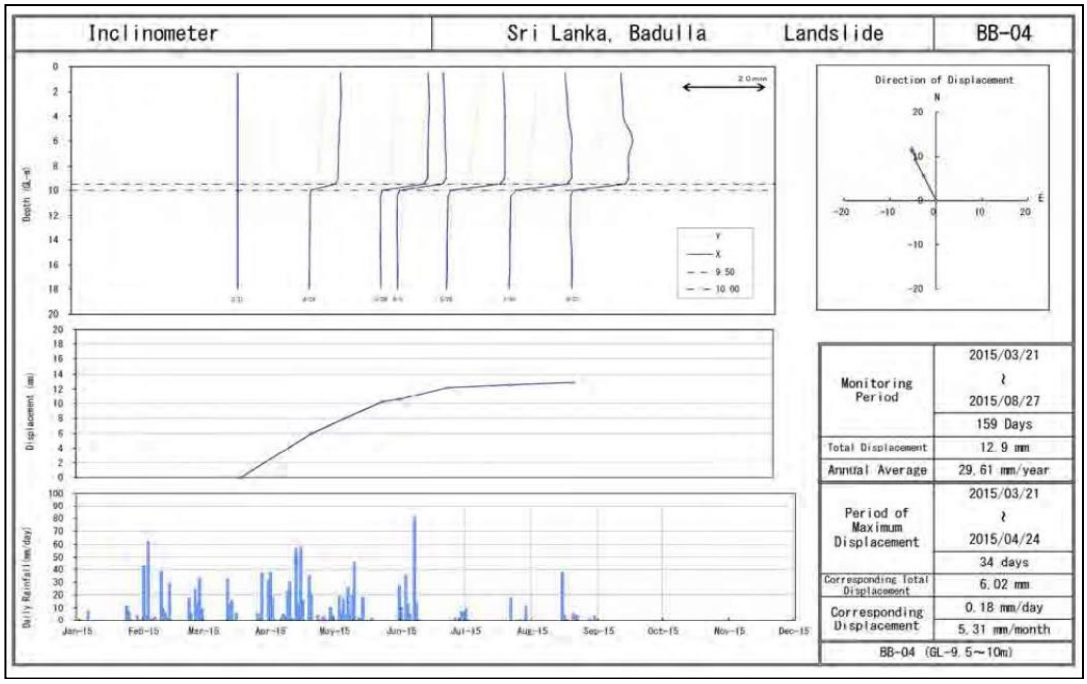

Figure 4.4 Inclinometer graph pertaining to BB 04

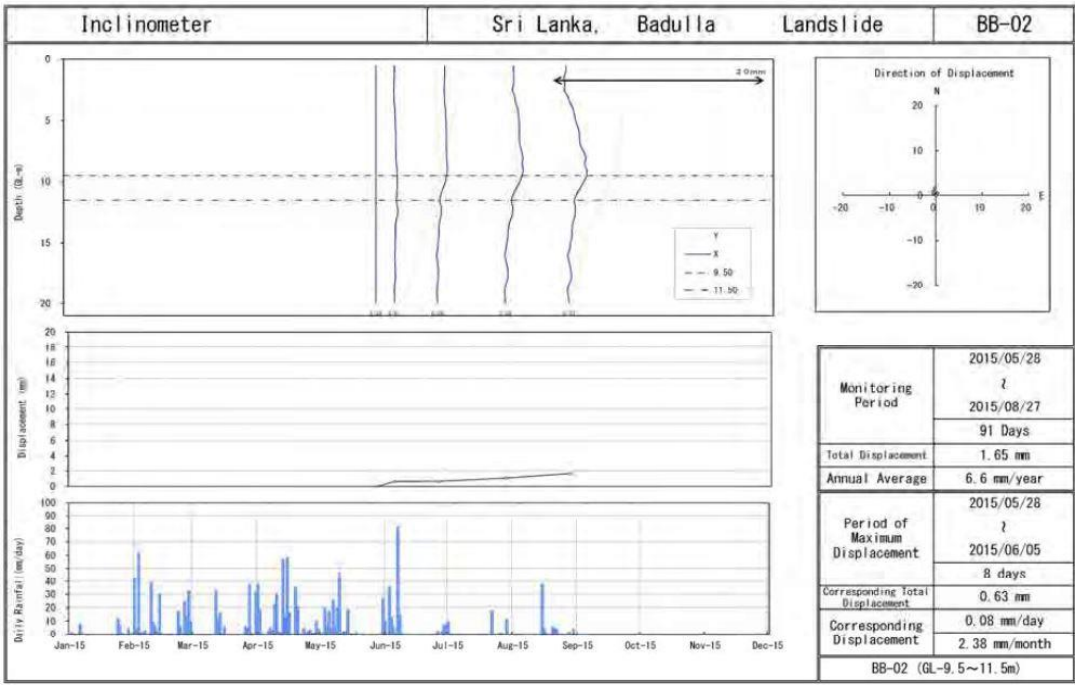

Figure 4.5 Inclinometer graph pertaining to BB 02

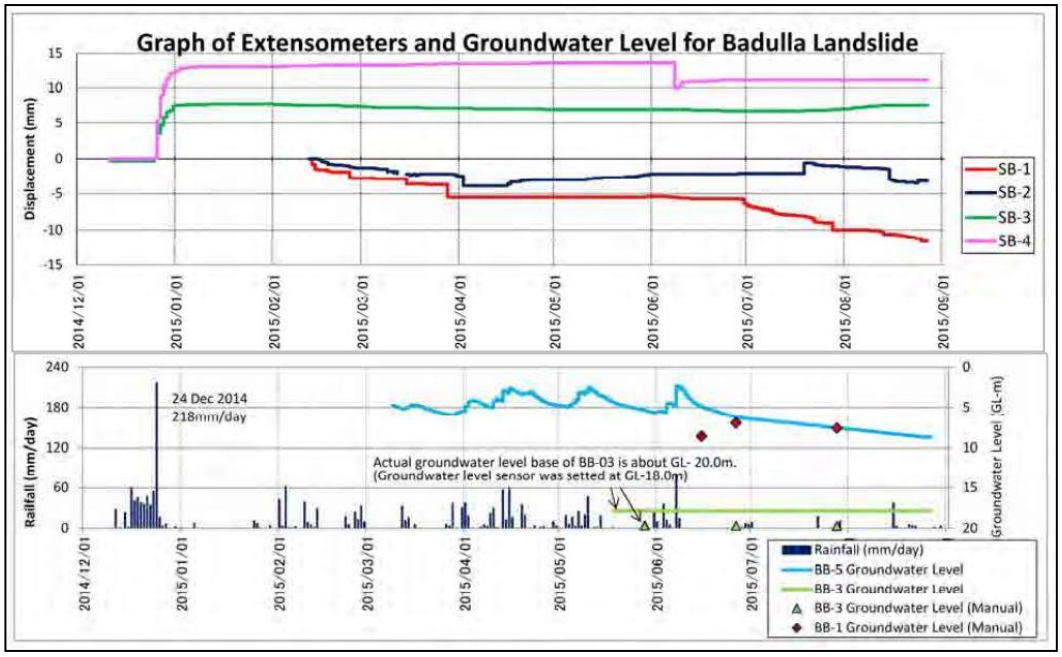

Figure 4.6: Graphs pertaining to extensometers (SB 01, 02, 03 and 04)

4.2.5 Ground water table

Depths to the ground water table encountered at each borehole location are given in Table 4.1. These depths indicate that the water table generally lies within the top colluvium layer of low permeability. The water table indicated in the boreholes is located at a depth of more than 7 m from the ground surface. However, during the periods of prolong heavy rainfalls, perched water table conditions had been observed in the landslide area. In addition to this, borehole water level sensors too have indicated a rise of ground water table after heavy rainfall events. These perched water levels have been observed very close to the ground surface level, indicating that about 7 -15 m rise of water level is possible at the site when under existing poor drainage conditions.

4.3 Geotechnical model of the Badulusirigama site

Mechanical and hydrological parameters for subsoil layers were determined based on the field SPT correlations available in the literature as well as experience gained from similar studies conducted in the past. Table 4.4 summarizes the parameters

derived for each soil layer. These parameters were used for soil and rock materials for the 2D and 3D numerical analyses.

Table 4.4: Summary of soil parameters used for different layers

Parameter / Layer	Density		Effective Cohesion (kPa)	Effective Friction angle (deg)	Elastic modulus (kPa)	Poisson s ratio	Void ratio	Saturated permeability ($mday^{-1}$)
	Bulk (kNm^{-3})	Saturated (kNm^{-3})						
Colluvium	15	16	2	22	12000	0.3	0.8	0.86
Completely to highly weathered rock	16	17	6	32	30000	0.3	0.5	8.6E-2
Moderately weathered rock	20	20	20	40	150000	0.2	0.2	8.6E-10

4.4 Summary

The methodical development of subsurface soil profiles and derivation of their strength parameters were discussed in this chapter. Site investigation data such as borehole logs, contour survey, geophysical survey and ground water monitoring wells were considered when deriving the subsurface conditions. The subsurface soil profile mainly consists of three soil layers; a 10 to 20 m thick colluviums layer at the top followed by a 10 to 20 m thick completely to highly weathered rock underlain by moderately weathered bed rock. After careful assessment of the investigated data, the mechanical and hydrological parameters for each subsoil layer were derived. These parameters were used as the inputs for the constitutive material models used in numerical simulations during this study.

Chapter 5

5 TWO DIMENSIONAL PLANE STRAIN ANALYSIS OF THE BADULUSIRIGAMA LANDSLIDE

5.1 Background

This chapter discusses the two dimensional (2D) plain strain analysis carried out to investigate the behaviour of Badulusirigama landslide. The complete analysis covering the process of infiltration and seepage and the stability of the slope under the resulting condition was done with SEEP/W and SLOPE/W software in GeoStudeo 2012 software package. Material parameters obtained through site investigations, discussed in Chapter 4 were used for the numerical model.

The initial model of the landslide was set up to yield pre-improvement stability conditions similar to site observations. Then, the landslide was assessed under the improved condition after installation of sub-horizontal drains. Further analyses were conducted to investigate the performance of the rectified site of the landslide during different anticipated critical rainfall weather events. The results obtained from these analyses are presented in this chapter.

5.2 Two dimensional plane strain idealization of the site profile

A 2D plain strain analysis was conducted using the GeoStudio 2012 software by Geo Slope international. A cross section along A1- A2 was selected so that the section passes through the centre line of the impending landslide and represents most critical terrain along the slope. Generally, plane strain models are adopted for long geotechnical problems that are uniform along the longitudinal direction. Although this condition is not satisfied by the geometric formation of the current geotechnical problem, selecting the most critical section for the analysis and assuming the plane strain conditions is deemed to yield worst case scenario performance for the landslide. The 3D model developed will be discussed in Chapter 6.

Analysis was conducted to assess both existing conditions and the behaviour after implementation of the rectification measures. Separate analysis were conducted for modelling the seepage and assessment of slope stability using the different modules available in the software.

5.3 Seepage analysis using SEEP/W module

GeoStudio 2012 software package comprise of a separate module SEEP/W, to conduct a seepage analysis. In this module, seepage analysis can be carried out under both steady state conditions and transient flow conditions. SEEP/W module operates on a basis of finite element formulation which enables more complex calculations related to both saturated and unsaturated conditions.

It is necessary to have a good understanding on the flow properties of the materials to specify the hydrological performance for the constitutive models in the numerical analysis. These characterizations are important to effectively guide the software to produce results which are closer to reality. When the soil is unsaturated, flow properties are not constant and are non- linear functions of the matric suction or the negative pore water pressure. The two main functions required to perform a seepage analysis using SEEP/W module are the Soil Water Characteristic Curve (SWCC) and Hydraulic Conductivity Function (HCF). SEEP/W provides a set of functions pertinent to different soil types, which can be used for most of the real world cases.

5.3.1 Soil water characteristic curve (SWCC)

SWCC describes the variation of the water content with negative pore water pressure or the matric suction in an unsaturated soil. It consists of three main regions, namely, boundary effect zone, transition zone and the residual zone. SWCC provides information about saturated water content, residual water content and the air entry value of the soil. Experimental determination of SWCC is tedious, time consuming and requires specially fabricated laboratory equipment. Whereas SWCC of a particular soil can be derived using pore size distribution and Atteberg limits (Aarya & Paris 1981: Zapata 1999). Considering these characteristics of the

soils encountered at the site appropriate SWCC curves available in SEEP/W module was adopted in the analysis.

5.3.2 Hydraulic conductivity function (HCF)

Permeability of an unsaturated soil is also a function of the matric suction. Tedious laboratory testing procedures are required to establish the permeability function of a given soil. However, there are number of methods available to predict the permeability function using indirect approaches. SEEP/W module provides two indirect methods to predict the HCF of a given soil, namely Fredlund and Xing (1994) and Van Genuchten (1980). For this analysis, Permeability function was estimated based on the method proposed by Van Genucthen (1980).

Table 5.1 indicates the soil properties used for seepage analysis. For the colluvium and completely weathered rock layer, SWCCs developed for silty-sand and silt were used, respectively, in the modelling. Figure 5.1 and 5.2 illustrates the SWCC's and HCF's used for colluvium and completely to highly weathered rock respectively.

Table 5:1: Soil properties for seepage analysis

Formation	Saturated Permeability (m/day)	SWCC	Permeability function
1.Colluvium	0.860	Silty Sand*	Estimation based on VG**
2.Completely to highly weathered rock	0.086	Silt*	Estimation based on VG**
3.Highly to moderately weathered rock	8.6E - 10	Saturated only material	

(a) *Built in function available in SEEP/W module

(b) **Based on the estimation method by Van Genuchten 1980 available in SEEP/W module

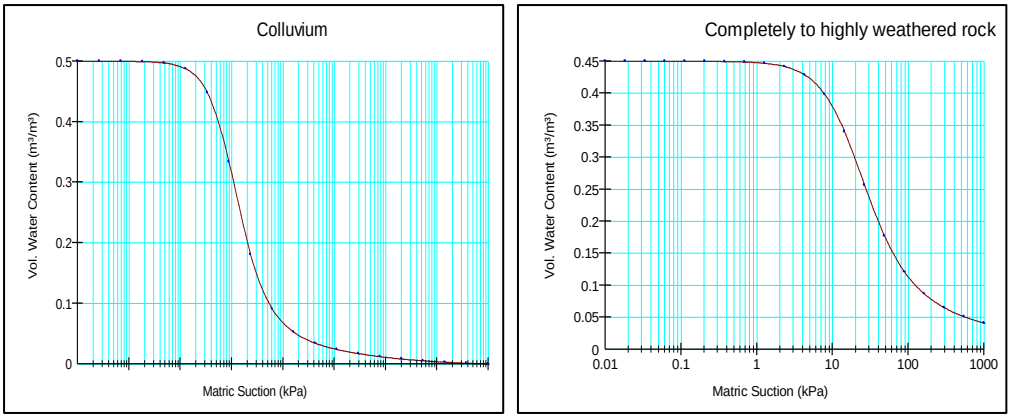

Figure 5.1: SWCC used in the analysis (a) Colluvium; (b) Completely to highly weathered rock

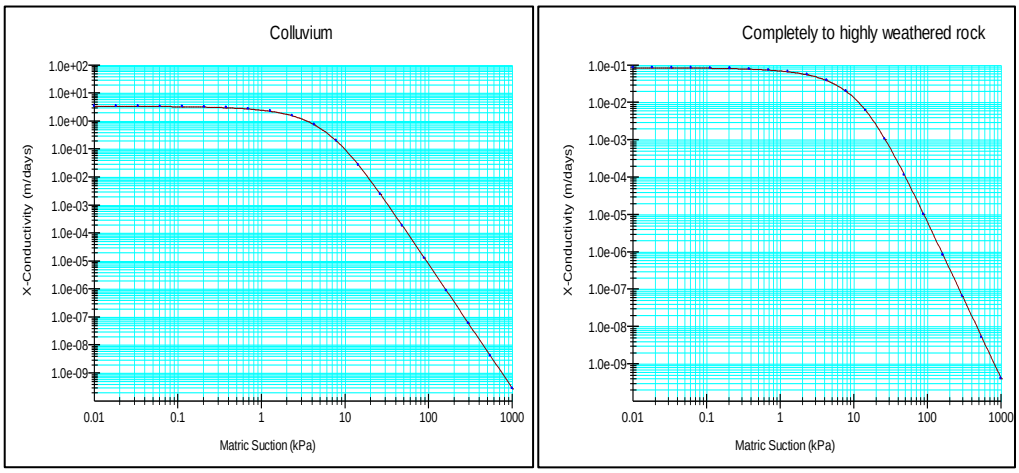

Figure 5.2: HCF"s used in the analysis (a) Colluvium; (b) Completely to highly weathered rock

5.4 Idealization of the cross section A1-A2 in SEEP/W

The hydraulic conductivity properties given in Table 5.1 were incorporated into the geotechnical model of the site developed in Chapter 4. The integrated model was then used to analyse the behaviour of the pore water pressure regime under different conditions. Figure 5.3 shows the profile through the cross section A1 – A2 drawn in the SEEP/W model. Table 5.2 summarizes the layer thicknesses. The cross section was subdivided into three components (i.e upper slide, middle slide and

lower slide) by vertical lines IJ and KL, in Figure 5.3. This is for the purpose of the assessment of stability which will be discussed in detail in the forthcoming sections.

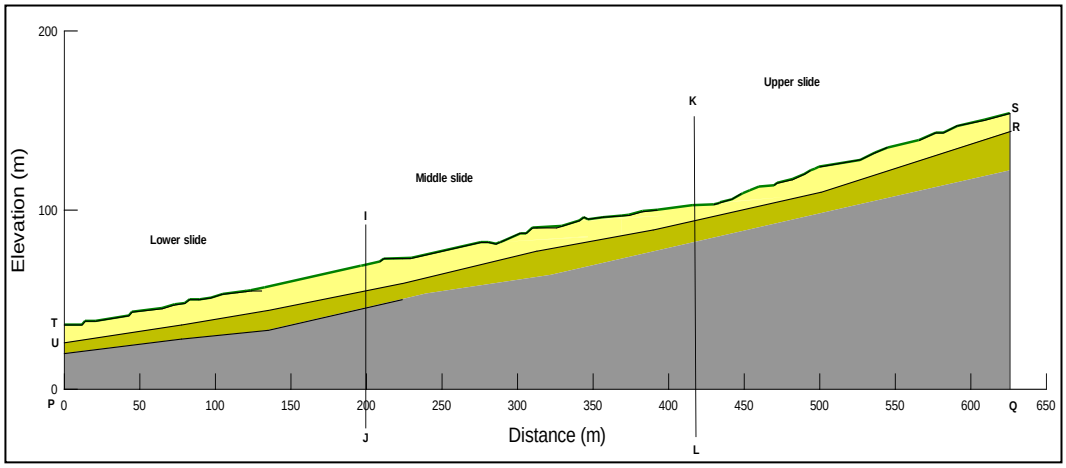

Figure 5.3 Cross section idealized in SEEP/W

Table 5:2: details of the subsoil /rock layers drawn in SEEP/W

Layer	Notation	Thickness range (m)
Colluvium layer		10 - 20
Completely to highly weathered rock		10 - 20
Highly to moderately weathered rock		Over 15

5.4.1 Boundary conditions

Figure 5.4 shows the hydraulic boundary conditions assigned to the model at the initial stage when no drains are installed and Table 5.3 summarizes details of the same.

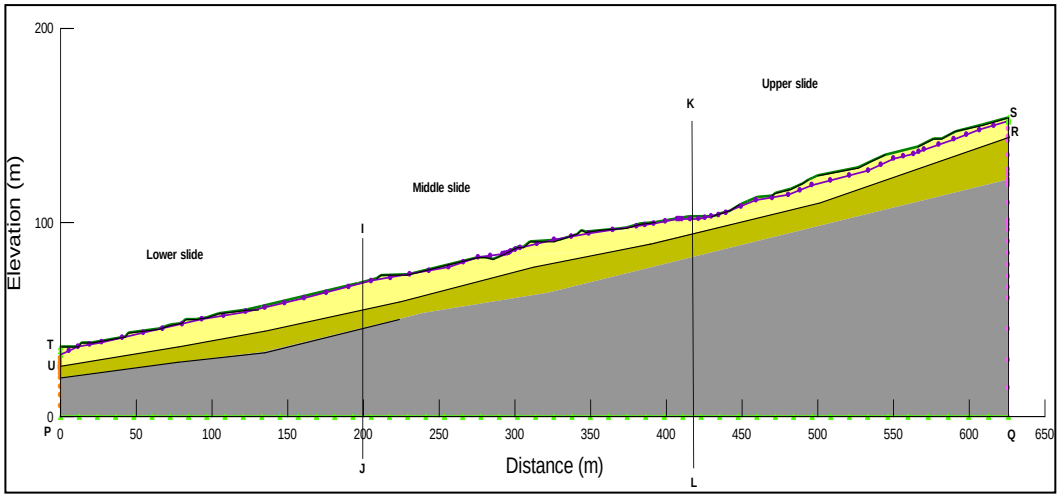

Figure 5.4 Model showing the assigned boundary conditions

Table 5:3: Description of the boundary conditions assigned

Boundary condition	**Type**	**Value**
PQ, RS, TU	Total flux	0 m^3s^{-1}
PU, QR	Total head	Height of the sides

5.5 Initial ground water table condition of the slope (prevailing condition)

An initial seepage analysis was conducted to set up the pore pressure profile of the site. For this analysis ground water table was assumed to be present at a depth of around 1 – 2 m below the existing ground level. The main reasons behind adopting a high ground water table for the analysis are; perched water table conditions observed at the site, indications of high ground water table in boreholes during rainy periods and excessive movements indicated in the monitoring instruments during heavy rainfall events. For example, the ground water table was encountered at 2.5 m below the ground level in BB 05 (refer section 3.8). The purple colour line in Figure 5.5 indicates the ground water table.

5.5.1 Initial pore water pressure profile derived from the ground water flow analysis

The steady state pore water pressure profile of the slope, derived from the steady state seepage analysis under the conditions discussed above, is presented in Figure 5.5.

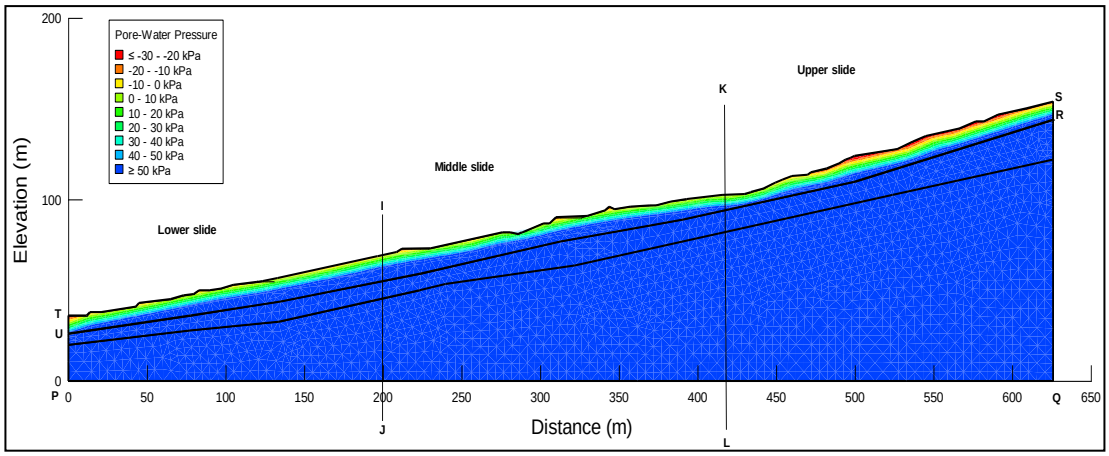

Figure 5.5 Variation of pore water pressure profile of the slope

The blue colour shading indicates the positive pore water pressures below the ground water table. Yellow to orange colour shadings indicate the matric suction profile generated through the seepage analysis. The results from the initial steady state seepage analysis was taken as the input to transient seepage analysis, simulated for different weather and groundwater conditions, as described in the succeeding sections.

5.6 Stability of the slope with high ground water table condition

The stability of the slope section was analyzed using the SLOPE/W module available in the GeoStudio 2012 software. The software is based on a limit equilibrium formulation for stability analysis and yields a FoS for the slope based on a specified method of slices. A coincise review of the limit equilibrium analysis is included in Chapter 2. These analyses were done using the Spencer's method which is regarded to possess a very accurate formulation.

The same cross section A1 – A2 was used to analyze the stability of the slope. Material properties used in slope stability analysis are presented in Table 5.4. These properties were deduced based on the lithological description of the soils encountered in boreholes, SPT N values, laboratory test results and local experience on similar sites. These values are quite different from those used in the study done by JICA reported in Chapter 3.

Table 5:4: Material properties assigned for stability analysis

Formation	Colour	Cohesion (kPa)	Friction angle (deg)	Unit weight (kN /m^3)
1.Colluvium		2	22	15
2.Completely to highly weathered rock		8	35	16
3.Highly to moderately weathered rock		20	40	17

5.6.1 Definition of the slip surfaces

SLOPE/W module possesses several methods to define the slip surface, namely entry and exit, grid and radius, fully specified and block specified. The applicability of each method depends on the nature of the problem to be addressed and the data in hand. In the case of Badulusirigama landslide, location and the extent of the slip surface was confirmed by means of comprehensive site investigation and monitoring programme. Hence, the fully specified slip surface definition, which enable the user to fully define the sliding surface, was adopted. Accordingly, the slip surfaces identified at the site during the preliminary investigations and monitoring (Section 3.8) were pre-defined in the SLOPE /W module. The cross section A1 – A2 is reproduced in Figure 5.6 incorporating the fully specified failure

surfaces used for stability analysis. The analysis was carried out using Spencer's method, which accounts for both force and moment equilibrium.

The lines marked as S1 - S2, S3 - S5 and S4 - S5 indicate the slip surfaces corresponding to each slide. Point O is the point about which the software computes the moment equilibrium.

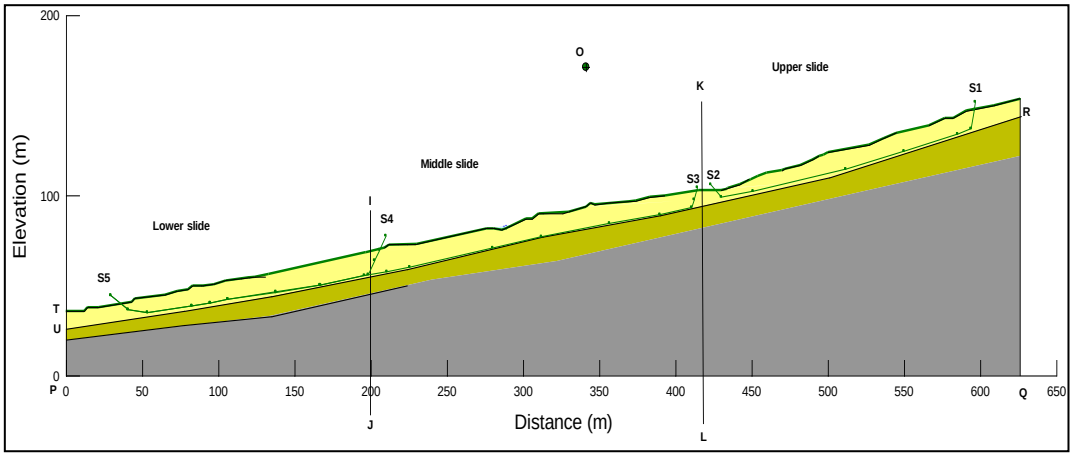

Figure 5.6 The slip surfaces of each slide are fully defined in SLOPE/W module

5.6.2 Results of the stability analysis for prevailing conditions

Table 5.5 summarizes the safety margins obtained for each slip surface. Figures 5.7, 5.8 and 5.9 presents the slip surfaces and the factor of safety values pertinent to each slip surface.

Table 5:5: Factor of safety values for prevailing conditions

Slide	Factor of safety
1. Upper	1.03
2. Middle	1.08
3. Lower	1.10

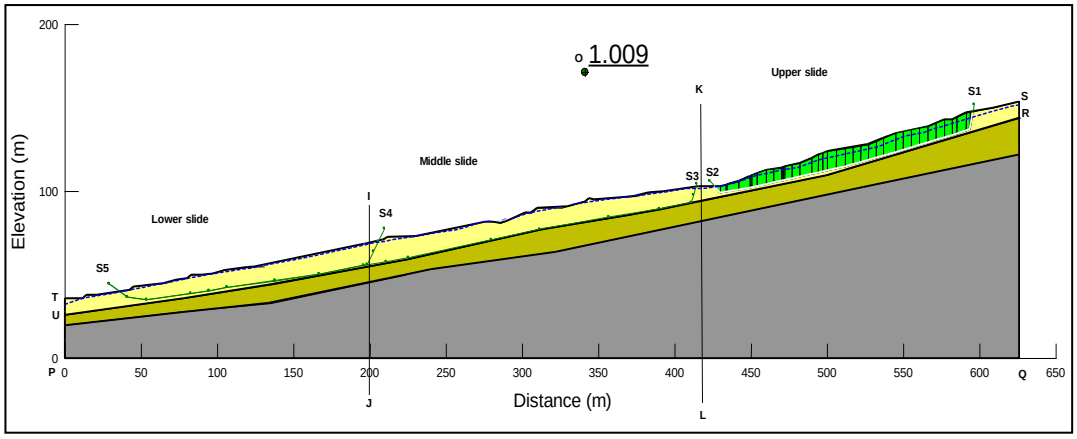

Figure 5.7 Safety margins of the upper slide

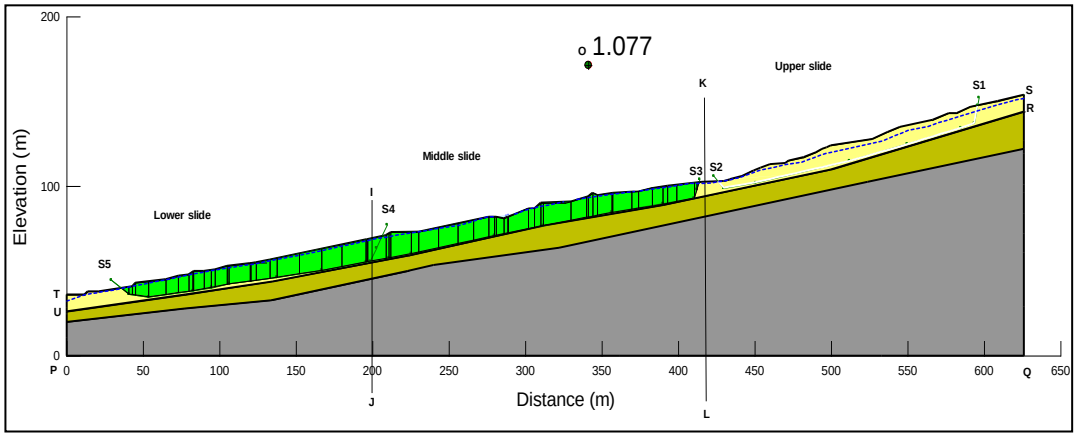

Figure 5.8 Safety margins of the middle slide

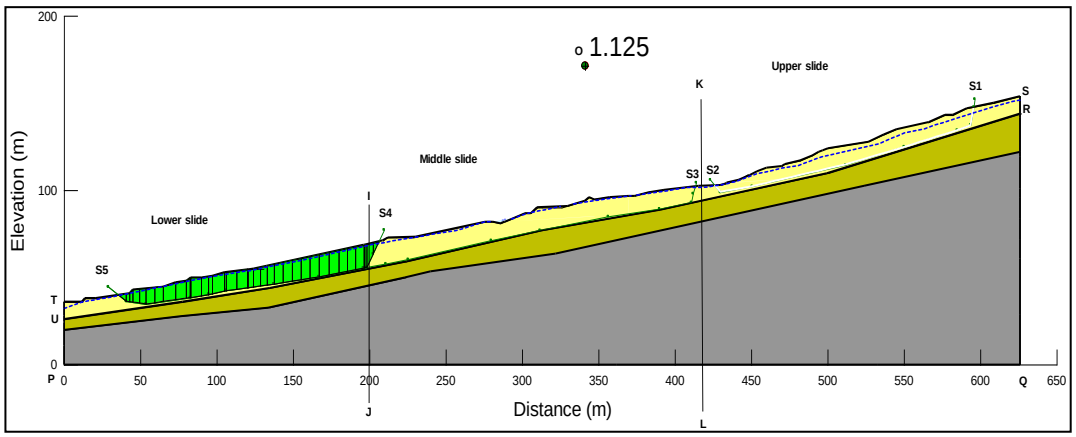

Figure 5.9 Safety margins of the lower slide

5.7 Modelling the effectiveness of rectification measures

5.7.1 Subsurface drainage improvement

The prime activity in enhancing the stability of the slope was to improve the drainage measures. This section examines the effectiveness of subsurface drainage improvement in enhancing slope stability. A substantial description on the subsurface drainage improvements done at the site has been given in Chapter 3 under the Section 3.10.1.Table 5.6 presents an outline of the implemented drainage network.

Table 5:6: Summary of the subsurface drains constructed at the site

Drainage fan	Elevation (mSL)	No. of drains in the fan	Length of a drain (m)	Diameter of a drain (mm)	Angle (deg)	
					In horizontal plane	Between two drains
A	710	8	45	100	5	10
B	704	8	45	100	5	10
C	690	8	45	100	3	10
D	682	9	60	100	3	10
E	662	9	60	100	3	10
F	651	9	55	100	3	10

5.7.2 Simulation of subsurface drainage improvement in two dimensional plain strain formation

Drains were simulated as lines in the SEEP/W model as shown in Figure 5.10. The ‘Seepage” boundary condition option available in SEEP/W module was used for

the sub-horizontal drains. When this boundary condition is used, the software initially assigns zero flux boundary condition at each drain and then reviews by the maximum pressure. Thus, if the calculated pressures at the drain nodes are greater than zero, solver automatically sets the nodal pressure values to zero. In other words, the total heads at the nodes are always kept equal to respective elevation head. This type of boundary condition permits the water out from the system if the pressures in the surrounding are positive or zero. Furthermore, this boundary condition does not allow the draining out of water in case of pressures in the surrounding are negative. Therefore, the drain would not become a source of water when the surrounding soil is unsaturated. This allows for the possibility of water table drop below the level of the drains during longer dry periods, representing the condition that would occur naturally. The subsurface drainage configuration of the slope is presented in Figure 5.10.

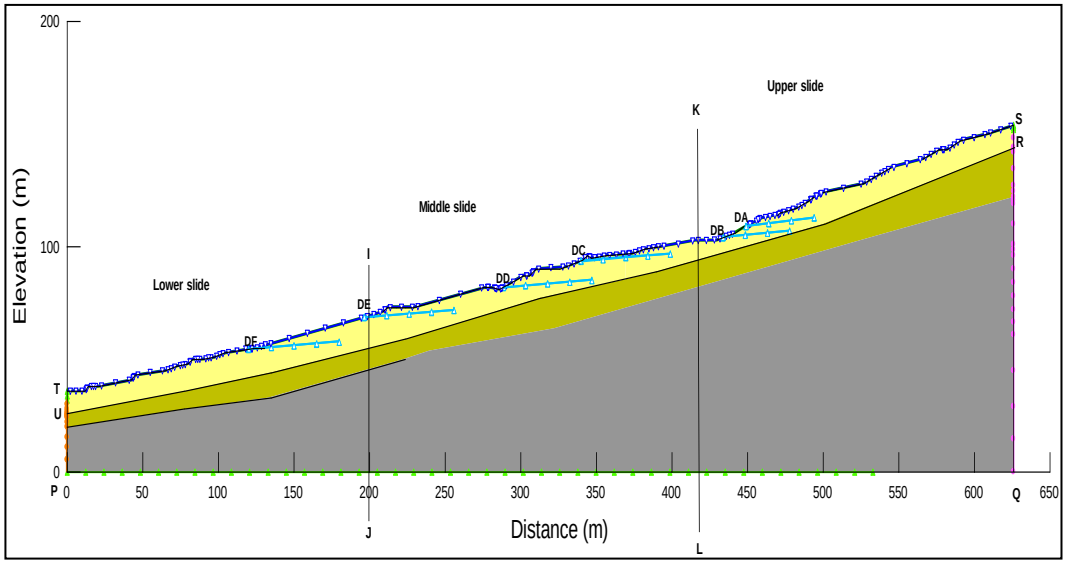

Figure 5.10 Drains simulated in the section A1 - A2

Drains representing the drainage fans A to F have been illustrated as DA to DF respectively in the Figure 5.10. Table 5.7 shows the details of the drains in the section. It is admitted that this is a simplification of the actual three dimensional situation at the site.

Table 5:7: Details of the drains simulated in Figure 5.10

Drain (D)	Length (m)	Inclination (deg)
DA	45	5
DB	45	5
DC	45	3
DD	60	3
DE	60	3
DF	55	3

5.7.3 Transient seepage analysis of the slope after drainage improvement

After implementing the sub-horizontal drains in the model, a transient seepage analyses were conducted for three cases as outlined here to investigate the effect of the drain construction sequence on the stability improvement of the slope. The three cases are:

Case 1: Simulating all six drains simultaneously

Case 2: Simulating top – down construction of drains

Case 3: Simulating bottom – up construction of drains

Table 5.8 summarizes the sequence of construction of subsurface drains under the three cases considered. When analyzing Cases 2 and 3 above, a time gap of 3 days was allowed prior to activation of the following drain to simulate the construction time required.

Table 5:8: Summary of drain installation sequence under each case considered

Day of installation of drains	Case 1	Case 2	Case 3
At the start	All drains	A	F
After 03 days	-	A,B	F,E
After 06 days	-	A,B,C	F,E,D
After 09 days	-	A,B,CD	F,E,D,C
After 12 days	-	A,B,C,D,E	F,E,D,CB
After 15 days	-	A,B,C,D,E,F	F,E,D,C,B,A

Pore water pressures profile deduced from the initial steady state analysis (Section 5.4) was used as the initial conditions for first transient analysis conducted under each case (i.e. at the start). The analysis stages in each Case were linked linearly, so that the pore water pressure conditions of the last stage is referred to set up the pore water pressure profile for the beginning of the following stage, during Case 2 and 3.

The transient analysis was set to continue for further 30 days after the date of installation of the final drain. Accordingly, the total time duration for each case was 48 days. The reason for extending the analysis for further time steps is to observe the temporal variation of the pore pressures, flow rates through drains as well as behaviour of the overall slope in terms of stability. No infiltration conditions were simulated during the period of analysis.

5.7.3.1 Flow rate through horizontal drains

SEEP/W module facilitates the computation of the total flux within a pre-defined section. This facility can be used to obtain the inflow to the drains. The flux can be obtained either using the concept of flux sections or accumulating the total nodal flux associated with the element of interest (i.e. drain). In this study, nodal flux

values corresponding to each drain region were plotted to identify the flux from the surrounding soil into subsurface drains.

Figures 5.11, 5.12 and 5.13 illustrate the variation of flux rate through drains for the Cases 1, 2 and 3, respectively.

In all the three cases, a maximum initial flow rate is reported by Drain-D (DD) which is at the mid-level of the slope. The initial flow rate of DD is about 29, 24 and 27 m^3/ day for Cases 1, 2 and 3, respectively. The second highest initial flow rate is observed in Drain-F (DF) which is at the toe of the slope, for all the three cases. In general terms drains in the toe area of the slope have higher initial flow rates than the drains in the top area of the slope. When compared the latter two cases (i.e. 2 and 3), which is the most likely practical approach of construction, drains at the lower regions of the slope have taken a slightly longer time durations to reach the steady flow rates. Furthermore, steady flow rates of drains at the bottom region of the slope are bit higher than that of drains in the top region. According to Figure 5.12, drains simulated in top down construction sequence (Case 2) have taken about 26 – 28 days to reach the steady flow rates. Whereas in bottom up construction sequence, drains have achieved steady flow rates within about 18 days (Figure 5.13). Also, the initial flow rate of the bottom most drain (Drain-F) is the same for both the cases (around 17 m^3/day) and it has the second highest flow rate in both the cases. This suggests that the bottom drains are the most effective in attracting water from the slope body. This should be compared with Table 5.9 and 5.10 where the improvement of FOS with time as the drainage occurs is presented.

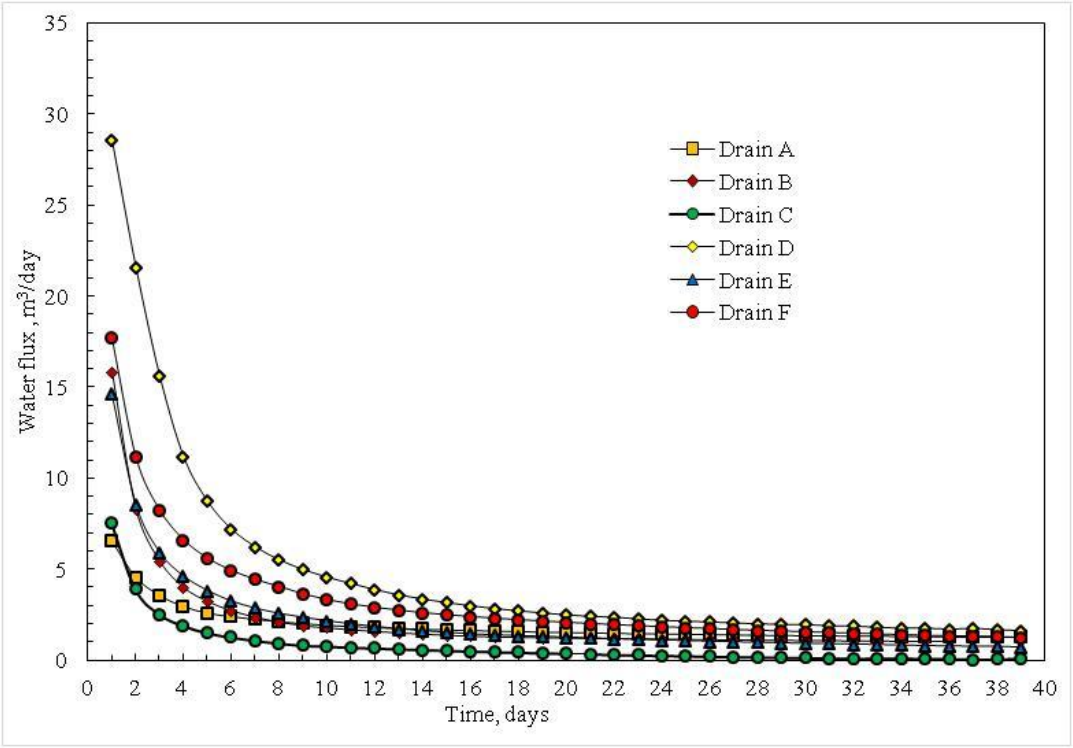

Figure 5.11 Variation of flux rate through drains for Case 1

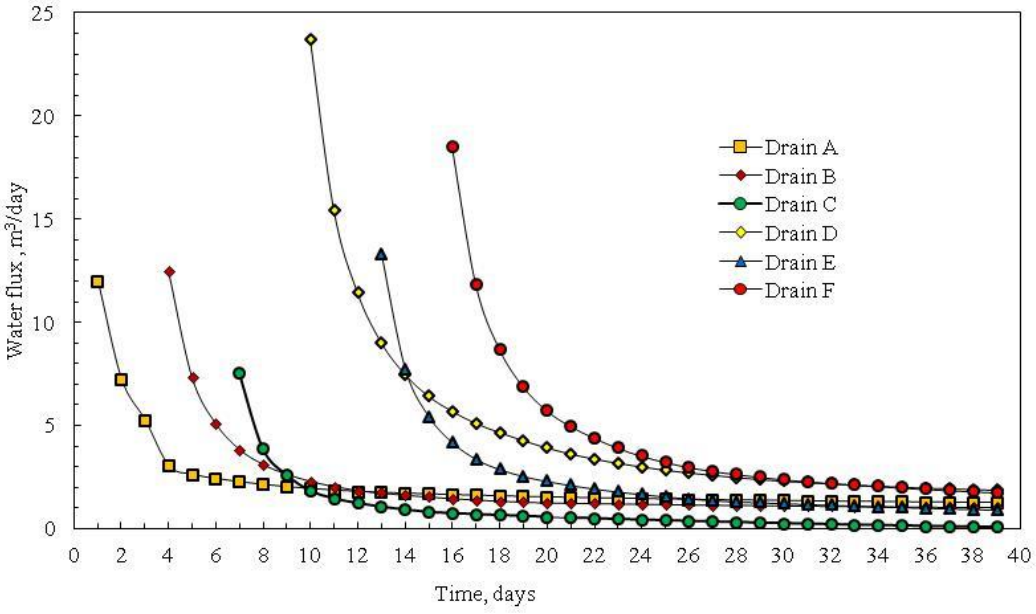

Figure 5.12 Comparison of the water flux into the drains for Case 2

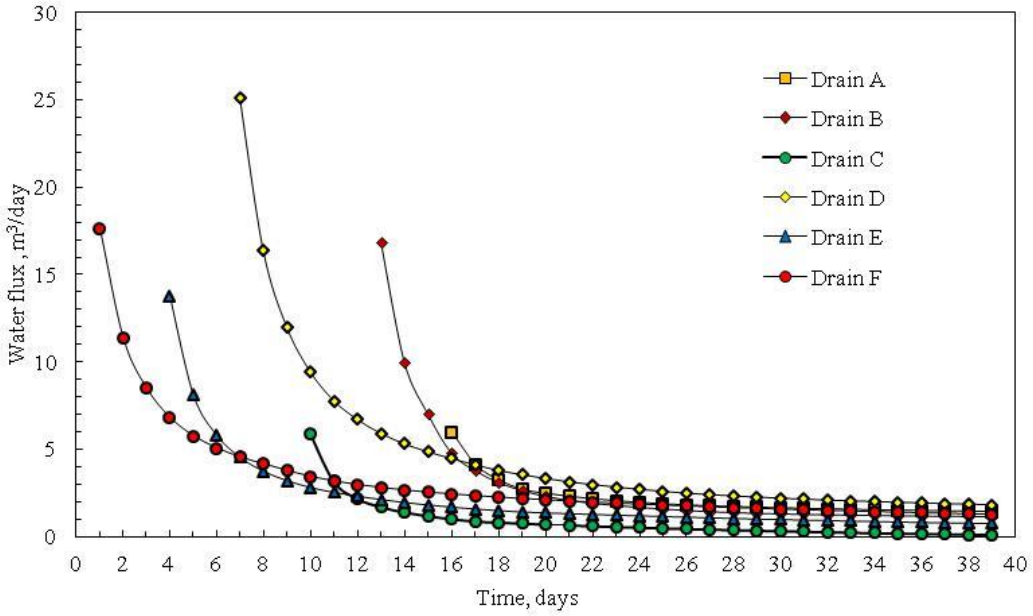

Figure 5.13 Comparison of the water flux into the drains for Case 3

5.7.3.2 Variation of the factor of safety of the slope

Variation of the factor of safety of the three slides with the time, after the sequential installation of the drains was studied. Figure 5.14, 5.15 presents the daily increase of the FoS with the installation of drains in two sequential construction processes Case 2 and Case 3. Figure 5.16 and 5.17 relates this to the installation of each drain and present it in the form of a percentage increase with respect to its initial FoS. Table 5.9 and 5.10 summarize the progressive percentage increase of factor of safety of each slide under the simulated construction sequences (i.e. Case 2 and Case 3).

A key feature to note is that the achieved final FoS by either construction sequence is the same for the respective slides. The difference is in the rate at it is achieved. This will give guidance on the most time efficient way to achieve the improvement on the way to the final result. This feature presented in Figure 5.16 and 5.17 is further elaborated in the proceeding sections.

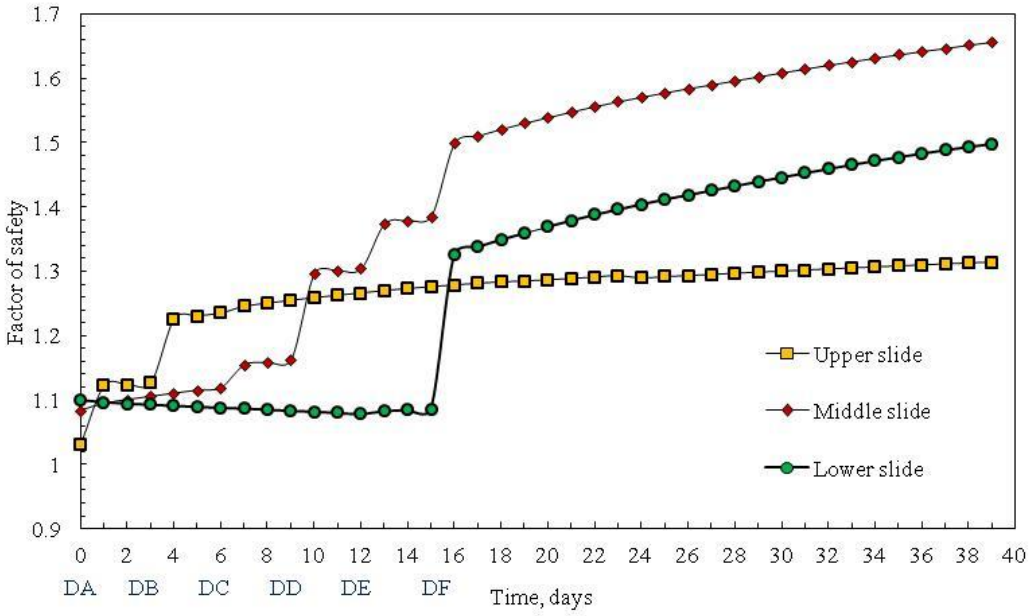

Figure 5.14 Variation of factor of safety of three slides under Case 2

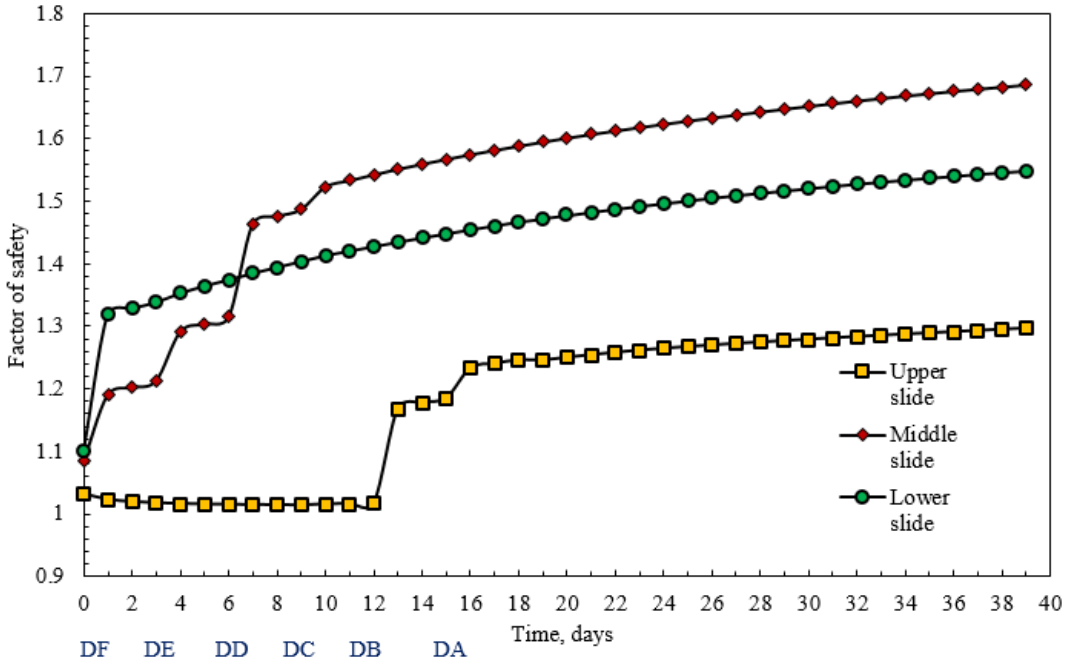

Figure 5.15 Variation of factor of safety of three slides in Case 3

Table 5:9: Percentage Improvement of factor of safety after drainage improvement under Case 2

Drainage improvement (Elapsed time, days)	Upper slide (F_{int}=1.03)			Middle slide (F_{int}=1.08)			Lower slide (F_{int}=1.10)		
	value	$\left(\frac{F_i - F_{i-1}}{F_{i-1}}\right)\%$	$\left(\frac{F_i - F_{int}}{F_{int}}\right)\%$	value	$\left(\frac{F_i - F_{i-1}}{F_{i-1}}\right)\%$	$\left(\frac{F_i - F_{int}}{F_{int}}\right)\%$	value	$\left(\frac{F_i - F_{i-1}}{F_{int}}\right)\%$	$\left(\frac{F_i - F_{int}}{F_{int}}\right)\%$
A (03)	1.13	9.2	9.20	1.11	2.0	2.0	1.09	-0.7	-0.7
AB(06)	1.24	9.7	19.7	1.12	1.2	3.2	1.09	-0.4	-1.1
ABC (09)	1.26	1.6	21.7	1.16	3.8	7.2	1.08	-0.4	-1.5
ABCD(12)	1.27	0.9	22.7	1.30	12.2	20.3	1.08	-0.5	-2.0
ABCDE(15)	1.28	0.8	23.7	1.39	6.2	27.8	1.09	0.7	-1.3
ABCDEF(18)	1.28	0.6	24.4	1.52	9.8	40.3	1.35	24.2	22.6

F_{int} = initial factor of safety of the slide

F_i = factor of safety at the i[th] stage

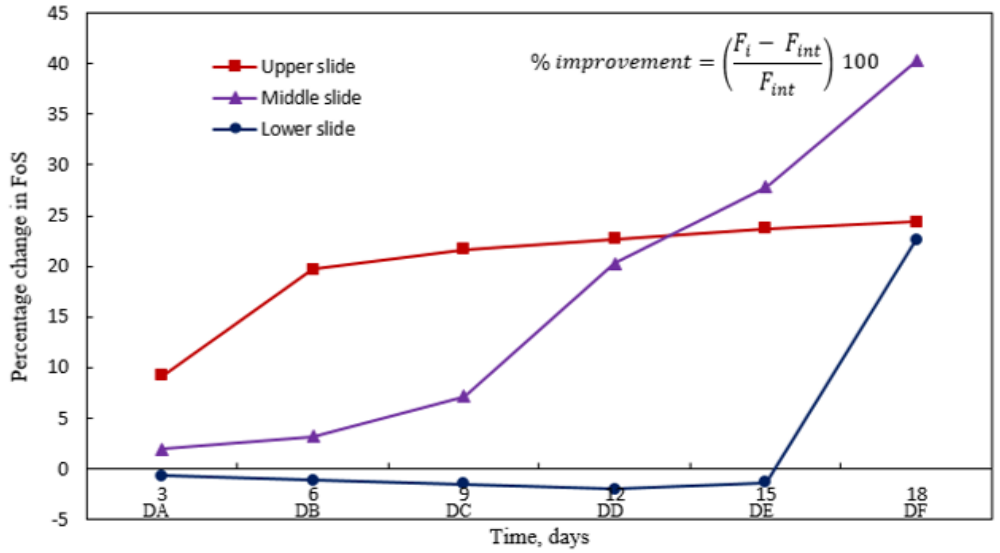

Figure 5.16 Percentage improvement in factor of safety of each slide with sequential construction under Case 2

Table 5:10: Variation of factor of safety after drainage improvement under Case 3

Drainage improvement (Elapsed time days)	Upper slide (F_{int}=1.03)			Middle slide (F_{int}=1.08)			Lower slide (F_{int}=1.10)		
	value	$\left(\frac{F_i - F_{i-1}}{F_{i-1}}\right)\%$	$\left(\frac{F_i - F_{int}}{F_{int}}\right)\%$	value	$\left(\frac{F_i - F_{i-1}}{F_{i-1}}\right)\%$	$\left(\frac{F_i - F_{int}}{F_{int}}\right)\%$	value	$\left(\frac{F_i - F_{i-1}}{F_{int}}\right)\%$	$\left(\frac{F_i - F_{int}}{F_{int}}\right)\%$
F (03)	1.02	-1.4	-1.4	1.21	11.9	11.9	1.34	21.	21.6
FE(06)	1.01	-0.2	-1.7	1.32	8.4	21.3	1.37	2.7	24.9
FED(09)	1.01	-0.1	-1.7	1.49	13.1	37.2	1.40	2.1	27.6
FEDC(12)	1.02	0.3	-1.5	1.54	3.7	42.3	1.43	1.7	29.7
FEDCB(15)	1.18	16.6	14.9	1.57	1.6	44.6	1.45	1.4	31.6
FEDCBA(18)	1.25	5.1	20.8	1.59	1.3	46.5	1.47	1.3	33.3

F_{int} = initial factor of safety of the slide

F_i = factor of safety at the ith stage

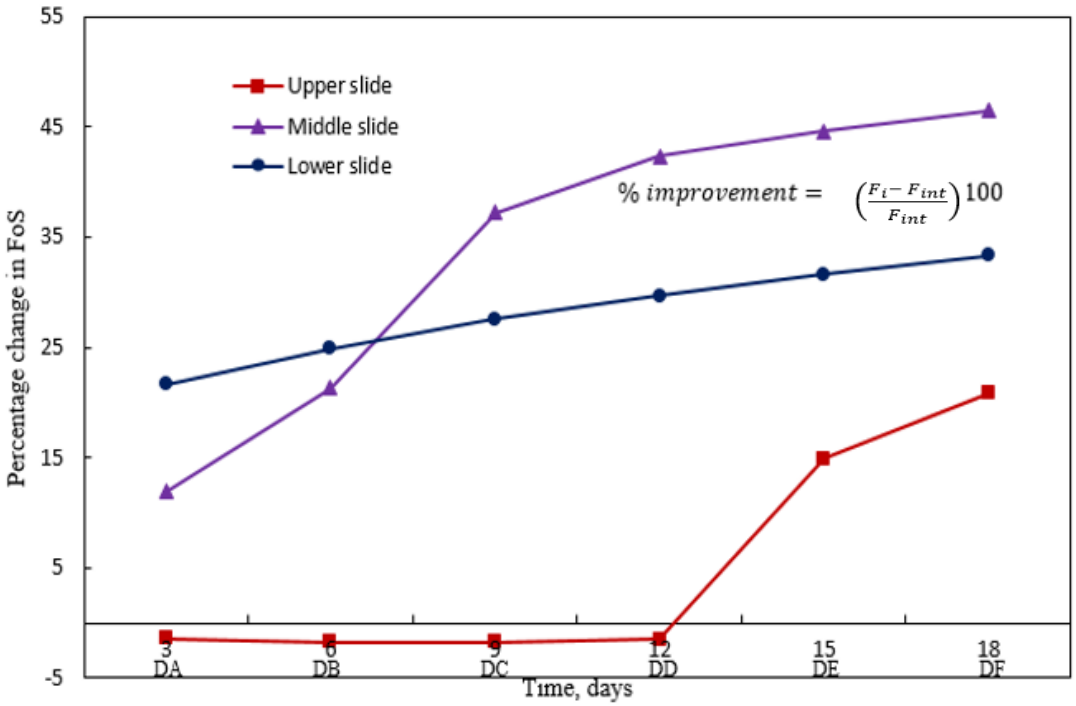

Figure 5.17 Percentage Improvement in factor of safety of each slide under sequential construction in Case 3

Factor of safety improvement under installation sequence - Case 2

As shown by Figure 5.16, a noticeable improvement of the factor of safety of the upper slide could be observed after the installation of Drain-A (DA) (i.e. from 1.0 to 1.1; 10%) pertaining to construction sequence Case 02, Safety margins have further increased to 1.2 since the installation of Drain-B (DB). Thereafter the installation of successive drains did not have a significant impact on factor of safety of the upper slide; only a little improvement has gained with the time. In contrast, installation of first three drains does not significantly contribute to enhance the factor of safety values of middle and lower slides. Factor of safety of the middle slide has increased from 1.15 to 1.30 (13 %) after the installation of DD. Further around 5 % and 20 % increments in the factor of safety value can be seen corresponding to installation of the next two drains (i.e. DE and DF). Figure 5.16 also indicates that the factor of safety of the lower slide has not increased during the installation of the first five drains. On the contrary, a slight decrease in the factor of safety can be traced, within the period of first 15 days. With the installation of the final drain DF, factor of safety of the lower slide has gained a significant improvement by about 20%, which is indicated by the rise of the graph from around 1.1 to 1.3.

Factor of safety improvement under installation sequence - Case 3

Figure 5.17 illustrates the variation of factor of safety values of the three slides under bottom up sequence of drain construction (i.e. Case 3). Lower slide has gained a factor of safety improvement of about 19% since the installation of DF. Thereon, factor of safety of the lower slide increases at a uniform rate with the installation of rest of the drains. However, a factor of safety value of above 1.4 has gained since the installation of DC. Meantime installation of drain DF caused a 10% enhancement of the factor of safety of middle slide. Rapid improvements of the factor of safety values are noticeable in the middle slide, soon after the installation of DE and DD. Factor of safety has been improved from 1.2 to almost 1.3, and 1.31 to 1.46 (i.e. 8.3% and 11.4%) after the installation of DE and DD, respectively. The factor of safety value of the upper slide has gained a significant

improvement only after the installation of DB. During the installation of four previous drains DF, DE and DD, factor of safety of the upper slide has increased slightly.

As displayed by Figures 5.16 and 5.17 the rate of increase in factor of safety is comparatively faster under construction sequence of Case 3 (i.e. bottom up construction). Both lower and middle slides have obtained significant improvements in factor of safety after 9 days (Figure 5.17), when bottom up construction procedure was followed. It is explicit that the highest percentage improvement in factor of safety of each slide (upper, middle and lower) has been gained immediately after the construction of toe drain for the respective slide. To sum up, these observations emphasize the importance of relative location of the drains in draining out water and improving the stability of slope within the least possible time period.

5.7.4 Performance of the rectified slope with subsurface drainage system during a typical rainfall event

An actual critical rainfall event (the most critical rainfall event since the installation of the monitoring system) occurred during the period of 01st of December 2014 to 31st of December 2014 (Section 3.4) was applied on the slope to investigate the performance of the subsurface drainage measures, during a subsequent critical rainfall. Rainfall event was simulated as a unit flux boundary condition, varying with time.

First, the transient analysis carried out for Case 3 was continued for some additional time period without any rainfall, until the pore water pressures stabilize. That is; until there were no significant variations occurred in the pore water pressure profile in between subsequent time steps. Results were saved after each time step and pore water pressure information of each time step was inspected to decide the termination criteria. The phreatic surface after 30 days from the completion of installation of drains appeared to be present below the level of the bottom most drain (DF). Consequently, the shallow depths of the slope (i.e above the drain level)

had become unsaturated and presence of negative pore water pressures was noted in the slope profile.

The most critical rainfall event applied on the slope is presented in Figure 5.18. Figures 5.19 presents the FoS values obtained in the three slides after the critical rainfall event.

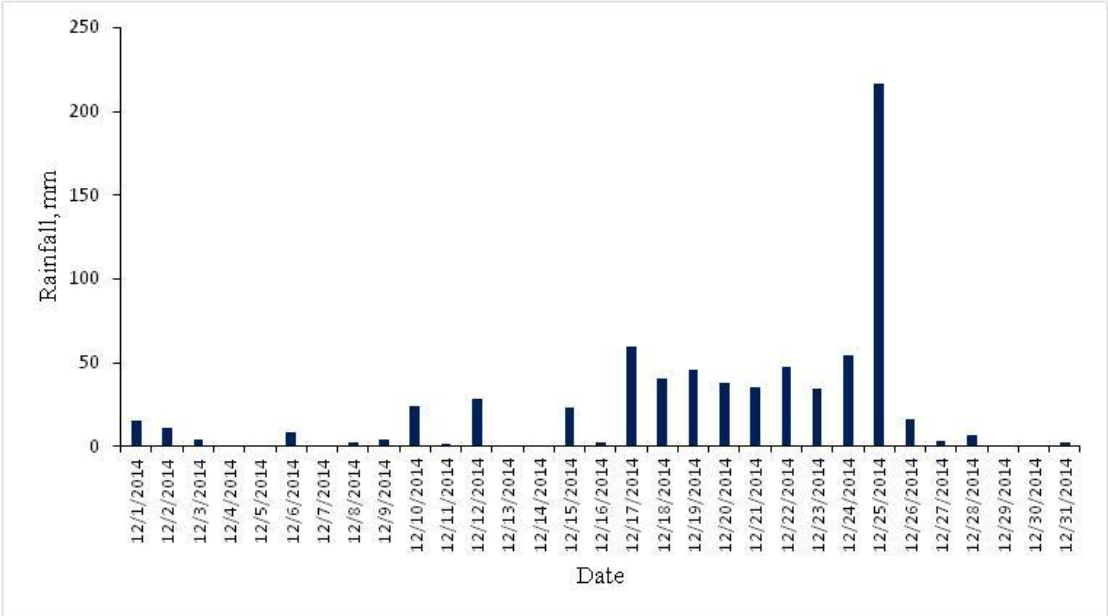

Figure 5.18 Rainfall event from 1st December to 31st December 2014

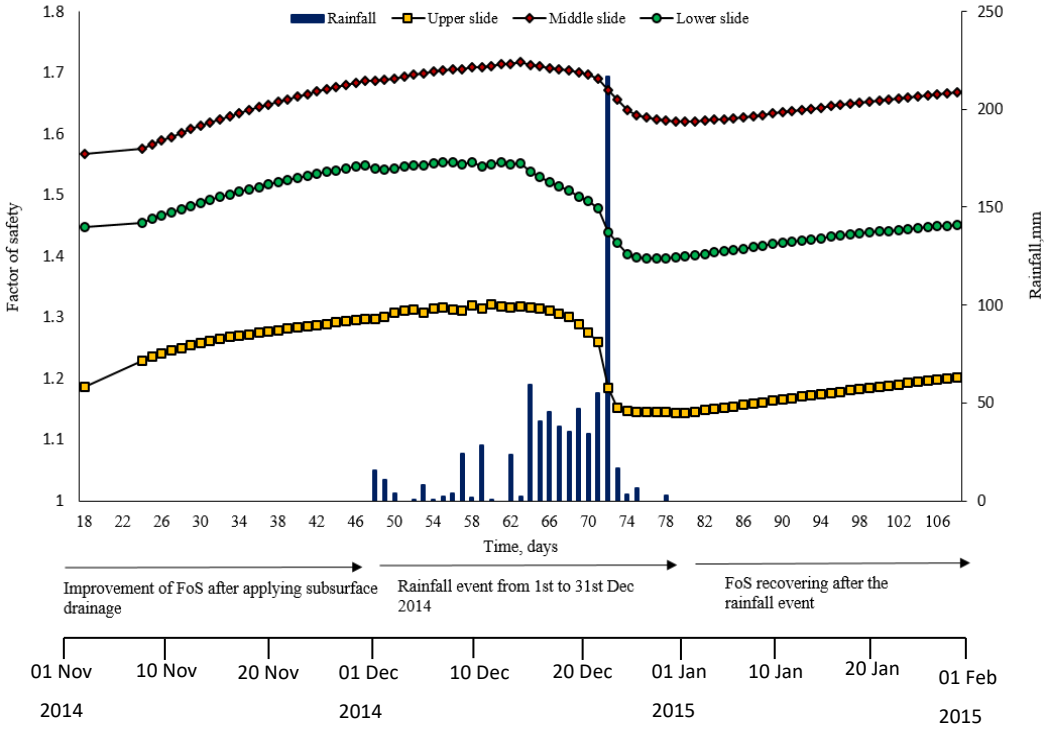

Figure 5.19 Variation of factor of safety of the upper slide after subsurface drainage improvement due a critical rainfall event

As illustrated in Figure 5.19 factor of safety of all three slides remains more or less unaltered until the rainfall event on 17th December 2014 occurs. After antecedent rainfall events of less than 30 mm, the site area has experienced a major rainfall of about 60 mm. Some consecutive rainfall events have occurred following the event on 17th December. Factor of safety values have started to decrease after the rainfall event on 17th December. The rate of decrease in factor of safety is almost same for the top two slides, and was comparatively high for the lower slide. After the critical rainfall event of 216 mm on 25th December 2014, factor of safety values have significantly decreased. Still the percentage reduction of factor of safety for all three slides is below 10. Factor of safety of the upper slide after the rainfall event on 25th December 2014 has reduced to 1.15, which was 1.25 before the rainfall event.

Factor of safety values of all the slides tend to increase after the cessation of the rainfall event on 25th December 2014 despite the occurrence of some minor rainfall events. However, the rate of factor of safety gain after the total rainfall event of 30

days was slower when compared to the rate of factor of safety improvement immediately after the application of subsurface drainage measures. The gradual increment of the FoS of the slope with time in the absence of any rainfall is due to draining out of groundwater along the slope, naturally facilitated by the drains installed.

5.8 Analysis of the composite slip surface

Another set of analyses were conducted to investigate the safety margins of a possible composite failure surface that combines the three failure surfaces. The three slip surfaces were identified at the site, based on the tension cracks observed at the surface, that separates the slides from one another. However, it is also possible that the three slides moved together through the common rupture surface present at the interface between weak, moderately weathered rock and the relatively strong highly weathered material. This will form one long sliding mass that starts from the upper area of the slope and ends at the toe of the slope.

Block specified slip surface definition was adopted to define the composite failure surface in the SLOPE/W software. In this method, slip surface is defined using three linear segments. The slip surfaces within the failure mass are established using the two grids defined at the toe and crest areas of the side. These lines are then extended according to the specified angles and their incremental variations to establish the ground surface intersection points at toe and the crest. When defining the slip surface for this particular composite slip surface, two grid blocks were drawn within the soil mass, encompassing the potential intersecting points of three line segments, identified from filed investigation data. Figure 5.20 illustrates the definition of the composite slip surface in section A1- A2.

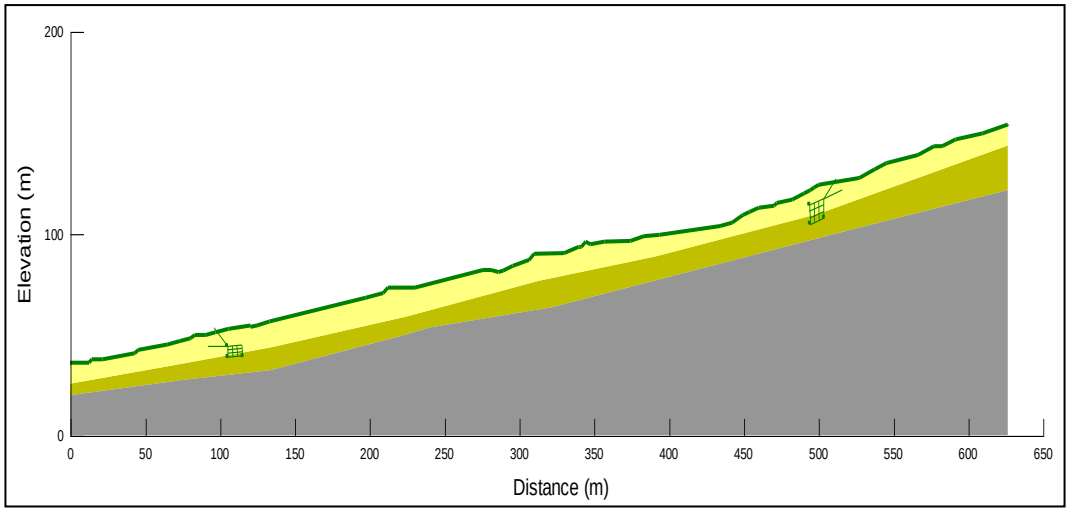

Figure 5.20 Definition of the composite slip surface using block specified method

Initially the stability of the composite slip surface under exiting high ground water table conditions was assessed. Figure 5.21 illustrates the composite slip surface with the lowest factor of safety, generated by the software in accordance with the defined blocks of grids. The resulting composite slip surface is quite similar to an integrated slip formed by three individual slip surfaces discussed in the previous sections. This has a FOS of 1.068 indicating closeness to failure.

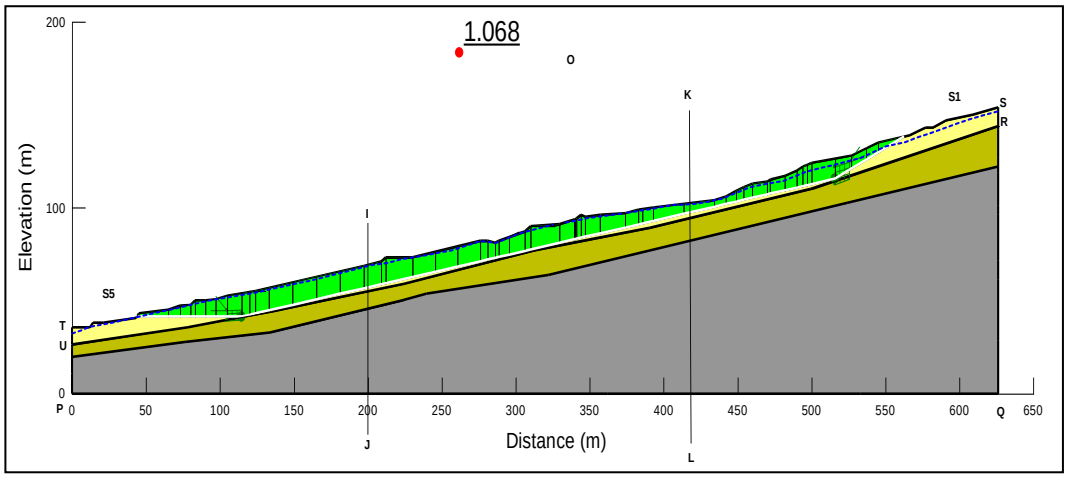

Figure 5.21 Factor of safety of the composite slip surface under existing conditions

5.8.1 Improvement of stability along the composite slip surface with the installation of subsurface drainage measures

Improvement of stability of the composite slip surface with the installation of sub surface drains under the sequences Case 2 and 3 was studied. When assessing the stability of the composite slip at each construction stage, the factor of safety value corresponding to the most critical slip was selected. Table 5.11 presents the variation of Factor of safety under each case considered. The improvement of the FOS with the sequential installation of drains is graphically presented in Figure 5.22. The percentage increase at each stage is also presented there.

Table 5:11: Variation of factor of safety of the composite slip under Case 2 and Case 3

Case 2 (F_{int}=1.07)				Case 3 (F_{int}=1.07)			
Drainage improvement (Elapsed time)	value	$\left(\frac{F_i - F_{i-1}}{F_{i-1}}\right)\%$	$\left(\frac{F_i - F_{int}}{F_{int}}\right)\%$	Drainage improvement (Elapsed time)	value	$\left(\frac{F_i - F_{i-1}}{F_{i-1}}\right)\%$	$\left(\frac{F_i - F_{int}}{F_{int}}\right)\%$
A(03)	1.082	1.31	1.31	F (03)	1.116	4.49	4.49
AB(0)6	1.146	5.91	7.30	FE(06)	1.176	5.38	10.11
ABC(09)	1.149	0.26	7.58	FED(09)	1.298	10.37	21.54
ABCD(12)	1.271	10.62	19.01	FEDC(12)	1.339	3.16	25.37
ABCDE(15)	1.346	5.90	26.03	FEDCB(15)	1.44	7.54	34.83
ABCDEF(18)	1.44	6.98	34.83	FEDCBA(18)	1.476	2.50	38.20
ABCDEF(1mon)	1.557	8.13	45.79	FEDCBA(1mon)	1.578	6.91	47.75
ABCDEF (3mons)	1.679	7.84	57.21	FEDCBA (3mons)	1.688	6.97	58.05

Again the proportion of factor of safety improvement is rapid when the drains are constructed in bottom up sequence. As per the graph (Figure 5.22), improvement in factor of safety after 18 days period compared to initial safety factor, is 38% for

Case 3 and only 35% for Case 2. The factor of safety obtained after a period of 30 days of construction is 1.56 (gain of 46%) and 1.58 (gain of 48%) for Case 2 and 3, respectively. After a period of about 90 days (3 months) since the completion of the construction of drains, factor of safety achieved under both the construction sequences (i.e. Case 2 and Case 3) has become similar; which is indicated by 57.2% and 58% improvement in FoS compared to initial FoS for Case 2 and 3 respectively.

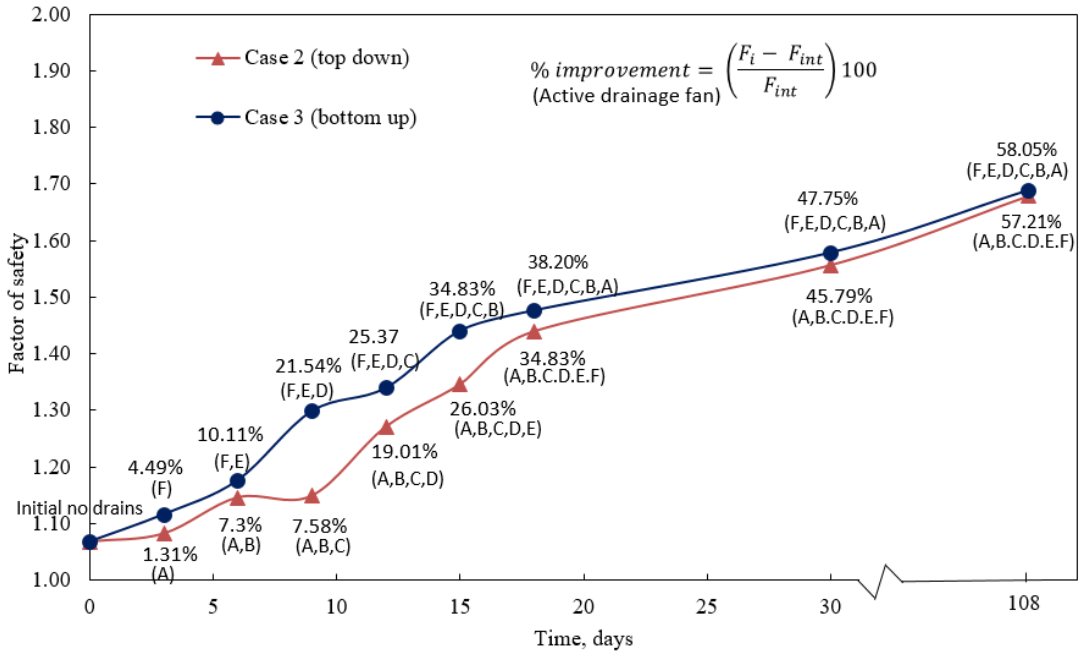

Figure 5.22 Variation of factor of safety of the composite slip surface under Case 2 & 3

Figure 5.23 (a) & (b) show the pore water pressure distribution wthin the colluvium soil layer, through the selected cross sections IJ and KL (Figure 5.21) before and one month after the competetion of installation of subsurface drains, respectively.

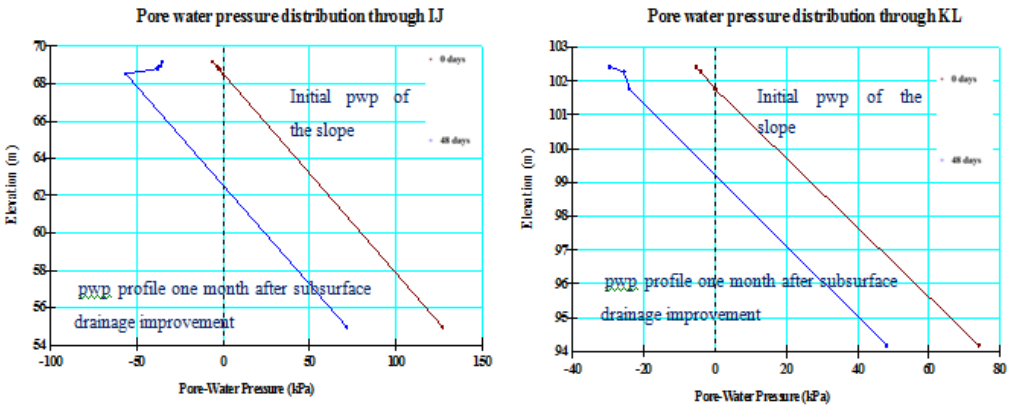

(a) (b)

Figure 5.23 Variation of the pore water pressure profile before and after subsurface drainage improvements: (a) Section IJ, (b) Section KL

Significant reuction in pore water pressures can be observered in both toe (Section IJ) and middle of the slope (Section KL). Phreatic surface has been dropped by 6.0 m in the toe of the slope and by 3.0 m at the middle of the slope, one month after completion of subsurface drainage installation.

5.8.1.1 Response of the composite slip to a typical rainfall event after rectification by installation of subsurface drainage network

The actual critical rainfall event discussed under section 5.7.4 was applied into the slope with the composite slip surface, to find out the ability of the drainage system to ensure the stability of the slope against that mode of failure. Figure 5.24 shows the factor of safety variation of the slope during the rainfall event. The improving factor of safety even during the rainfall event indicates that the rainfall events from day 49 to day 65 have no influence on the safety margins of the slope. Factor of safety starts to drop after the 50 mm rainfall on 65th day. Minimum factor of safety after the rectification measures has been recorded on the 79th day, which is six days after 215 mm rainfall event on day 73. Nevertheless, the safety margins of the slope is still well above the value of 1.40. Figure 5.25 shows the failure surface with the least safety margin during the rainfall event.

Due to the fine grained nature of the shallow sub soils, comparatively high residual water contents prevail during the unsaturated state. Thus, when the rainfall starts, subsurface flow channels are more easily established interconnecting pore spaces (Collinz & Zindarcic 2004). Therefore, the probability of creating near surface saturation zones is less likely once the flow paths are established between the drains and the ground surface. Although the shallower depths are saturated, the excess water is drained out. Hence, the system will reach an equilibrium state.

Figures 5.26 (a) & (b) illustrate the pore water pressure profiles, through the slope sections IJ and KL, during the rainfall events. At the initiation of the rainfall event, soil possesses a high infiltration capacity as indicated by relatively high initial matric suction (around -40 kPa). When the rainfall intensity is lower than the infiltration capacity, the water flow is governed by the infiltration capacity, i (see equation 5.1), of the soil. Therefore, all the water will infiltrate in such conditions (Gavin & Xue 2008)

$$i = K\frac{S_y}{y} \quad \ldots\ldots\ldots (5.1)$$

Where, K is the permeability of the wetted zone, $\frac{S_y}{y}$ is the hydraulic gradient due to matric suction

It is evident from Figure 5.26 that there is no significant positive pore water pressure development in shallow depths of the slope, either in the toe area or middle region, during and after the rainfall event when the subsurface drains are installed in the slope. Also, the absence of perched water table conditions at shallower depths suggests that the wetting front has reached the subsurface drains at an acceptable rate. It further implies that the hydraulic conductivity values of the top soil layers are sufficiently high, so that the water can be effectively drained out from soil before it gets stagnant and contributes to the rise of the ground water table.

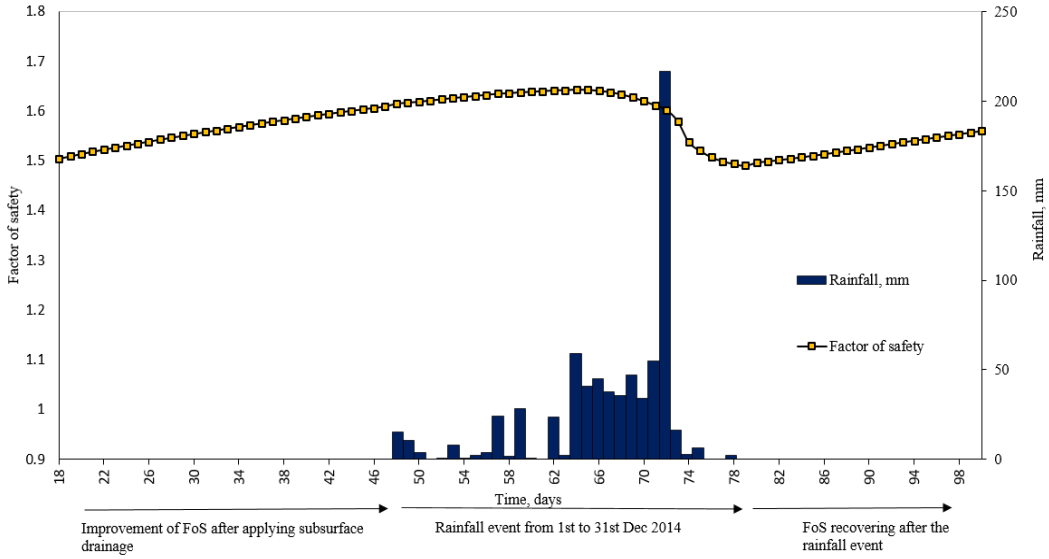

Figure 5.24 Variation of factor of safety of the composite slip corresponding to rainfall event from 1st to 31st December 2014

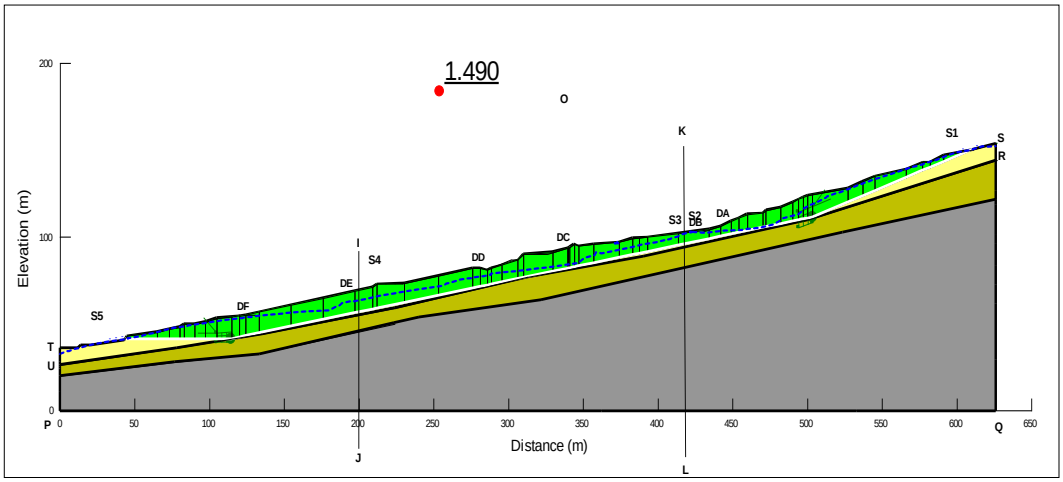

Figure 5.25 Most critical failure surface during the rainfall event

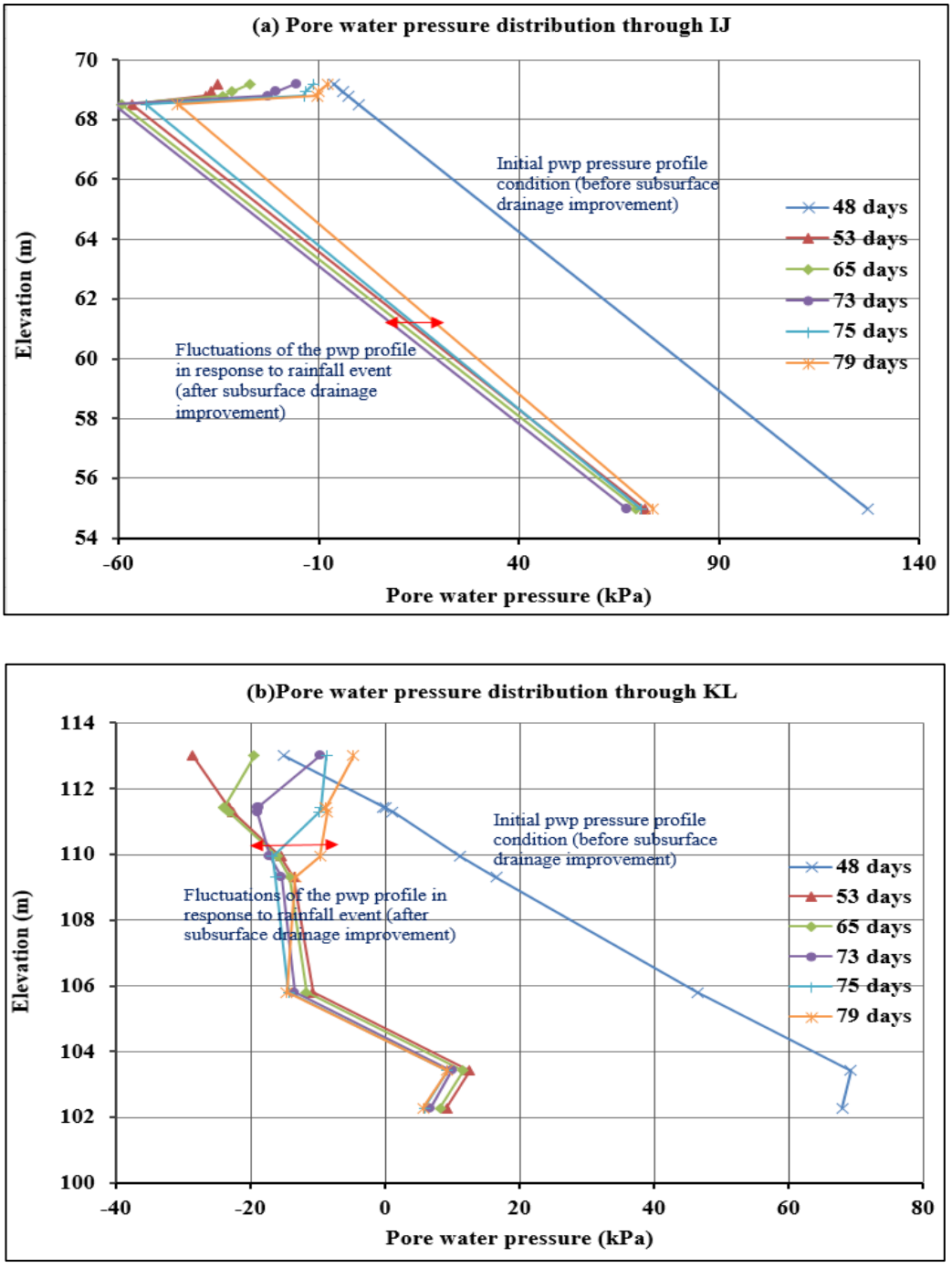

Figure 5.26 Pore water pressure variation during the actual rainfall event: (a) Section IJ, (b) Section KL

5.9 Effect of surface vegetation on the stability of the slope

In this section, the impact of selected surface vegetation cover on the slope, on the stability was assessed. The term “selected surface vegetation” implies that the new

vegetation was systematically introduced to existing vegetation to cover up the bare areas of the slope. The intentions of introducing vegetation were to control the surface erosion and increase the shear capacity of the top soil layer to withstand possible localized shallow failures.

The effects of surface vegetation were incorporated to the model based on laboratory tests conducted to assess the soil behaviour within the vegetated zone. In this section, the new material parameters obtained for the vegetated soil using laboratory tests are first described. The incorporation of effects of vegetation into the numerical model is discussed afterwards.

5.9.1 Selection of the plant species

A set of plant species was selected from the central highlands of Sri Lanka, especially from the landslide prone slopes. When selecting the plants, several factors such as evaporation capacity, root morphology, anchoring effect etc. were taken into consideration. From the selected plant species, several roots having different diameters were obtained for tensile strength tests of roots. The average diameter variation of the selected roots were 2 to 10 mm. Altogether roots from 15 different plant species were analysed.

5.9.2 Root tensile strength tests

Root tensile strength tests were conducted in the laboratory using Dynamometer universal tensile and compression test machine (Model LW 6527, WC DILLON & Co Inc, USA) (Figure 5.27). This device combines three functions: (1) traction force generation, (2) measuring load and displacement, and (3) data acquisition.

When clamping the roots, a cotton textile bandage was wrapped around the griping ends of the roots to increase the grip and to minimize the damage to the roots. The initial root length was set to 150 mm. The root diameter was measured at both ends and the middle using a Vernier calliper. The maximum force at the breaking point was recorded. The following equation was used to calculate the root tensile strength.

$$T_i = \frac{F_{max}}{\pi\left(\frac{D^2}{4}\right)} \ldots\ldots\ldots\ldots (5.2)$$

where, F_{max} is the maximum force (N) needed to break the root and D is the mean root diameter (mm).

Table 5.12 summarizes the root tensile strength values obtained for different species.

Table 5:12: Root tensile strength of selected species

No.	Species Name	Diameter Range (mm)	Tensile strength range (MPa)
1	Syzygium aromaticum (Clove)	1.37 – 2.30	40.08 – 165.01
2	Theobroma cacao (Cocoa)	2.03 – 2.78	48.29 – 25.77
3	Trema orientalis (Gaduma)	4.15 – 4.52	10.14 – 12.23
4	Macaranga peltata (Kanda)	2.20 – 2.60	10.31 – 11.07
5	Cinnamomum verum (Cinnaman)	4.42 – 5.48	21.75 – 22.41
6	Myristica fragans (Nutmeg)	2.28	27.19
7	Calliandra calothyrsus	8.70	9.89
8	Eucaliptus grandis	5.97 – 8.37	10.51 – 42.78
9	Bauhinia racemosa (Maila)	5.12 – 6.79	9.53 – 10.84
10	Camellia sinensis (Tea)	8.77 – 10.077	3.25 – 2.46
11	Azadirachta indica (Neem)	5.35	17.44
12	Clidermia hirta (Kata-kalu bowitiya)	5.14	9.44
13	Osbeckia octandra. (Heen-bowitiya)	5.08	9.66
14	Lantana camara (Hinguru)	6.80	5.40
15	Coffea Arabica (Cofee)	2.63 – 9.00	14.69 – 28.67

Figure 5.27 Root tensile strength testing using Dynamometer

5.9.3 Modelling the root tensile strength

The contribution of the root tensile strength in enhancing the effective cohesion of the soil was studied using the relationships discussed in Chapter 2. In this analysis, it was decided to use *Syzygium aromaticum* species which is commonly known as Clove as a possible vegetation cover for the Central highlands of Sri Lanka. The effectiveness in increasing the shear capacity of the soil in shallower depths was assessed using the numerical model.

Average root cohesion was calculated presuming a planting configuration parallel to slope contour using varying spaces between lines from 0.5m to 2m. It was noted that root cohesion was greater when the spacing between the rows of plants were a minimum. A root area ratio, A_R/A (Equation 2.4) of 0.25% was assumed for Clove for a depth of 2m based on field experience in calculating the average root cohesion. Equation 2.7 was used to calculate the root cohesion of the vegetated soil. Table 5.14 illustrates the values obtain for Clove tree, for different spacing's.

Table 5:13: Root cohesion of Clove tree for different spacing's

Width of plant row (l_r) (m)	Average root cohesion (MPa) for different spacing between each plant row (l_s) (m)			
	2.0	1.5	1.0	0.5
0.5	0.010	0.012	0.016	0.020

5.9.4 Hydraulic conductivity of the vegetated layer

After introducing the proposed vegetation, the slope will ultimately experience a mixed vegetation. Due to the presence of variable root structures representing mixed vegetation, preferential flow paths could create in the shallower depths, increasing the soil permeability (Ni et al., 2018). Ni et al., (2018) has experimentally discovered that around 5 – 6 time increase of saturated hydraulic conductivity can take place when grass and tree type mixed vegetation is present, compared to that of the bare soil. Accordingly, in this study, it was assumed that the initial saturated hydraulic conductivity of the bare soil layer is increased by fourfold due to the combine effect of mixed vegetation.

5.9.5 Stability analysis of the vegetated slope

In this analysis, a separate layer namely, "Colluvium after vegetation" which is of thickness about 2 m (representing the average root depth zone of Clove tree) was introduced. This layer was assigned with the modified shear strength parameters given in Table 5.14. A spacing of 2m was considered between plant rows.

The conditions of the slope, after the modification to account for the effect of surface vegetation, were then considered to investigate the impact of the vegetation on slope stability. A strength reduction factor of 1/3 was applied on the cohesion values derived based on laboratory tests and empirical relationships to account for possible variations in the experimental studies and uncertainty. Figure 5.28 shows the slope profile modified after introducing vegetation.

Table 5:14: Modified soil strength parameters after introducing vegetation

Formation	notation	Cohesion (kPa)	Friction angle (deg)	Unit weight (kN /m3)
1. Colluvium after Vegetation		5	22	15
2. Colluvium		2	22	15
3. Completely to highly weathered rock		8	35	16
4. Highly to moderately weathered rock		20	40	17

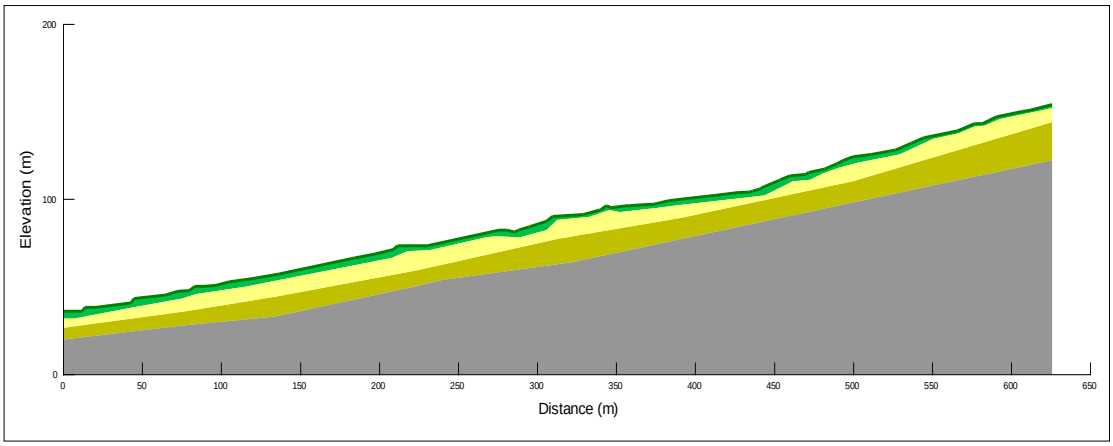

Figure 5.28 Slope profile after introducing the effect of vegetation

Numerical model developed during the previous analysis was modified accordingly integrating the new layer. By the time of the implementation of vegetation, the subsurface drainage system had already been installed (Case 3) and had functioned for a period of one month.

Factor of safety improvement of the slope corresponding to the implementation of each mitigation measure is summarized in Table 5.15. Figure 5.29 shows the safety margins of the critical slip surface. Hybrid measures have improved the initial safety margins of the slope by 71% after a period of 49 days since the commencement of the construction of drains (i.e. one month after the completion of the drainage construction).

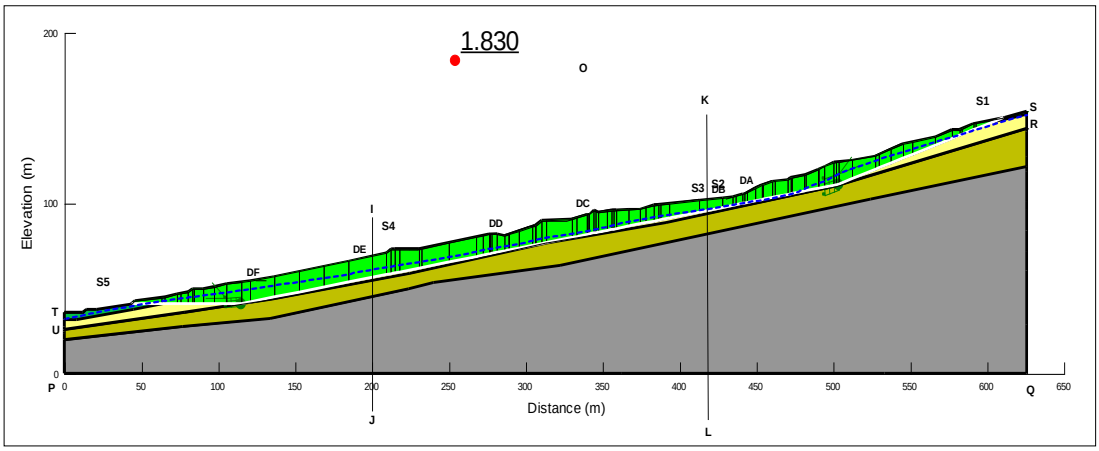

Figure 5.29 Critical slip surface after implementing hybrid measures

Table 5:15 Variation of factor of safety after improving subsurface drains and vegetation

	Stability improvement measure			
	Subsurface drainage		Subsurface drainage and vegetation	
Factor of Safety (F_{int}=1.07)	FoS (48 days)	$\left(\frac{F_i - F_{int}}{F_{int}}\right)\%$	FoS (49 days)	$\left(\frac{F_i - F_{int}}{F_{int}}\right)\%$
	1.58	47.8	1.83	71

5.9.6 Response of the hybrid mitigation system to an actual rainfall event

The same rainfall event discussed under the Sections 5.7.4 and 5.8.2 was applied on the slope rectified with hybrid mitigation measures to study its response. Figure 5.30 presents the variation of the factor of safety under the applied rainfall event.

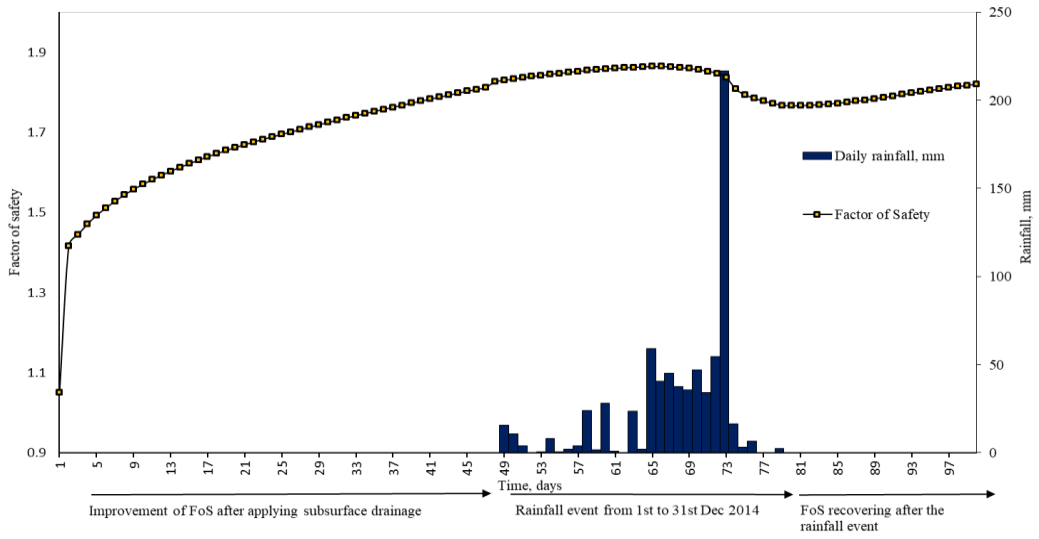

Figure 5.30 Variation of the factor of safety after implementing hybrid mitigation measures, corresponding to an actual rainfall event

Response of the pore water pressure regime of the slope along the cross sections IJ and KL, during the rainfall event is shown in Figure 5.31.

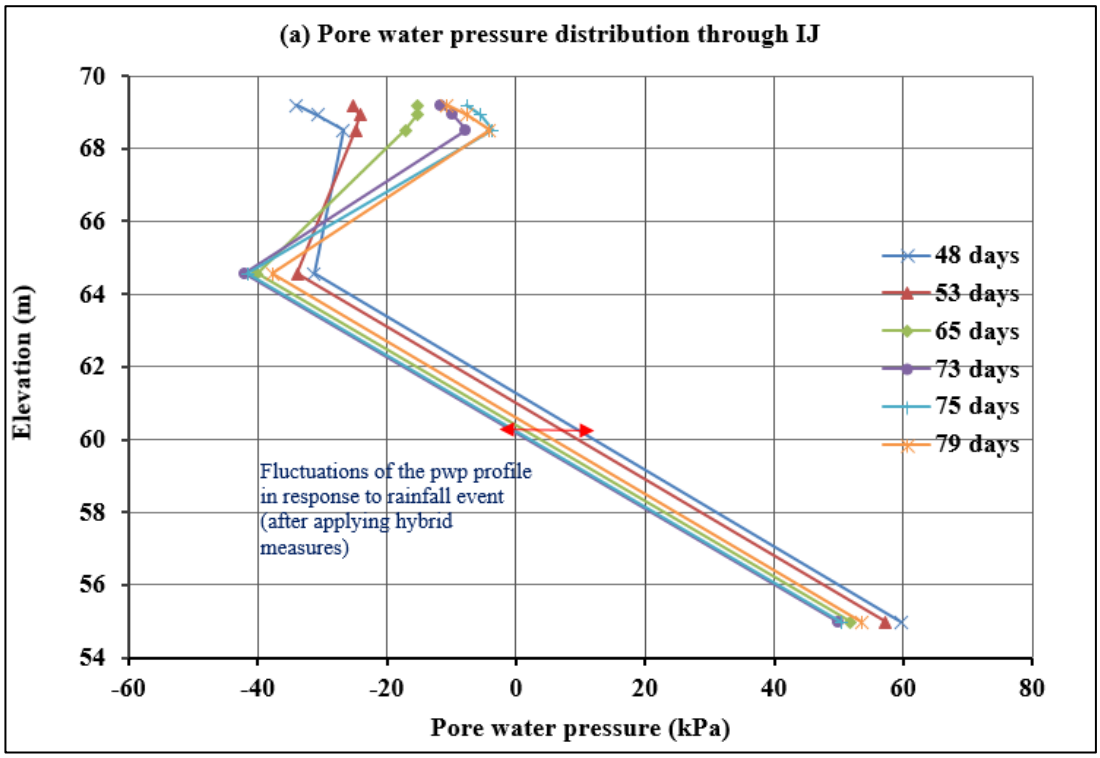

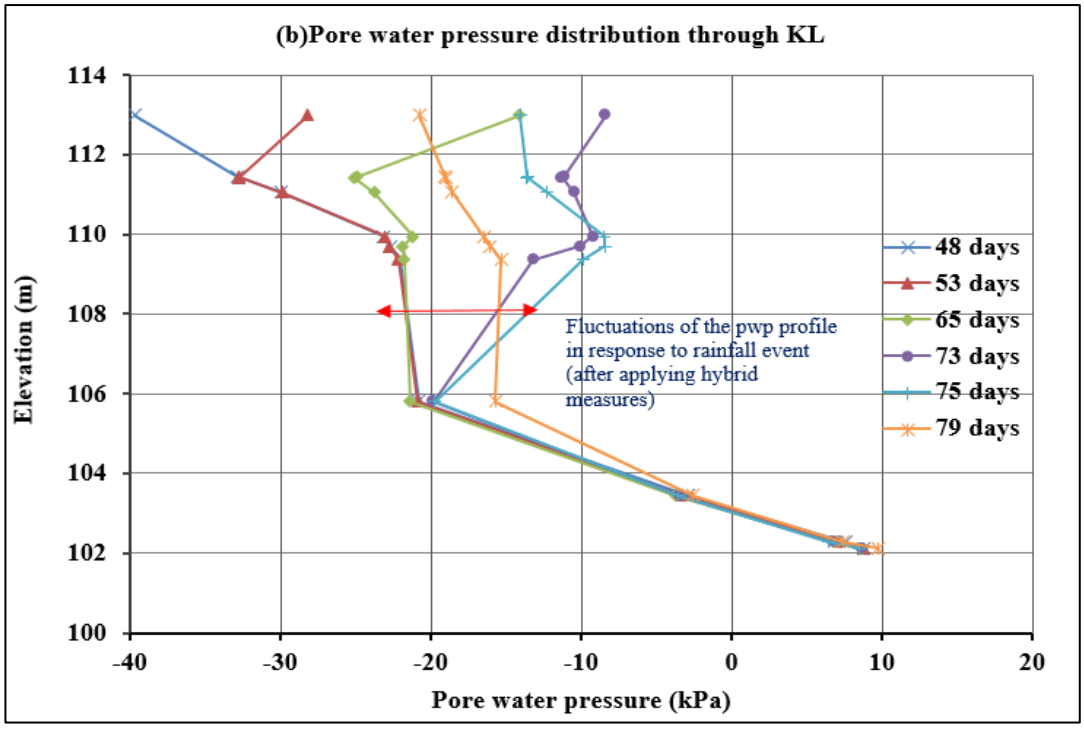

Figure 5.31 Variation of the pore pressure profile of the slope after implementing hybrid measures under the actual rainfall event: (a) Section IJ, (b) Section KL

The response of the pore water pressure profile in the shallower depths of the slope (predominantly in the initially unsaturated zone) after implementing hybrid measures are quite different to the same when only the subsurface drainage network is there. Along both the investigated cross sections, the likelihood of generating near surface saturated zones in the shallower depths are high (Figure 5.31) when hybrid measures are applied. Due to the increase in the hydraulic conductivity in the shallow depths caused by from vegetation, a large area of the initially unsaturated zone tends to achieve a state of saturation. Meantime, due to relatively high permeability in vegetated soil than in the bare soil, negative pore water pressures are unlikely to be maintained. This is a different observation from the case without vegetation, where preferential flow paths towards the ground water table were generated. The contrast in hydraulic conductivity at the interface of the two soil layers (i.e. vegetated soil and bare soil) discourages water entering the low permeable medium (bare soil), thus helping the accumulation of water in high permeable medium (vegetated soil). Therefore, when the vegetation was applied to

the slope, the rise in ground water table at both the slope sections investigated, is less than 1.0 m.

5.10 Summary

In this chapter, significance of subsurface drainage measures in enhancing the stability of the Badulusrigama Landslide was assessed in 2D plane strain conditions. Effects of different subsurface drainage construction sequences were discussed in detail. Performance of the mitigation measures were evaluated under different rainfall conditions. A critical rainfall envelope leading to slope instability at Badulusirigama landslide, after implementing hybrid mitigation measures has been developed incorporating the past landslide records with the results obtained from the analysis. Finally the impact of surface vegetation cover on the stability of the slope was investigated.

The numerical analysis conducted in 2D plane strain formulation, considering different internal and external factors that govern the stability of a slope, indicates that the use of subsurface drainage networks in the Badulusirigama landslide has substantially improved the stability of the slope. Improvement of the factor of safety value of the slope is rapid when the subsurface drains are constructed commencing from the toe region of the slope. Also, drains in the middle and toe of the slope yield high water contents than drains in the upper part of the slope during prolong rainfall events. In designing drains, it is pivotal to have a sound knowledge on the flow control parameters such as hydraulic conductivity, soil –water retention behaviour as well as the matric suction profile of the slope during prolonged dry periods. It is explicit from the analysis conducted, that the efficiency of the drains is greatly dependent on these parameters.

An appropriate vegetation type should be carefully selected after examining the different impacts on the slope. Meanwhile increasing the shear capacity in the shallower depths, root systems could create easy flow paths for water and thereby increase the permeability of the shallow soils, which in turn has an adverse impact

on the stability of the slope. Most of these findings could be generally applied when studying the stability related problems in Central Highlands of Sri Lanka.

The slope seemed to possess adequate safety margins even when exposed to excessive rainfall events, as indicated by the critical rainfall intensity vs duration envelop developed using the numerical model.

Chapter 6

6 DEVELOPING A THREE DIMENSIONAL FINITE ELEMENT MODEL OF THE BADULUSIRIGAMA LANDSLIDE

6.1 Background

Chapter 5 presented 2D numerical models for stability and seepage analysis of Badulusirigama landslide. However, as also discussed in Chapter 5, a 2D plane strain model is not the ideal approach for the simulation of a terrain such as Badulusirigama landslide which is highly variable in both transverse and longitudinal directions, Therefore, in this chapter, an effort was taken to develop a 3D finite element model for the analysis of seepage and stability of the Badulusirigama landslide. Conditions at Badulusirigama landslide hold special challenges for a development of 3D model, which are not encountered in modelling regular geotechnical problems. Some of them are; highly non-uniform terrain and different in-situ stress profile compared to horizontal ground, larger area of land under consideration and unique arrangement of sub-surface drains adopted in the project. The techniques used to address these challenges in developing the 3D model will be discussed in detail in this chapter. After successfully implementing the 3D model, analyses were conducted to assess the stability of the slope with and without sub-surface drainage improvements. Further, the response of the slope to an adverse rainfall event after implementation of stability measures was also studied and discussed in detail.

6.2 PLAXIS 3D software for stability modelling

PLAXIS 3D is a three dimensional finite element programme capable of simulating different geotechnical phenomena. The programme incorporates many analysis methods which are needed to simulate different geotechnical conditions such as flow conditions, stress conditions and stability assessments. In this study, the following analysis types have been utilized to generate the 3D model.

Plastic analysis

Plastic anaylsis is a basic analysis type available in PLAXIS 3D software. This is one of the most widely used analysis types in geotechnical practice. A plastic analysis is performed based on the small deformation theory. For the basic soil models, plastic analysis does not consider a limitation in time. Rather, this analysis technique provides a continuation of computations until an equilibrium state is achieved.

Full coupled flow - deformation analysis

Fully coupled analysis is used when it is required to analyze the behaviour of pore pressure changes and deformation simultaneously. This method addresses the time dependant behaviour of the problem. In a fully coupled analysis, the soil deformations and pore pressure changes are co-dependent, where stress increments and deformations in soil due to pore water pressure dissipation and pore water pressure changes due to external load induced deformations are coordinated iteratively until the equilibrium is reached. This analysis is carried out in terms of the total pore pressure in the system; i.e. the software can generate both steady state pore pressure and excess pore pressure components. This type of analysis enables the generation of unsaturated zone above the water table by taking into account the reduction in permeability and degree of saturation.

Safety analysis

In PLAXIS, safety analysis is performed based on the C – phi reduction technique. At a given stage During a C – phi reduction analysis, the values of the soil strength parameters are defined by a multiplier, $\sum M_{sf}$

$$\sum M_{sf} = \frac{\tan \Phi_{input}}{\tan \Phi_{reduced}} = \frac{C_{input}}{C_{reduced}} \ldots\ldots\ldots \quad (6.1)$$

Parameters with the subscript “input” refer to the initial properties entered for the material. At the outset of the analysis M_{sf} is set to 1. Then at the each step, the value of M_{sf} is increased by 0.1 and strength parameters are reduced accordingly, as

shown in equation 6.1. By default, the number of calculation steps is set to 100. If the full failure mechanism has been developed at the end of defined number of calculation steps, then the factor of safety is equal to the value of $\sum Msf$. However, the failure mechanism and the $\sum Msf$ vs. displacement curve should closely be observed to accurately identify the development of the failure mechanism as well as the approaching $\sum Msf$ to a constant figure.

6.3 Development of three dimensional profile for the model

The three dimensional profile of the site was developed in the model based on the contour survey data and lithological data obtained during field investigations, as outlined in detail in Chapter 3 and Chapter 4

In the 3D model, soil layering of the subsoil profile was developed using the borehole elements available in the "Soil" module. Table 6.1 presents the thicknesses of the different sub soil / rock layers. However, the facilities available in this module cater only to build the basis shape of the slope. The more specific variations of the ground surface that were captures by the contour survey was introduced to the model in "structures" module in the program. This technique allowed the featuring of some hilly areas of the slope which were especially targeted during subsurface drainage treatment. Thus, building those features in the 3D model enables the opportunity to observe the localized effects of the drains more realistically.

Linear elastic perfectly plastic behaviour with Mohr – Coulomb failure criteria was assumed for all soils layers in the model. The properties of the subsoil layer were assigned as detailed in Chapter 04. During the safety analysis, however, the assignment of Mohr – Coulomb material model for top most soil layer resulted in very shallow and localized failures with lower FoS. This is due to the localized variations of the slope and these small slides are not of interest in the current analysis. Therefore, in order to avoid shallow failures and to direct the program to look for overall failure surface of the slope, a thin layer of near surface zone with linear elastic properties was defined. In this near surface zone, the elastic material

properties were kept as same as for the rest of the colluviums soil, however, plastic behaviour was not specified. Table 6.1 illustrates the notation used for different soil layers in the 3D model.

Table 6:1: Notation used for different subsurface layers in 3D model

Layer	Notation
1. Colluvium	
2. Completely weathered rock	
3. Highly to moderately weathered rock	

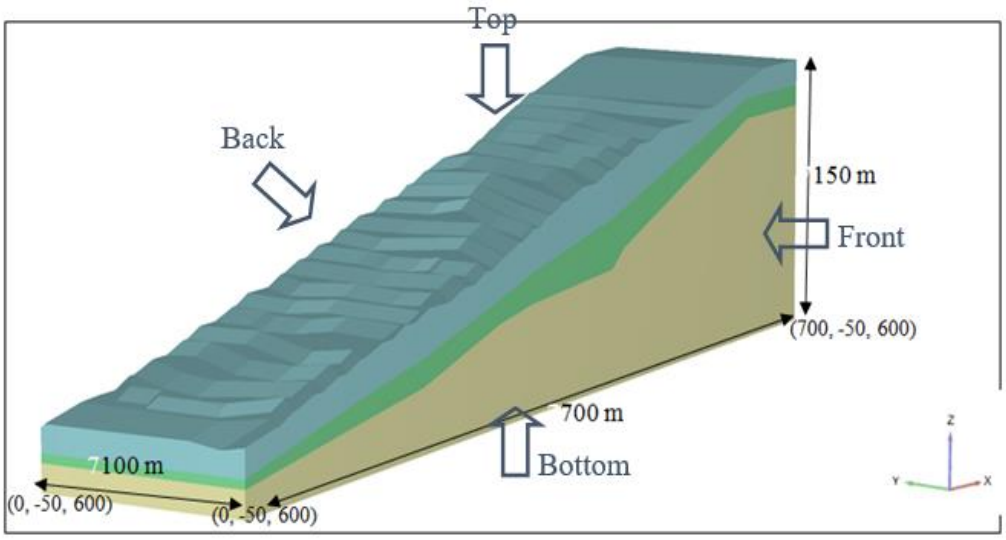

Figure 6.1 PLAXIS 3D model of Badulusirigama Landslide

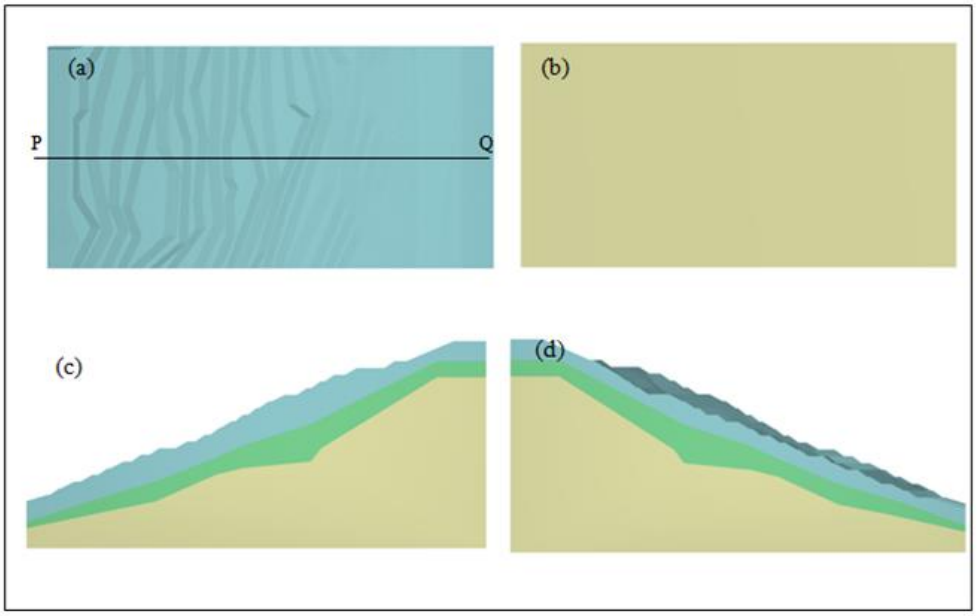

Figure 6.2 Model from the different viewpoints (a) top view, (b) bottom view, (c) front view, (d) back view

Figure 6.1 illustrates the three dimensional model worked out for the site based on the available information and Figures 6.2 (a), (b), (c) & (d) show the model from different viewpoints. The total length in X direction is 700 m, width in Y direction 100 m and height in Z direction is 150 m, in the model.

6.4 Model boundary conditions

6.4.1 Displacement boundary conditions

PLAXIS automatically assigns the certain displacement boundary conditions at the model boundaries unless prescribed otherwise. The default boundary conditions were suitable for this model. Accordingly, the following displacement boundary conditions have been used in the model. A graphical presentation is given in Figure 6.3.

- Vertical model boundaries parallel to the YZ plane: Symmetric boundary conditions were used. Displacements are fixed in X – direction (u_X =0) and free in Y and Z direction.

- Vertical model boundaries parallel to the XZ plane: Symmetric boundary conditions were used. Displacements are fixed in Y - direction (u_Y =0) and free in X and Z direction.
- The bottom boundary of the model is fixed in all direction ($u_X = u_Y = u_Z$ =0)
- The ground surface is free in all directions.

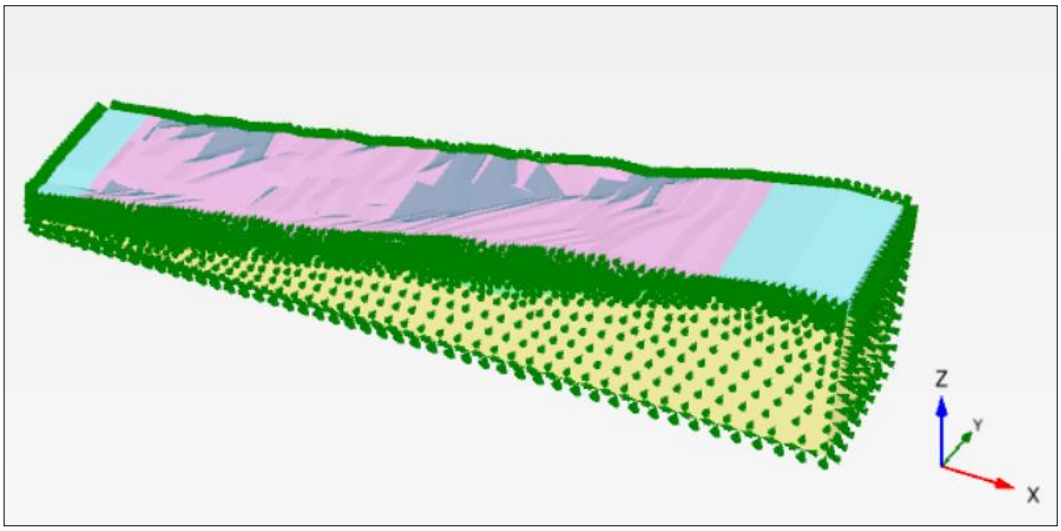

Figure 6.3: Displacement boundary conditions assigned for the model

6.4.2 Flow boundary condition

Ground water table was defined based on the field observed ground water levels, using the borehole water level option available in PLAXIS 3D. Accordingly, ground water table for the entire model has been generated using the water levels defined in the boreholes.

The seepage boundary conditions were altered accordingly during the infiltration analysis to simulate different precipitation conditions. The "Precipitation" boundary condition available in "Flow conditions" module of the software was used for this purpose.

Figure 6.4 and 6.5 indicates the initial ground water table of the slope. The thick blue line indicates the initial ground water table. In PLAXIS, compressive forces are denoted by a negative sign as per the sign convention. Variation of ground water

head within the model along the cross section P–Q (see Figure 6.2(a)) is shown in Figure 6.4. Figure 6.5 shows the pore water pressure contours along selected cross section of the slope. Steady state pore water pressure varies from about 0 to 1500 kPa below the level of the water table. Above the water table suction varies from 0 to 100 kPa as illustrated in the shaded plot in Figure 6.5.

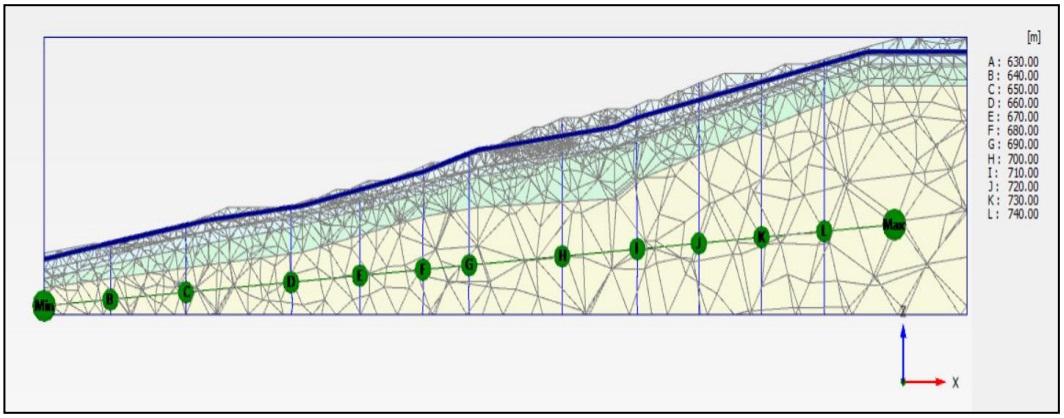

Figure 6.4 Variation of the ground water head within the shown in a cross section along the centre line of the slope

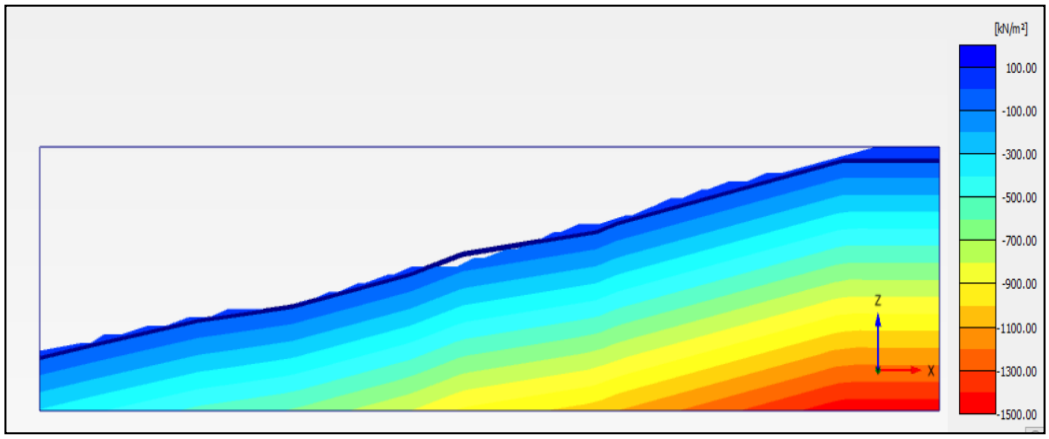

Figure 6.5 Variation of the pore water pressure along the section PQ

6.5 Finite element mesh

In solving finite element problems, it is mandatory to generate an appropriate finite element mesh according to the problem definition. In this analysis, the mesh coarseness option “fine” was used. Table 6.1 gives a description on the finite

element mesh. Figure 6.6 shows the finite element mesh generated for the problem. The mesh shown in Figure 6.6 was used in all the analysis conducted in this chapter.

Table 6:2: Details of the finite element mesh

Mesh type	Fine
Number of elements	111279
Number of nodes	156096
Average element size	5.382 m
Maximum element size	60.59 m
Minimum element size	6.286E – 3 m

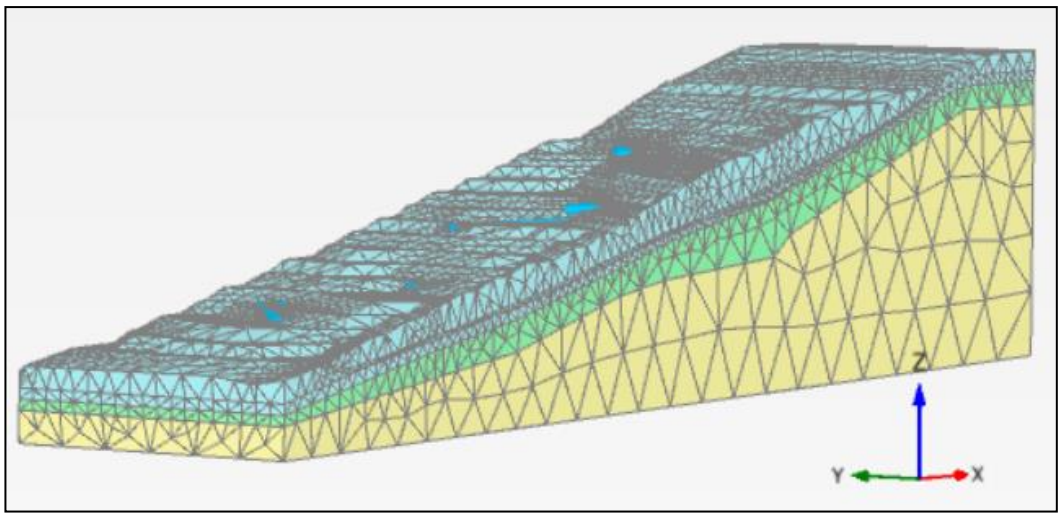

Figure 6.6 Finite element mesh generated for the problem

6.6 Establishment of initial geo-static stresses of the ground

In solving geotechnical problems using finite element approach, first, the initial stress profile of the problem should be established. PLAXIS finite element programme enables the establishment of initial stress condition using either of K_0

procedure, gravity loading and field stress method. In this study initial stress condition of the slope was established using the K_0 procedure.

It is noteworthy to discuss here that, K_0 procedure is recommended for generating initial stress conditions in problems with horizontal or nearly horizontal ground surface formations. This technique is not recommended to very steep ground surfaces such as in current case history analyzed, because, the K_0 procedure is not capable of generating the shear stresses in the elements that are actually present in sloping grounds. Therefore, once K_0 procedure is carried out on a steep slope there can be out of balance forces remaining in the soil elements. In order to overcome this short-coming, as recommended in PLAXIS manual, a plastic stage analysis was carried out immediately after the K_0 procedure. This procedure is termed as running a "plastic – nil phase". During a plastic stage analysis, the imbalanced forces are brought to equilibrium; however, this may cause some deformations in the ground. Therefore, for the current model, the deformations after the plastic stage were thoroughly scrutinized to make sure that the displacement during this stage are small enough to not to alter the existing geometry of the initial model. In this analysis, the deformations experienced during the plastic stage were less than 0.5 m. This was deemed as not affecting to original shape of the ground, given the large dimensions of the overall model as well as sensitivity of contour survey data.

As a second check on the correct establishment of the initial geostatic stresses, the development of failure points on the soil body was also inspected. The output of the initial K_0 procedure indicated a limited number of plastic points and tension points as well as no extreme displacements. This suggests that the out of balance forces developed for the sloping ground are not deviated far from the equilibrium condition. Therefore, the equilibrium state stress regime in the sloping ground can be successfully established in the model by conducting a subsequent plastic analysis following the initial K_0 step. The displacements calculated during this plastic phase were set to zero before commencing the subsequent phase to ensure that the initial displacements of the ground are zero before commencing any succeeding calculations.

Alternative to the aforementioned K_0 procedure followed by a plastic – nil phase, the gravity loading procedure can also be adopted to establish the geostatic stresses in a sloping ground. This procedure allows for the generation of shear stresses in the soil elements during the gravity loading analysis itself. However, the shear stresses developed in this analysis type are based on the Poisson's ratio values and are not based on the specified k_0 values as of a geotechnical engineer would prefer. Therefore, if the gravity loading procedure is adopted, it is recommended to adjust the soil Poisson's ratio to reflect the required k_0 values. Later, in the subsequent analysis stages to the gravity loading analysis, a new set of material properties should be assign to the model with the correct combinations of k_0 and Poisson's ratio values in order to obtain the accurate results for the model.

The initial stress condition of the slope was established as per the k_0 procedure described above. Figure 6.7 shows the initial stress condition of the slope after establishment of initial geostatic stresses. The directions of the principal stresses that are deviated from vertical – horizontal directions indicate the formation of shear stresses within the soil body. The maximum effective principal stress value of the sloping ground pertaining to the existing condition was 1430 kPa.

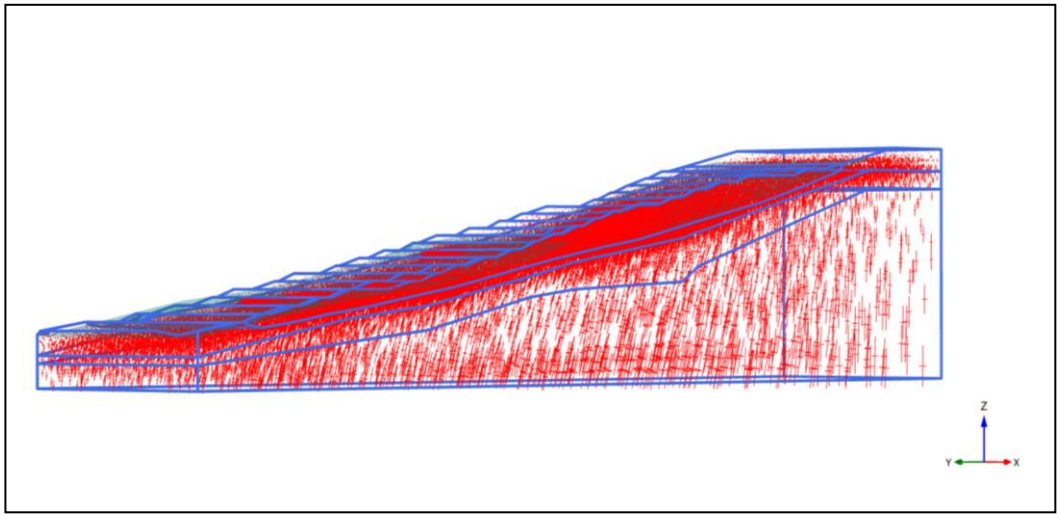

Figure 6.7 Initial principal stress profile of the site

6.7 Analysis of the stability of the slope

Stability of the slope was assessed under prevailing conditions and after introducing subsurface drainage measures using the 3D model, as discussed in following sections.

6.7.1 Stability of the slope under prevailing conditions

After setting up the initial conditions of the ground, stability of the slope, under the prevailing conditions was assessed. Figure 6.8 illustrates the incremental shear strains developed in the model at the last time step of the c-Phi reduction procedure. As seen in the figure, larger shear strain increments are formed along the slip surface of the slope. The shaded line in light blue colour in Figure 6.8 indicates the deviatory shear strains developed along the failure plane. This is due to the slip of the upper soil mass, causing shear at the interface between the sliding and stable zones. Figure 6.9 and 6.10 show vectors and contours of the incremental displacements developed along the slip surface, respectively. Incremental displacements are an indication of the moving soil mass. A 3D view of the failure mass under existing ground conditions is presented in Figure 6.10.

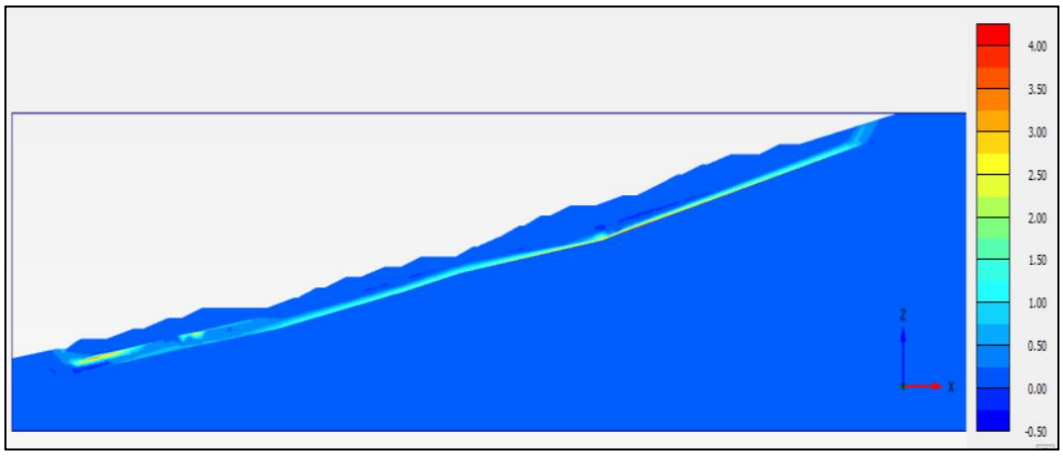

Figure 6.8: Deviatoric shear strains along the failure plane

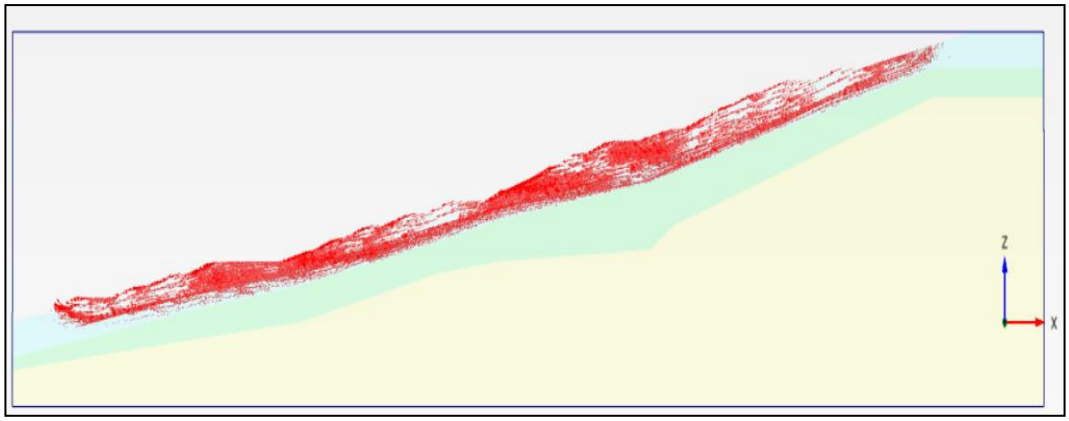

Figure 6.9: Vectors showing incremental displacements in the moving mass

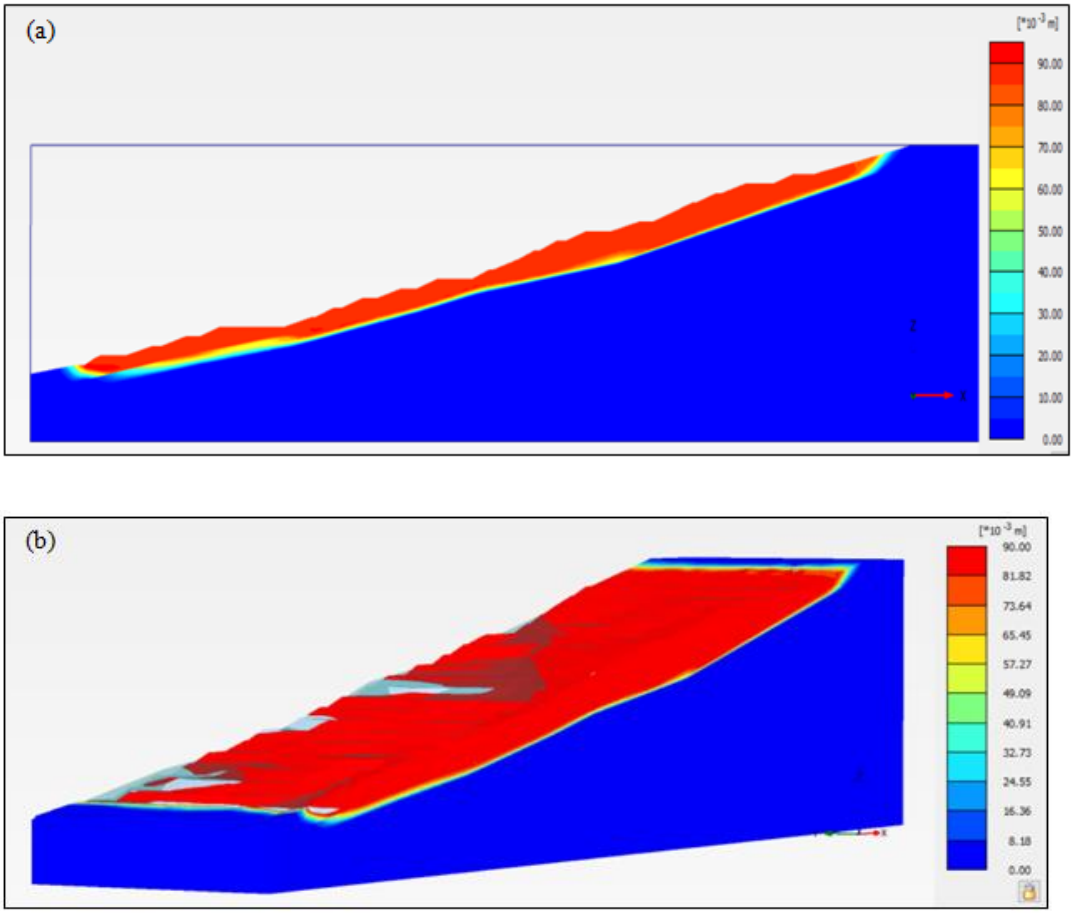

Figure 6.10: Shadings indicating the incremental displacements in the moving mass (a) along the section PQ, (b) 3D view

When conducting a safety analysis, the slip surface in the model output was closely examined to confirm the development of a potential overall failure surface rather

than localized small failures surfaces. Also, the evolution of FoS with the number of iterations in the safety analysis was well examined to confirm that the FoS has reached a stable condition within the specified number of iterations (100 iterations in current case). The FoS vs Time step curve should appear more or less constant without large fluctuation to accept the final result as the FoS of the slope. In cases where it was not stable, number of calculation stages were increased from its default value to arrive at steady factor of safety values. Initial factor of safety value of the slope with existing high ground water table conditions (without subsurface drains), was determined to be 1.086 (Figure 6.11).

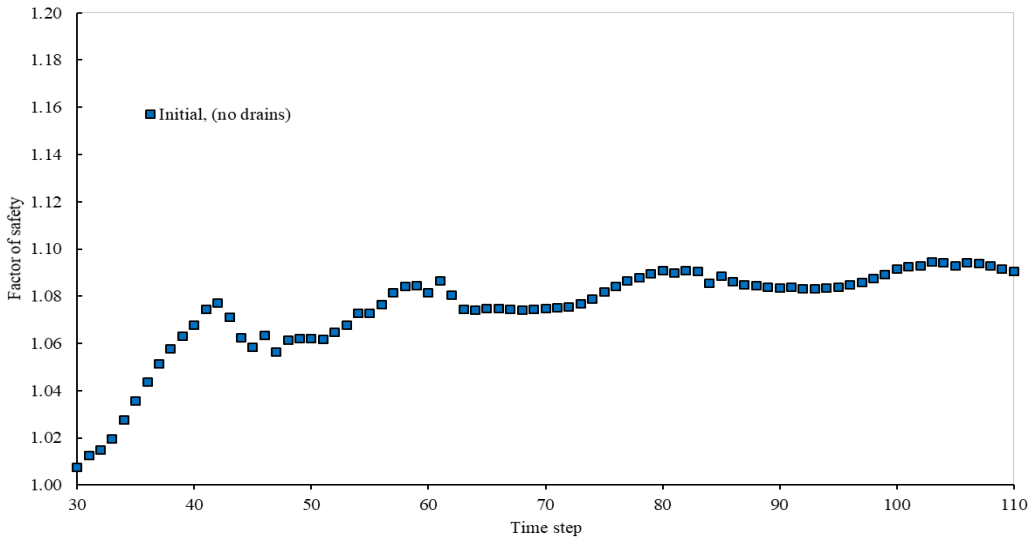

Figure 6.11: Plot showing the initial factor of safety of the slope

During the 2D plane strain analysis base on limit equilibrium approach, slip surface was fully specified based on the field investigation data. In 3D finite element analysis which is based on a finite element formulation, the critical slip surface was obtained using stress – strain analysis, without predefining the failure surface. The close agreement between the of the slip surface generated in the 3D model and the predefined composite slip surface considered in the 2D analysis, indicates that the 3D model developed for Badulusirigama Landslide is significantly representative of the actual field condition. Further, the factor of safety of the critical slip surface

obtained from 3D finite element analysis, which is generated through stress - strain analysis (1.086) procedure is more or less similar to that of 2D plane strain analysis (1.068) that is derived based on force and moment equilibrium.

6.8 Performance of the slope after implementation of fan –type subsurface drainage

The main aim of performing the 3D analysis is to investigate the impact of fan – type subsurface drainage improvement in enhancing the stability of the slope. Details of proposed subsurface drainage system (i.e. number of drains, length and etc.) were discussed in section 3.10.1 in Chapter 3. Table 6.3 gives the spatial arrangement of drains in the 3D system. The spatial arrangement of the subsurface drainage fans are shown in Figure 6.12.

Table 6:3: Spatial arrangement of the drainage system in 3D formulation

Drain	Drain length (m)	Angles (deg)		Coordinates at the drain mouth (m)			Coordinates at the drain end point (m)		
		Vert. plane	Hori. pl	X	Y	z	X	Y	Z
DA1	45	-40	5	449	-4.2	710	483	-33.0	713.92
DA2	45	-30	5	449	-4.2	710	488	-26.6	713.92
DA3	45	-20	5	449	-4.2	710	491	-19.5	713.92
DA4	45	-10	5	449	-4.2	710	493	-12.0	713.92
DA5	45	0	5	449	-4.2	710	494	-4.2	713.92
DA6	45	10	5	449	-4.2	710	493	3.6	713.92
DA7	45	20	5	449	-4.2	710	491	11.2	713.92
DA8	45	30	5	449	-4.2	710	488	18.2	713.92
DB1	45	0	5	412	-29.2	704	457	-29.2	707.92
DB2	45	-10	5	412	-29.2	704	456	-37.0	707.92
DB3	45	-20	5	412	-29.2	704	454	-44.5	707.92
DB4	45	-30	5	412	-29.2	704	451	-51.6	707.92
DB5	45	-40	5	412	-29.2	704	446	-58.0	707.92
DB6	45	-50	5	412	-29.2	704	441	-63.5	707.92
DB7	45	-60	5	412	-29.2	704	434	-68.0	707.92
DB8	45	-70	5	412	-29.2	704	427	-71.3	707.92
DC1	45	-80	3	340	-40.0	690	348	-84.3	692.36
DC2	45	-70	3	340	-40.0	690	355	-82.2	692.36
DC3	45	-60	3	340	-40.0	690	362	-78.9	692.36
DC4	45	-50	3	340	-40.0	690	369	-74.4	692.36
DC5	45	-40	3	340	-40.0	690	374	-68.9	692.36
DC6	45	-30	3	340	-40.0	690	379	-62.5	692.36
DC7	45	-20	3	340	-40.0	690	382	-55.4	692.36
DC8	45	-10	3	340	-40.0	690	384	-47.8	692.36

Drain	Drain length (m)	Angles (deg)		Coordinates at the drain mouth (m)			Coordinates at the drain end point (m)		
		V2ert. plane	Vert. plane	X	Y	Z	X	Y	Z
DD1	60	0	3	288	-8.3	682	347	-8.3	685.14
DD2	60	-9	3	288	-8.3	682	347	-17.7	685.14
DD3	60	-18	3	288	-8.3	682	344	-26.8	685.14
DD4	60	-27	3	288	-8.3	682	341	-35.5	685.14
DD5	60	-36	3	288	-8.3	682	336	-43.6	685.14
DD6	60	9	3	288	-8.3	682	347	1.0	685.14
DD7	60	18	3	288	-8.3	682	344	10.2	685.14
DD8	60	27	3	288	-8.3	682	341	18.9	685.14
DD9	60	36	3	288	-8.3	682	336	26.9	685.14
DE1	60	-50	3	196	-41.7	662	235	-87.6	665.14
DE2	60	-40	3	196	-41.7	662	242	-80.2	665.14
DE3	60	-30	3	196	-41.7	662	248	-71.6	665.14
DE4	60	-20	3	196	-41.7	662	252	-62.2	665.14
DE5	60	-10	3	196	-41.7	662	255	-52.1	665.14
DE6	60	0	3	196	-41.7	662	256	-41.7	665.14
DE7	60	10	3	196	-41.7	662	255	-31.3	665.14
DE8	60	20	3	196	-41.7	662	252	-21.2	665.14
DE9	60	30	3	196	-41.7	662	248	-11.7	665.14
DF1	55	-30	3	106	-27.1	651	154	-54.5	653.88
DF2	55	-20	3	106	-27.1	651	158	-45.9	653.88
DF3	55	-10	3	106	-27.1	651	160	-36.6	653.88
DF4	55	0	3	106	-27.1	651	161	-27.1	653.88
DF5	55	10	3	106	-27.1	651	160	-17.5	653.88
DF6	55	20	3	106	-27.1	651	158	-8.3	653.88
DF7	55	30	3	106	-27.1	651	154	0.4	653.88
DF8	55	40	3	106	-27.1	651	148	8.2	653.88
DF9	55	50	3	106	-27.1	651	141	15.0	653.88

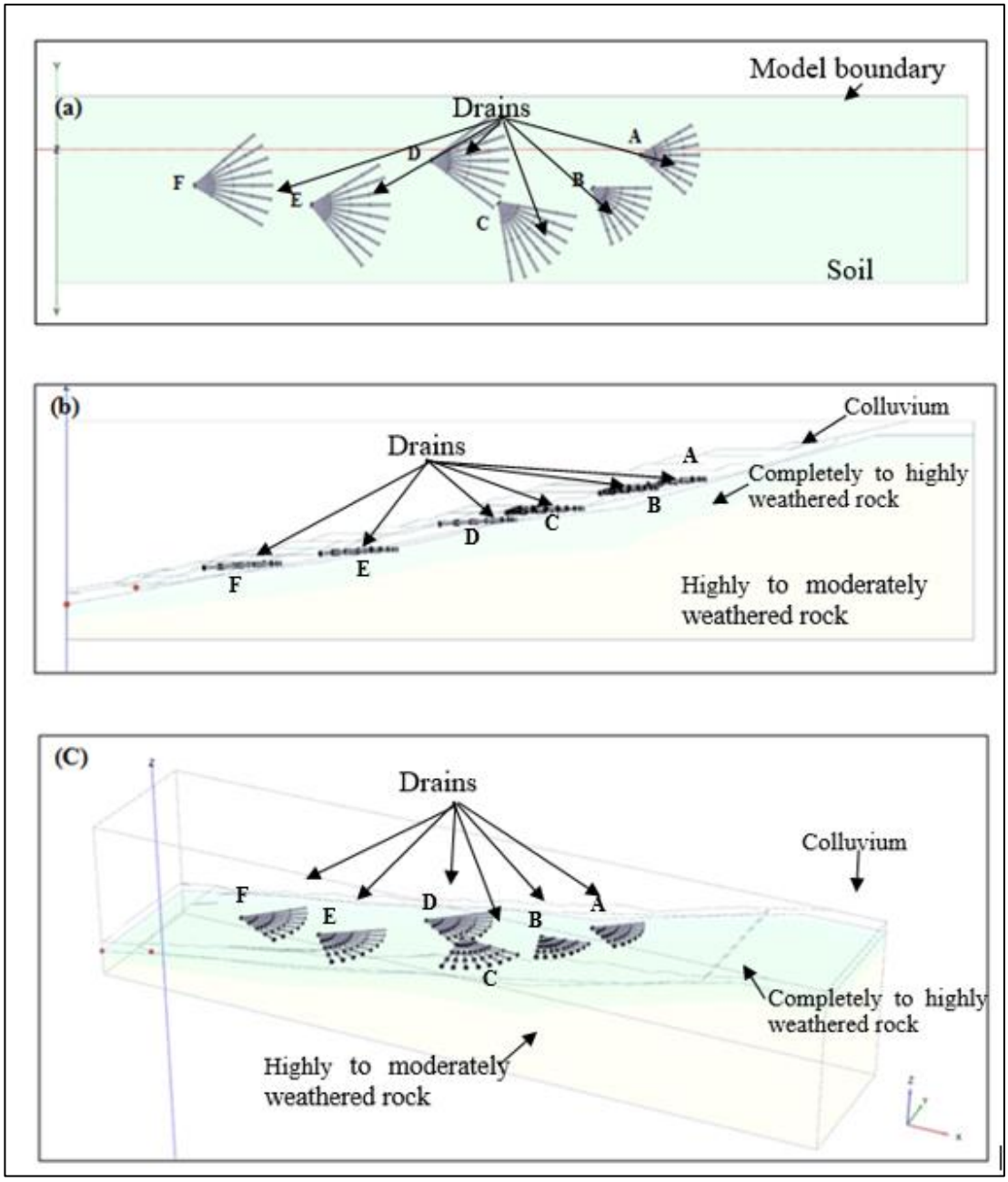

Figure 6.12 Spatial arrangement of the subsurface drainage system (a) top view, (b) front elevation, (c) perspective view

To simulate the subsurface drains in the model “line drain” option available in the software was used. The pore water pressure value inside the drain was set to zero. To simulate the functioning of drains in 3D finite element formation, fully coupled flow deformation analysis type was adopted.

Six fan type drainage arrangements were modelled in both top down (Case 2) and bottom up (Case 3) construction sequence. The case "simulating all drains simultaneously", the Case 1 investigated under 2D plane strain analysis, was eliminated here due to practical constrains applicable when it comes to real world applications. The cases considered in the analysis are:

Case 2: Simulating top – down construction of drains

Case 3: Simulating bottom – up construction of drains

Improvement of the safety margins of the slope was observed after the construction of each drainage fan. In this regard the fully coupled deformation analysis was followed by the safety analysis. After activating all the drains, analysis was further extended for a period of one year, to investigate the variation of the phreatic surface and improvement of the factor of safety of the slope in long term. Table 6.4 summarizes the sequence of simulation under the each case considered.

Table 6:4: Sequence of simulation under the each case considered.

Day of installation of drains	Case 2 construction staging	Case 3 construction staging
At the start	Construct Fan A	Construct Fan F
After 03 days	Construct Fan B	Construct Fan E
After 06 days	Construct Fan C	Construct Fan D
After 09 days	Construct Fan D	Construct Fan C
After 12 days	Construct Fan E	Construct Fan B
After 15 days	Construct Fan F	Construct Fan A

6.8.1 Variation of the water table and stability of the slope under Case 2

Figure 6.13 shows the variation of the ground water table with drainage improvement following the Case 2, along cross section P-Q defined in Figure 6.2(a). The approximately vertical blue lines in the figures indicate the total head contours.

Figure 6.13 illustrate the changes in the ground water table, 3 days after activation of each drainage fan. The fluctuations of the ground water table cannot be directly observed in the figures due to the small scale of the overall model, relative to the couple of meters fluctuation in the water table. However, the water head variation can be observed by referring to the total head contours shown in approximately vertical lines in the figures. In each of the case, the contours were requested across the same reference points (shown in green). It can be seen from Figure 6.13(a), through to Figure 6.13(g), that the total head contours have been gradually changed from perfectly vertical contours to broken contours near the surface. In Figure 6.13(a), the total head contours are vertical and straight, indicating constant total head (elevation head + pore pressure head) along the line. When it comes to Figure 6.13(g), the total head contours are broken and the contours near the ground surface have moved toward uphill. This is due to the reduction of pore water pressure in the near surface zone bringing the total head values low. This observation of gradual change clearly indicated the variation of the ground water table with ongoing drainage with the installation of subsurface drains.

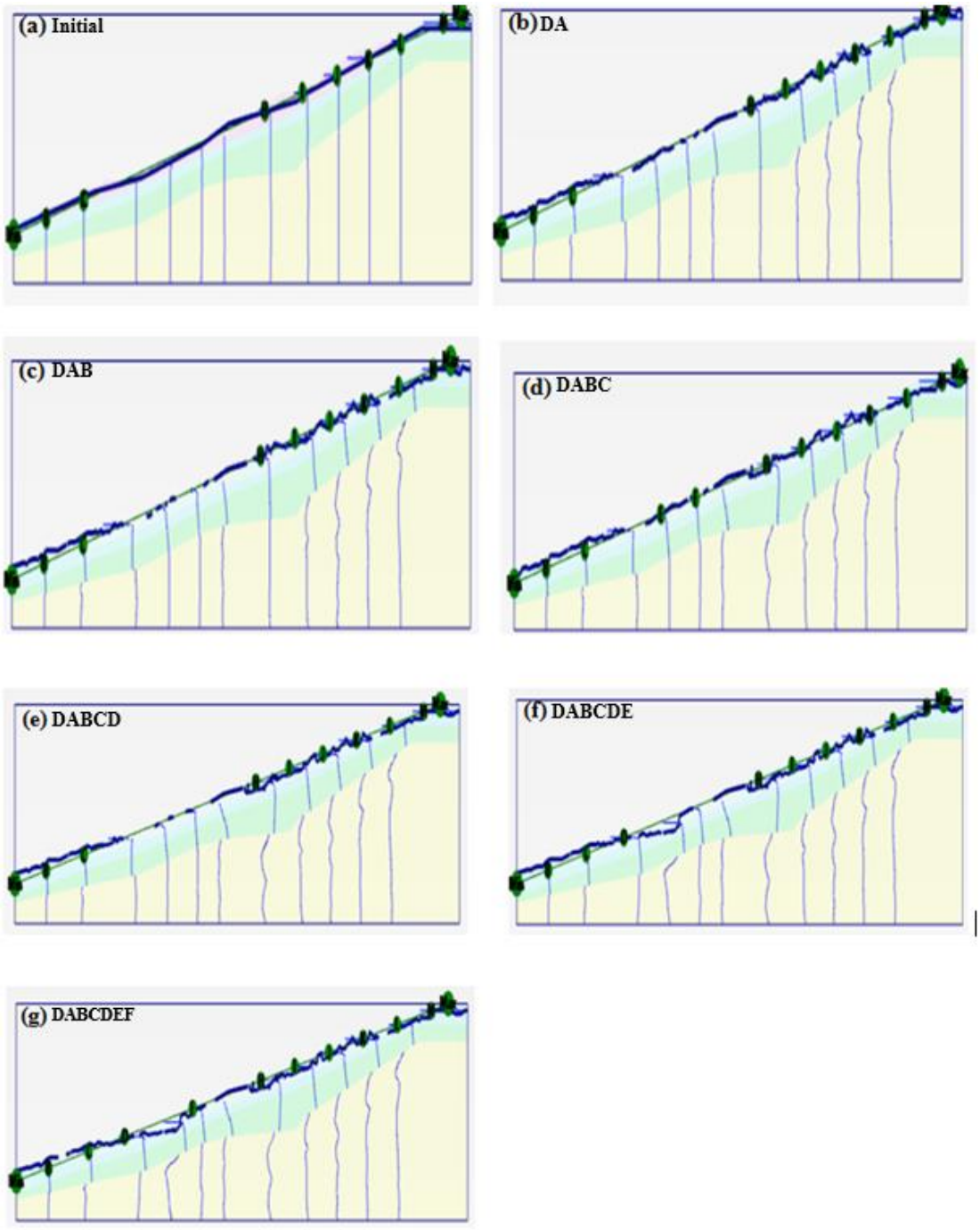

Figure 6.13: Variation of the ground water table with drainage improvement: Case 2- top down (a) Initial, (b) DA, (c) DAB, (d) DABC, (e) DABCD, (f) DABCDE, (f) DABCDEF

6.8.2 Variation of the water table and stability of the slope under Case 3

Figure 6.14 shows the variation of the ground water table with drainage improvement following the Case 3, along cross section P-Q.

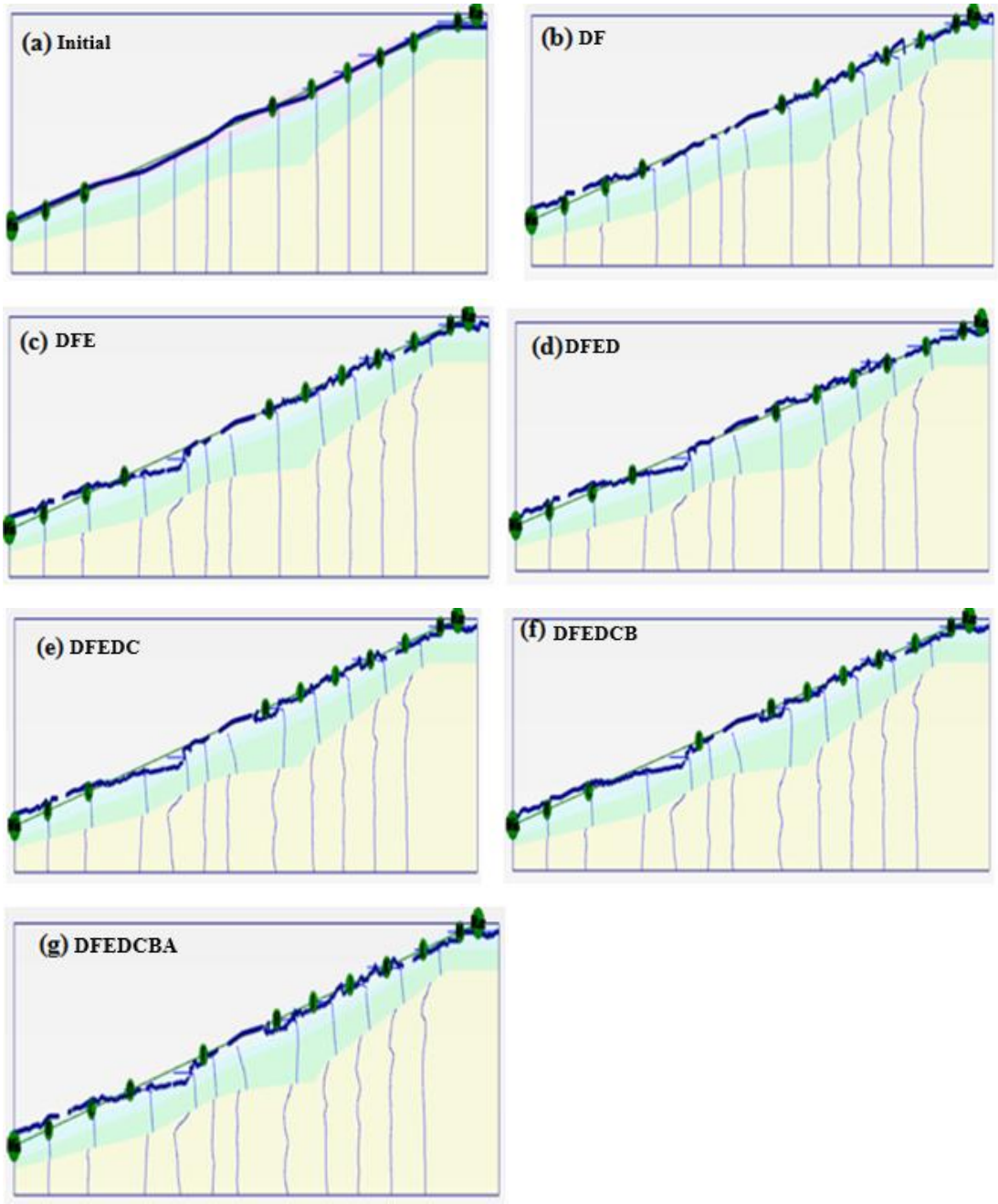

Figure 6.14: Variation of the ground water table with drainage improvement: Case 2 -Bottom up (a) Initial, (b) DF, (c) DFE, (d) DFED, (e) DFEDC, (f) DFEDCB, (f) DFEDCBA

A close observation of the variation of ground water table under the two cases considered, revels that, when the drains are constructed in bottom – up sequence, the ground water table at the top and the bottom of the slope are similar (Compare Figure 6.13(b), (c) and for Case 2 and Figure 6.14 (b) (c)) for Case 3 .

6.8.3 Comparative improvement of the factor of safety under two cases

While the actual construction stage and timing for the installation of drainage system are not available, in the current analysis, it was assumed that each fan of drains is constructed at 3 days intervals as presented in Table 6.3. The construction of the drains were simulated in the model by activating the line elements corresponding to the drains at respective time intervals. Factor of safety analyses of the improved slope, were doneat end of 3 days after activation of each drainage fan. Figure 6.15 and Figure 6.16 show the variation of the factor of safety of the slope after implementation of the drainage measures, in Case 2 and Case 3, respectively, with iteration steps. The stabilized factor of safety values obtained after the iterative time steps in each construction stage under Case 2 and Case 3 are presented in Table 6.5.

Under Case 2, Construction of fans of drains A results in an improvement of factor of safety by 5.5 % initially. The construction of fan B thereafter did not cause any significant increase. The condition was same for both fan C and Fan D where improvements were observed to be around 2 %, 1.6% respectively, when compared to the preceding installation. In contrast, installation of fan E, which is closer to toe of the slope, resulted in a factor of safety improvement of 4.3 % compared to previous installation. Installation of fan F resulted in a further increase of only 1.04%. Installation of all drains caused an improvement of 15.3% when compared with the initial factor of safety. Under Case 2 construction sequence, improvement of factor of safety when compared to initial factor of safety of the slope, is more significant in during the installation of drain fans near the toe. Installation of first four fans (A, B, C & D) has resulted in 10.5 % improvement and thereafter installation of fan E has improved to 15%. Installation of fan F has caused a significant further contribution towards the improvement of factor of safety.

Under Case 3, construction of fans of drains F resulted in an improvement of factor of safety by 5.9 %. Installation of the next drainage fan has resulted in further improvement of factor of safety by 5 %. Accordingly, in contrast to Case 2, improvement of factor of safety after the installation of first two fans of drains (F and E) have caused an overall factor of safety improvement of 11%. In addition, initial factor of safety has improved by 15 % after the completion of the installation of initial four fans of drains (F, E, D, and C). However, installation of two final fans of drains B and A has not yielded much further improvement in the factor of safety.

To sum-up, the rate of improvement of the factor of safety is higher when the drains are constructed in a bottom up sequence. However, final safety margins achieved by the slope for both construction sequences are almost similar.

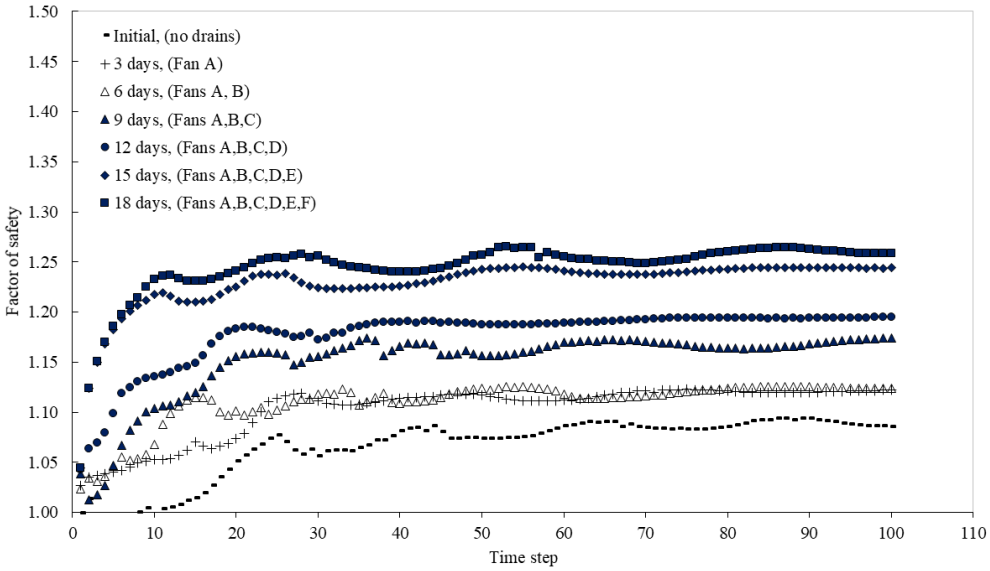

Figure 6.15: Variation of factor of safety pertaining to Case 2

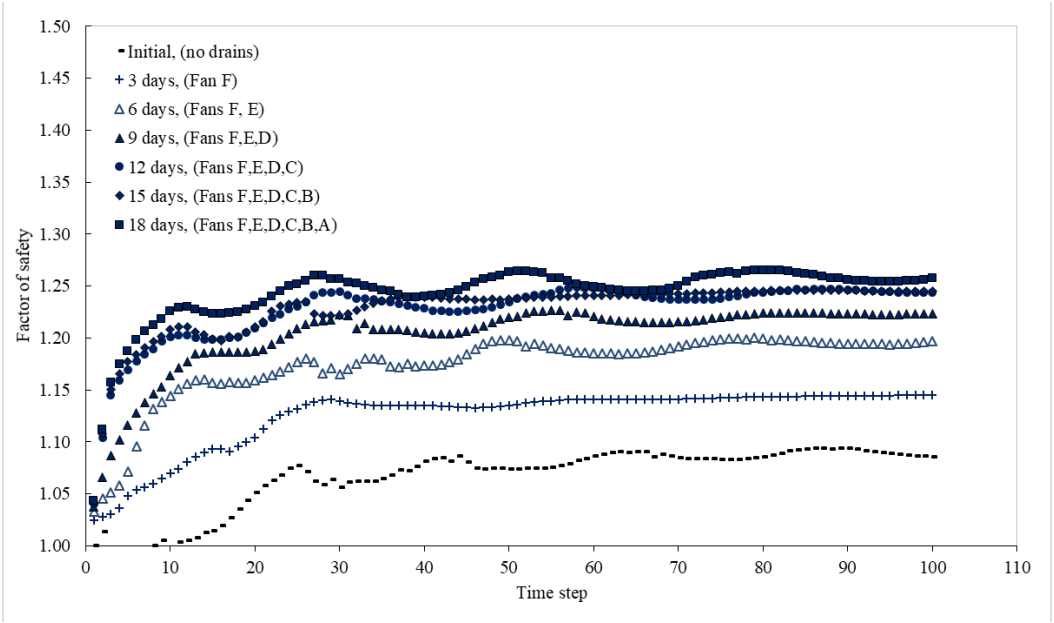

Figure 6.16: Variation of factor of safety pertaining to Case 3

Table 6:5: Percentage variation of the factor of safety for the two construction cases

Case 02 (F_{int}=1.086)				Case 03 (F_{int}=1.086)			
Drainage improvement (Elapsed time)	value	$\left(\frac{F_i - F_{i-1}}{F_{i-1}}\right)\%$	$\left(\frac{F_i - F_{int}}{F_{int}}\right)\%$	Drainage improvement (Elapsed time)	value	$\left(\frac{F_i - F_{i-1}}{F_{i-1}}\right)\%$	$\left(\frac{F_i - F_{int}}{F_{int}}\right)\%$
A(03)	1.146	5.52	5.52	F (03)	1.15	5.89	5.89
AB(0)6	1.157	0.96	6.54	FE(06)	1.207	4.96	11.14
ABC(09)	1.181	2.07	8.75	FED(09)	1.227	1.66	12.98
ABCD(12)	1.2	1.61	10.50	FEDC(12)	1.248	1.71	14.92
ABCDE(15)	1.252	4.33	15.29	FEDCB(15)	1.248	0.00	14.92
ABCDEF(18)	1.265	1.04	16.48	FEDCBA(18)	1.264	1.28	16.39

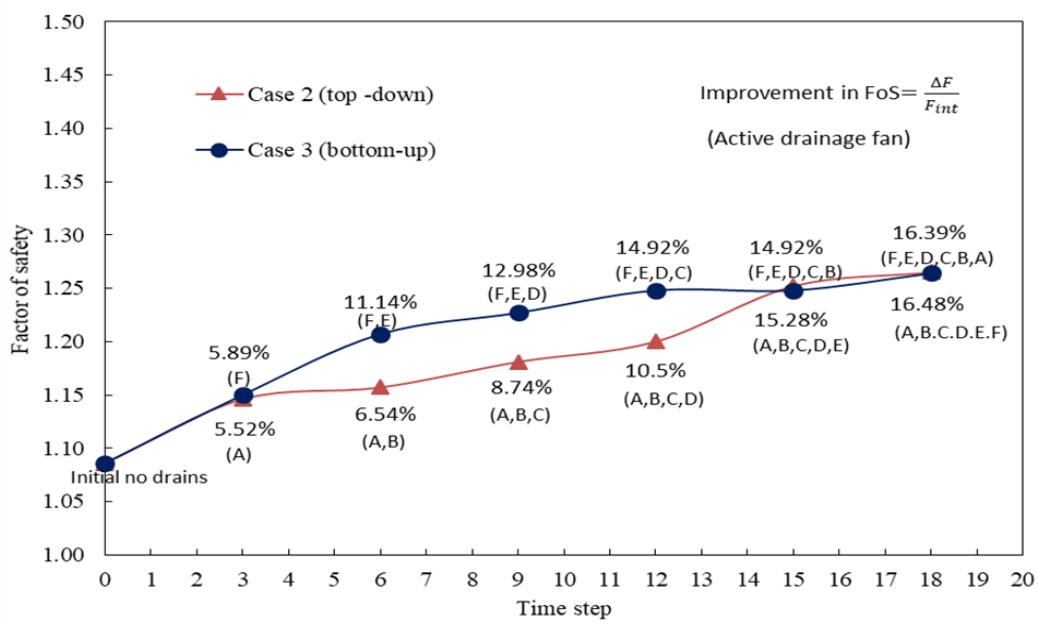

Figure 6.17 Plot showing the variation of factor of safety with time under two cases

When the safety analysis was extended for a period of three months under both cases, the factor of safety value obtained at the end of 18th day, remain unchanged. In other words, no further improvement of factor of safety value was observed in the 3D model, whereas in the 2D limit equilibrium analysis, factor of safety of the slope kept gradually increasing with the time.

It is evident that the initial factor of safety obtained for the slope is more or less similar using both analytical techniques. In addition, factor of safety improvement during the implementation of drainage measures follow a similar trend in both 2D and 3D models, with a higher rate of improvement when the bottom - up construction sequence is adopted. The achieved FoS of the 3D studies can be compared only with the FoS values of the composite failure surface. In 2D plane strain analysis, the factor of safety was improved from 1.07 to 1.44 (35 %) under Case 02 and 1.47 (38 %) under Case 03, during the first 18 days (i.e. drainage installation period). The factor of safety improvement in 3D finite element analysis under the same circumstances was 1.086 to 1.26 (16 %) for both Case 02 and 03.

The reasons for the difference could be; the difference in two analytical approaches and the impact of 3D effect. The 3D effect could affect either positively or negatively towards the improvement of the factor of safety.

6.9 Performance of the radial drainage network in response to an actual rainfall event

The critical rainfall event (from 01st December 2014 to 31st December 2014) simulated in section 5.7.4 under 2D plane strain analysis was applied to the rectified 3D slope to observe the performance. Infiltration event corresponding to each day was defined as a surface flow boundary under "model condition" module using the "Precipitation" option available in PLAXIS 3D. To complete the function, following three parameters have to be defined accordingly;

q: Infiltration

Ψ_{max}: Maximum pore pressure head relative to the elevation of the boundary

Ψ_{min}: Minimum pore pressure head relative to the elevation of the boundary

In this analysis infiltration, q, was changed accordingly and Ψ_{max} and Ψ_{min} were set to their default values, as recommended in the PLAXIS manual. The rainfall simulation was commenced on the 19th day after improving all the subsurface drainage measures. By this period slope had reached its maximum safety margins as confirmed by extended safety analysis.

The safety margin of the slope was assessed on selected days during and after the rainfall event. These days were selected based on the variation of the rainfall event and the factor of safety was observed after the selected days. Table 6.6 summarizes the percentage variation of factor of safety with time. Figure 6.18 presents the variation of the factor of safety of the slope during the rainfall event.

Table 6:6 Percentage variation of factor of safety

Elapsed time (days)	value	$\left(\frac{F_i - F_{int}}{F_{int}}\right)\%$
23	1.254	-0.63
28	1.262	0.00
33	1.245	-1.35
38	1.121	-11.17
43	1.110	-12.04
44	1.120	-11.25
46	1.146	-9.19
49	1.21	-4.12
53	1.25	-0.95

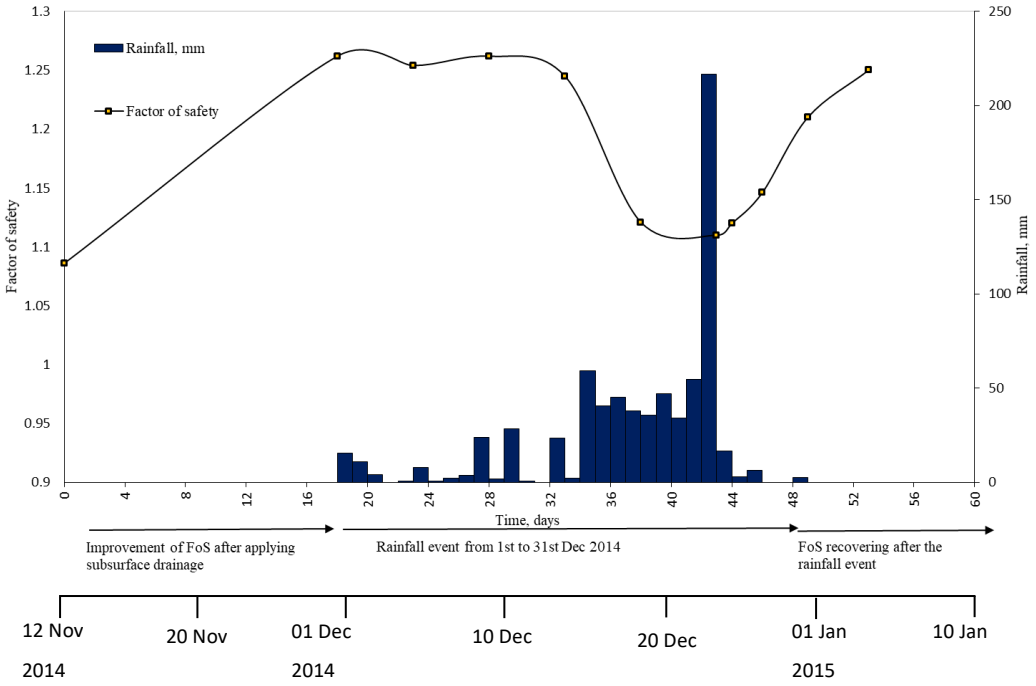

Figure 6.18: Variation of the factor of safety of the slope corresponding to actual rainfall event

During the first 15 days where the accumulated rainfall was less than 50 mm, the safety margins of the slope seems to be steady. However, after five to six day with

a cumulative rainfall of 250 mm, factor of safety has dropped to a value of 1.12. Further, it is observed that the reduction of factor of safety during forthcoming 5 days with a cumulative rainfall event of around 400 mm (from day 38 to 43) is not that drastic compared to initial drop in factor of safety (i.e. 1.254 to 1.121). The reason behind this might be because, by this time due to the reduction of suction in the soil, the infiltration capacity would have been reduced. As a result, more rain water will contribute to runoff without infiltrating into the slope. In both 2D and 3D analyses pertaining to the rainfall event, the maximum percentage reduction in factor of safety from its initial values are similar. In Section 5.9.6, the analysis conducted for composite slip surface resulted in a reduction of factor of safety from 1.76 to 1.64 (Figure 5.29), which is about 10%. However, 2D and 3D analysis follow different trends in variation of FoS, where in 2D analysis, minimum factor of safety was recorded after the rainfall event of 218 mm on 25th day. In 3D model, the minimum factor of safety was recorded after a total antecedent rainfall of 250 mm. Figure 6.19 indicates the variation of ground water table during the rainfall event.

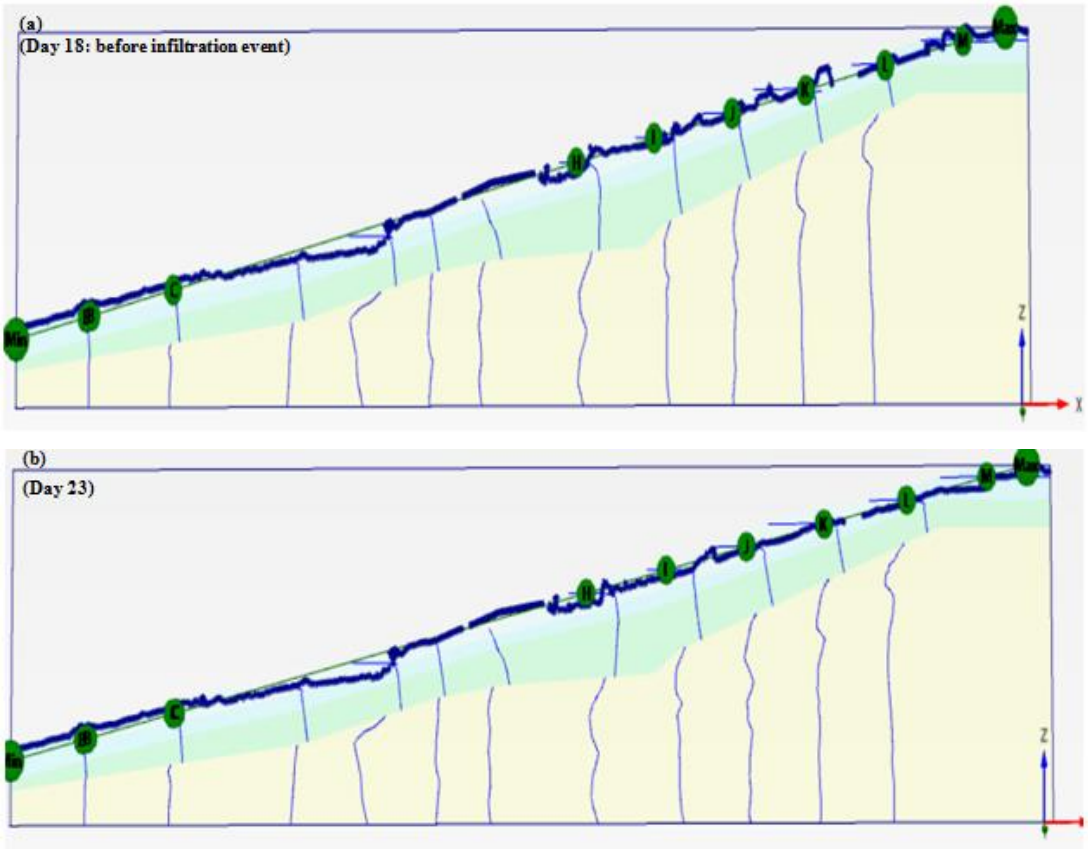

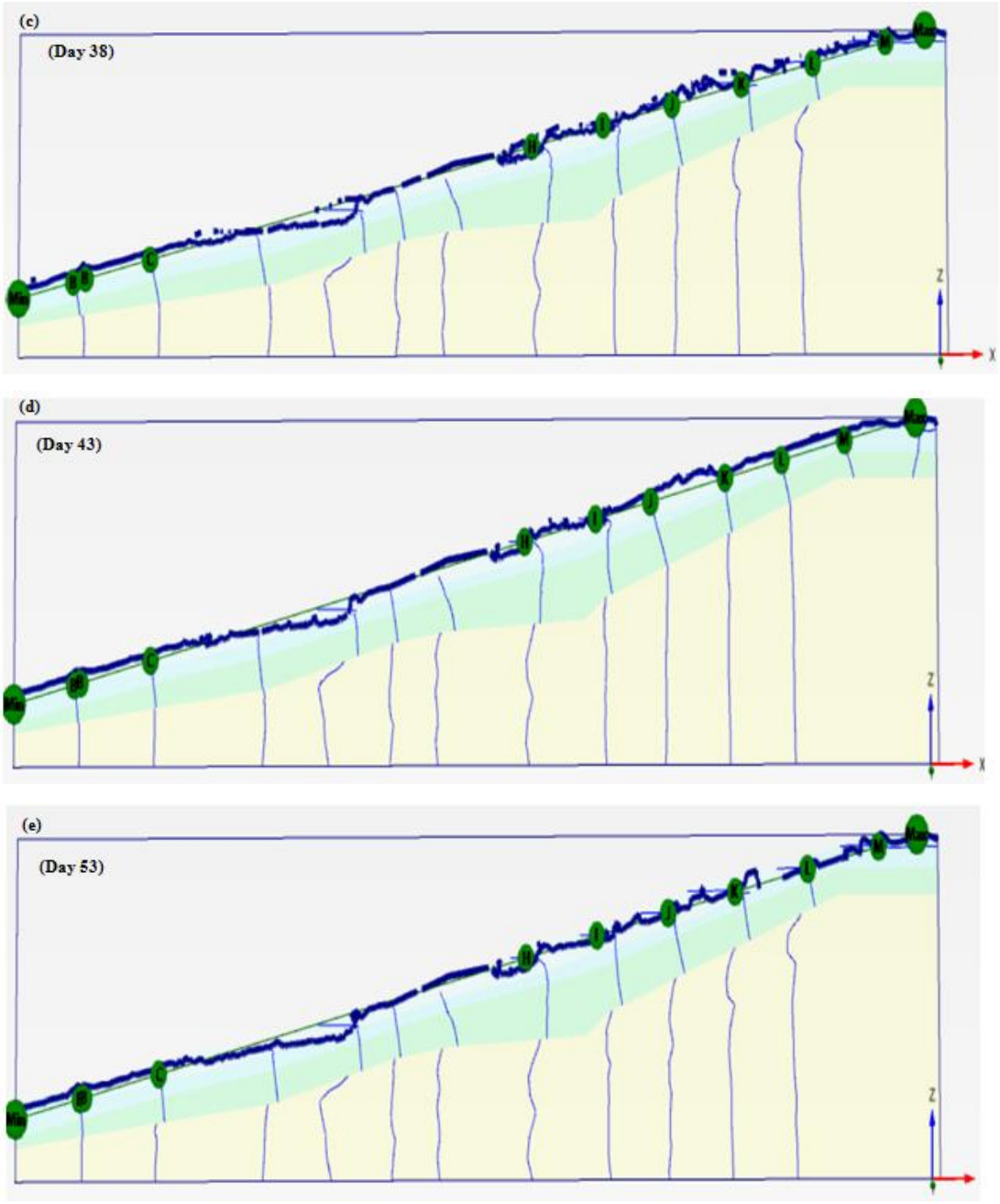

Figure 6.19: Variation of ground water table due to critical rainfall event: (a) Day 18, (b) Day 23, (c) 38, (d) Day 43, (e) Day 53

It can be seen that the ground water table in the upper slope has risen during the rainfall event during the day 33 to 37 as indicated in Figure 6.19(c). Ground water heads have further increased during the next five days as shown in Figure 6. 19 (d). The fluctuations of the ground water table can be figured out by closely observing

the relative movements of the vertical lines indicating the ground water head (appear in light blue colour). Therefore, it can be concluded that the safety margins of the slope has reduced due to the rise of ground water table in the upper region of the slope.

6.10 Commentary on the developed 3D finite element model for Badulusirigama landslide

The three dimensional model developed in preceding sections represents the full scale of the slope. Also a fare attempt has been made to simulate the actual uneven ground surface. Unlike in 2D plane strain conditions, in 3D finite element modelling, selection of soil parameters should be carefully done (in case they are not available from laboratory tests). Otherwise severe convergence, difficulties, large displacements and much deviations from general conditions would occur. All these matters should be collectively addressed while developing the 3D slope model as well as analyzing under different conditions. Effect of radial type subsurface drainage system can only be simulated using 3D formulation.

Use of finite element approach to determine the factor of safety of this landslide has certain advantages. FE method has the ability to conduct stress strain analysis which is missing in limit equilibrium approach. This fact is significant in handling these type of complex geometries (Memon 2018). In reality, transient water flow and deformations occur simultaneously. These simultaneous events could be modelled using fully coupled flow deformation analysis, with finite element technique. Also, conventional limit equilibrium approaches could overestimate the factor of safety values of the slope when it involves complex geometries, non-circular failure surfaces and layer stratifications (Giam & Donald 1989).

A sound understanding of the soil parameters and the way they are correlated with each other are required during modelling as well as interpreting the results. Lack of knowledge in these areas would lead to tedious procedures.

6.11 Summary

In this chapter, Badulusirigama Landslide is modelled in 3D finite element formulation in real scale. Stability of the slope has been assessed under existing high ground water table conditions. Radial drainage network introduced to improve the stability of the slope has been fully simulated in the 3D analysis. Improvement of the factor of safety of the landslide was investigated under different drainage construction methods. Actual rainfall event was simulated on the slope to study the variation of factor of safety in response to the rainfall event.

The initial factor of safety calculated for 3D slope model with high ground water table conditions is 1.086. Values obtained from two methods (2D and 3D approaches) are almost identical, which was 1.07 for composite slip surface analyzed using 2D plane strain conditions. However, the improvement in factor of safety obtained from 2D limit equilibrium method and 3D finite element method after installation of the drains were different. The 2D model showed higher improvement of factor of safety whereas the 3D model indicated less improvement. Yet the trends in the factor of safety variation were similar in both models. The reasons for the differences in the factor of safety obtained through the two models can be two fold; differences in the two analysis methods used in the two models namely, limit equilibrium method and the finite element method, and the effect of the 3D geometry which was included in the 3D model and not included in the 2D model.

The slope reached maximum safety margins within a period of 18 days after construction of drains. The final rate of improvement of the factor of safety was higher when subsurface drainage improvement was implemented in a bottom up sequence. The final factor of safety value reached by the slope was same under both top - down and bottom - up construction methods. Drainage measures were observed to be effectively functioning during the critical rainfall event simulated. Factor of safety value was maintained above 1.1 during excessive 5 day rainfall events of 400 mm.

Chapter 7

7 CONCLUSIONS AND RECOMMENDATIONS

7.1 Conclusions

Sub-horizontal drains have been in use all over the world for rectification of slopes and enhancement of stability. Despite being a popular solution, there are no systematic methods for the design of sub-horizontal drainage measures. This results in very elaborate designs, which are mainly based on designer's experience and confidence. Nevertheless, a widely adopted guide for the design of sub-horizontal drains may not be practical due to vast variation of slope behaviour depending on the hydraulic characteristic, climatic conditions, site geology, human intervention etc., specific to each site. However, with the increasing demand for different infrastructure facilities and consequent migration of some constructions into hilly areas, geotechnical engineers are facing the challenge to further optimize their designs. The critical issue with sub-horizontal drain improved slopes when optimizing and implementing safety limitations is the lack of understanding on the effectiveness of sub-horizontal drains in maintaining the water table at sufficiently low levels. Ever increasing number of massive slope failures and landslides in different regions of the world emphasizes the need to apply a more comprehensive assessment of slope stabilization through sub surface draining technique.

In this study, one of the large landslides improved with sub-horizontal drains was investigated in detail, to understand its behaviour in the short and long term. Badulusirigama landslide, used in this study is located in the Badulla administrative district of Sri Lanka. This was identified as a slow moving landslide with a sliding mass volume of about 600000 m^3 and was rectified with the use of surface and subsurface drains. The subsurface drains were of fan type arrangement and installed at six different elevations along the axis of the landslide.

7.1.1 Two dimensional analysis

The state of the slope prior to implementation of the rectification and the effect of rectification measures were initially modelled in two dimensions, with a finite element based seepage analysis through commercial software SEEP/W and limit equilibrium based commercial software for stability anaysis SLOPE/W. The comprehensive geotechnical investigation process conducted at the field could identify three different failure surfaces; upper, middle and lower. Hence the limit equilibrium analyses were done using "fully specified" failure surface option using following the Spencer's method which is applicable to both circular and non-circular failure surfaces and considers both force and moment equilibrium.

Ideally, the concept of adopting a plane strain model to represent a section of a long geotechnical problem that is uniform along the longitudinal direction is not suitable for the Badulusirigama landslide, as this is located on a highly inconsistent hilly terrain. However, a 2D plane strain simulation was adopted in the current study, on the basis of replicating the most critical section of the site in the model. Thus, it was deemed to yield worst-case scenario performance for the landslide.

The results of the 2D analysis illustrated that the state of instability prevailed at the site was improved significantly by the installation of sub surface drains. The sequence of drain installation had an impact on the gradual achievement of factor of safety. It was shown that, with a bottom up sequence of drain installation, the safety margin as indicated by FoS, increased faster than in the case of a top down sequence of installation. With the completion of the installation of all the drains, the final factors of safety achieved by the two different construction sequences were similar.

The 2D seepage analysis revealed that the subsurface drains located in toe and middle areas of the slope releases comparatively large amounts of water during an event of rainfall. The middle and lower drains were more efficient in discharging ground water compared to top drains, in the absence of rainfall as well. This

observation emphasizes that toe drains are the most effective in improving the factor of safety against slope instability that could trigger by heavy rainfalls.

Subsequently, the process of stabilization of the slope with sequential installation of drains was simulated with the composite failure surface, which included the three failure surfaces mentioned above. In that anlaysis also, the bottom up sequence of installation was found to achieve a more rapid increase of factor of safety than the top down sequence. The final FOS achieved after installation of all the drains was similar for both sequences.

The response of the rectified slope to a critical design rainfall was then evaluated. The results of the analysis revealed that with the critical rainfall of total 725 mm that spanned over 30 days with low initial intensities and a peak intensity of 216 mm/day after 24 days, an adequate factor of safety was maintained in the rectified slope throughout. There was a sharp reduction of FOS soon after the peak rainfall at 25^{th} day but the slope could recover and the FOS increased as the rainfall intensity reduced.

The effectiveness of using surface vegetation cover in conjunction with subsurface horizontal drains was also studied using the 2D plane strain model. The roots of the vegetation can enhance the effective cohesion of the top soil layer and also increase the hydraulic conductivity within the rooted zone. These effects contributed to another 8 – 9% increase in factor of safety of the slope.

7.1.2 Three dimensional analysis

The two dimensional analysis performed is a significant simplification of the actual conditions when considering the morphology of the slope and the arrangement of drains. A real scale 3D finite element model was successfully developed for the site, using PLAXIS 3D software. The model also included the fan type radial drainage network as well as the surface irregularities of the slope.

The stability analysis technique available in the Plaxis software automatically detects the critical failure surface based on a stress and displacement analysis.

Hence, no pre assumptions were made on the critical failure surface in the 3D FEM analysis. However, the critical failure surface predicted using the 3D FE model was very similar to the composite failure surface identified at the Badulusirigama landslide.

The initial safety margins of the slope assessed using 2D limit equilibrium and 3D finite element approaches were in close agreement. However, the factor of safety values predicted after the slope rectification, by the 3D finite element model and the 2D limit equilibrium method were different. Generally, the 3D model indicated a lower FoS than the 2D model. This can be attributed to the different analysis techniques used to obtain the factor of safety in the two methods. The 2D model uses limit equilibrium method whereas the 3D model uses finite element based c-phi reduction technique.

Similar to the 2D analysis, 3D stability analysis also indicated a faster improvement of factor of safety when bottom up construction procedure was used, when compared with top down construction sequence. Nonetheless, the final FoS achieved after complete installation of the six drainage fans were similar from both construction sequences.

When tested for a critical rainfall event, the 3D model showed a drop in FoS sooner than the 2D model. Even though some subsequent heavy rainfall was received after the FoS has dropped, no further significant reduction of factor of safety was observed in 3D model. This can be because the 2D plane strain model assumes continuous drains in the out of plane direction of the model and thus accounts a higher effectiveness than the actual scenario. Whereas in the 3D model, the localized influence zones of the drain network are better represented.

7.2 Recommendation for future work

In this analysis, SWCC and permeability characteristics of particular soils were obtained using limited amount of laboratory data and information available in the literature. Extensive studies should be conducted to establish these unsaturated soil properties pertinent to native soils using both direct measurements and empirical correlations based on particle size distribution and Atterberg limits. Further, variation of these properties with different vegetation should be studied.

Model can be further calibrated using monitoring data available from the site. Thereby, predictions could be made with regard to pore water pressure variation of the slope corresponding to known rainfall intensities.

Functions of vegetation such as diverting rainfall, minimizing the impact on the slope surface and etc. should be further studied by instrumentation of the slope to obtain changes in moisture content and matric suction in response to different rainfall events. This would enable identification of the most appropriate vegetation types for bio- engineering measures.

The effect of possible clogging / malfunctioning of some of the drains in the long run and anticipated risks of the landslide failure if such condition occur could be extensively studied.

References

Ali, F.H. and Osman, N., 2008. Shear strength of a soil containing vegetation roots. Soils and Foundations, 48(4), pp.587-596.

Bethlahmy, N., 1962. First year effects of timber removal on soil moisture. Hydrological Sciences Journal, 7(2), pp.34-38.

Bishop, A.W., 1955. The use of the slip circle in the stability analysis of slopes. Geotechnique, 5(1), pp.7-17.

Bishop, D.M. and Stevens, M.E., 1964. Landslides on logged areas in southeast Alaska. US Forest Service research paper NOR;-1.

Brinkgreve, R.B.J., Swolfs, W.M. and Engine, E., 2017. Plaxis users manual. Balkema, Rotterdam (The Neetherlands).

Cai, F., Ugai, K., Wakai, A. and Li, Q., 1998. Effects of horizontal drains on slope stability under rainfall by three-dimensional finite element analysis. Computers and Geotechnics, 23(4), pp.255-275.

Cebada, D.P., 2017. Assessment of the role of vegetation as part of ecosystem-based risk reduction measures used for shallow-landslides in Rasuwa district, Nepal. Unpublished master thesis, University of Twente, Enschede.

Chok, Y.H., 2008. Modelling the effects of soil variability and vegetation on the stability of natural slopes (Doctoral dissertation), School of Civi, Enginerring and Minning Engineering, The University of Adelade.

Chok, Y.H., Jaksa, M.B., Kaggwa, W.S. and Griffiths, D.V., 2015. Assessing the influence of root reinforcement on slope stability by finite elements. International Journal of Geo-Engineering, 6(1), p.12.

Collins, B. D, and Znidarcic, D. 2004. Stability analyses of rainfall-induced landslides. Journal of Geotechnical and Geoenvironmental Engineering. ASCE. April 2004, Vol. 130, No. 4, 362–372

Collison, A.J.C. and Anderson, M.G., 1996. Using a combined slope hydrology/stability model to identify suitable conditions for landslide prevention by vegetation in the humid tropics. Earth surface processes and landforms, 21(8), pp.737-747.

Cook, D.I., Santi, P.M. and Higgins, J.D., 2008. 2007 AEG Student Professional Paper: Graduate Division: Horizontal Landslide Drain Design: State of the Art and Suggested Improvements. Environmental & Engineering Geoscience, 14(4), pp.241-250.

Coppin NJ, Richards IG. (1990) "Physical effects of vegetation". In Use of Vegetation in Civil Engineering, Coppin NJ, Richards IG (eds).

Coppin, N. J., Barker, D. L. & Richards, I. 1990. Use of vegetation in civil engineering. Butterworths, London.

Cornforth, D.H. and Cornforth, D., 2005. Landslides in practice: investigation, analysis, and remedial/preventative options in soils. J. Wiley.

Department of Navy, 1971. Design Manual, Soil Mechanics, Foundations, and Earth Structures, NAVFAC DM-7, Naval Facilities Engineering Command, Philadelphia.

Dharmasena UNKP, Bandara KN, Karunawardena WA, Kulathilaka SAS,. 2015. Back analysis and the rectification of failed cut slope at Southern Expressway. In: Proceedings of the International Conference on Geotechnical Engineering, Colombo, Sri Lanka

Dias, A.S., Pirone, M. and Urciuoli, G., 2017, May. Review on the methods for evaluation of root reinforcement in shallow landslides. In Workshop on World Landslide Forum (pp. 641-648). Springer, Cham.

Donald, I.B. and Giam, P.S.K., 1989. Example problems for testing soil slope stability programs (No. 8/1989).

Donald, I.B. and Giam, S.K., 1988. Application of the nodal displacement method to slope stability analysis. In Fifth Australia-New Zealand conference on geomechanics: prediction versus performance; Preprints of papers (p. 456). Institution of Engineers, Australia.

Duncan, J. M. (1996). “State of the art: limit equilibrium and finite-element analysis of slopes.” Journal of Geotechnical Engineering, 122(7), 577-596

Duncan, J.M., 1996. State of the art: limit equilibrium and finite-element analysis of slopes. Journal of Geotechnical engineering, 122(7), pp.577-596.

Elia, G., Cotecchia, F., Pedone, G., Vaunat, J., Vardon, P.J., Pereira, C., Springman, S.M., Rouainia, M., Van Esch, J., Koda, E. and Josifovski, J., 2017. Numerical modelling of slope–vegetation–atmosphere interaction: an overview. Quarterly Journal of Engineering Geology and Hydrogeology, 50(3), pp.249-270.

Endo, T. and Tsuruta, T. (1969) “The effect of the tree's roots upon the shear strength of soil”. Annual Report, Hokkaido Branch, Forest Experiment Station USA, pp167-182.

Fellenius, W., 1936. Calculation of stability of earth dam. In Transactions. 2nd Congress Large Dams, Washington, DC, 1936 (Vol. 4, pp. 445-462).

Fredlund, D. G., and Rahardjo, H. (1993). Soil Mechanics for Unsaturated Soils, Wiley, New York.

Fredlund, D.G. and Krahn, J., 1977. Comparison of slope stability methods of analysis. Canadian geotechnical journal, 14(3), pp.429-439.

Geotechnical Investigation for the slope movements in the railway track at Ihalakotte,2016, National Building Research Organization

Ghestem, M., Veylon, G., Bernard, A., Vanel, Q. and Stokes, A., 2014. Influence of plant root system morphology and architectural traits on soil shear resistance. Plant and Soil, 377(1-2), pp.43-61.

Gjetvaj, V., Znidarčić, D., Szavits-Nossan, A. and Popović, N., 2009, January. Increase of slope stability with time by drilled drains. In 17th International Conference on Soil Mechanics and Geotechnical Engineering.

Gray DH, Oshashi H (1983) Mechanics of fiber reinforcement in sand. J Geotech Eng ASCE 109:335–353

Gray, D.H. & Sotir, R.B. 1996. Biotechnical and Soil Bioengineering Slope Stabilization A Practical Guide for Erosion Control. John Wiley & Sons.

Gray, D.H. & Sotir, R.B. 1996. Biotechnical and Soil Bioengi-neering Slope Stabilization A Practical Guide for Erosion Control. John Wiley & Sons.

Gray, D.H. and Leiser, A.T., 1982. Biotechnical slope protection and erosion control. Van Nostrand Reinhold Company Inc..

Gray, D.H., Barker, D., 2004. Root-soil mechanics and interactions. In: Bennett, J.J., Simon, A. (Eds.), Riparian Vegetation and Fluvial Geomorphology. Water Science and Applications vol. 8, pp. 113–123.

Greenwood, J.R., 2006. SLIP4EX–A program for routine slope stability analysis to include the effects of vegetation, reinforcement and hydrological changes. Geotechnical & Geological Engineering, 24(3), p.449.

Greenwood, J.R., Norris, J.E. and Wint, J., 2004. Assessing the contribution of vegetation to slope stability. Proceedings of the Institution of Civil Engineers-Geotechnical Engineering, 157(4), pp.199-207.

Griffiths, D.V. and Lane, P.A., 1999. Slope stability analysis by finite elements. Geotechnique, 49(3), pp.387-403.

Hidalgo, C.A., Vega, J.A. and Obando, M.P., 2018. Effect of the Rainfall Infiltration Processes on the Landslide Hazard Assessment of Unsaturated Soils in Tropical Mountainous Regions. Engineering and Mathematical Topics in Rainfall, pp.163-185.

Huang, Y. H., 1975. "Stability Charts for Earth Embankments," Transportation Research Record 548, Transportation Research Board, Washington, DC, pp. 1-12.

Huang, W., 2018. Stability of unsaturated soil slopes under rainfall and seismic loading (Doctoral dissertation).

Huang, Y.H., 1983. Stability analysis of earth slopes. Springer Science & Business Media.

Janbu, N., 1959. Stability analysis of slopes with dimensionless parameters. Harvard University, Division of Engineering and Applied Physics.

Janbu, N., 1973. Slope stability computations. Publication of: Wiley (John) and Sons, Incorporated.

JICA 2015,Proposal for Rectification on Landslide, Slope Failure and Rock Fall in Pilot Sites, Japanese International Corperation Agency

Jotisankasa, A. & Sirirattanachat, T. 2017. Effects of grass roots on soil-water retention curve and permeability function. Canadian Geotechnical Journal. 54(11): 1612-1622.

Jotisankasa, A., Coop, M. & Ridley, A. 2009. The mechanical behaviour of an unsaturated compacted silty clay. Geotechnique59(5): 415-428.

Jotisankasa, A., Kulsawan, B., Toll, D.G. and Rahardjo, H., 2008. Studies of rainfall-induced landslides in Thailand and Singapore. In Unsaturated Soils: Advances in Geo-Engineering-Proceedings of the 1st European Conference on Unsaturated Soils, E-UNSAT (Vol. 2008, pp. 901-907).

Jotisankasa, A., Mairaing, W. and Tansamrit, S., 2014. Infiltration and stability of soil slope with vetiver grass subjected to rainfall from numerical modeling. In Proceedings of the 6th International Conference on Unsaturated Soils, UNSAT (pp. 1241-1247).

Kankanamge, L., Jotisankasa, A., Hunsachainan, N. and Kulathilaka, A., 2018. Unsaturated Shear Strength of a Sri Lankan Residual Soil from a Landslide-Prone Slope and its Relationship with Soil–Water Retention Curve. International Journal of Geosynthetics and Ground Engineering, 4(3), p.20.

Kleppe, J. H. and Denby, G. M., "Design and Performance of Horizontal Drains" (1984). International Conference on Case Histories in Geotechnical Engineering. 8.

Knappett, J.A. and Craig, R.F., 2012. Basic characteristics of soils. Carig's Soil Mechanics, pp.3-38.

Kozlowski TT (1971) Growth and development of trees, vol 2. Academic Press, New York

Krahn, J., 2004. SLOPE/W: Complete Set of Manuals. Krahn, ed., Calgary, Alta., Canada.

Kulathilaka SAS, Kumara LM (2011) Effectiveness of surface drainage in enhancing the stability of cut slopes during the periods of heavy rain. J Inst Eng Sri Lanka, 127–137

Kulathilaka SAS, Sujeevan V (2011) Rain-triggered slope failures in unsaturated residual soils. J Sri Lankan Geotech Soc 6:20–26

Lau, K.C. and Kenney, T.C., 1984. Horizontal drains to stabilize clay slopes. Canadian Geotechnical Journal, 21(2), pp.241-249.

Lau, K.C. and Kenney, T.C., 1984. Horizontal drains to stabilize clay slopes. Canadian Geotechnical Journal, 21(2), pp.241-249.

Mahannopkul K, Jotisankasa A (2019) Influence of root suction on tensile strength of Chrysopogon zizanioides roots and its implication on bio-slope stabilization. Journal of Mountain Science 16(2). https://doi.org/10.1007/s11629-018-5134-8

GeoStudio manual. "Seepage modeling with SEEP/W." (2012)

Matthews, C., Farook, Z. & Helm, P.R. (2014). Slope stability analysis – limit equilibrium or the finite element method? Technical Paper. Ground Engineering. May. pp. 22-28.

Memon, M.Y., 2018. A Comparison Between Limit Equilibrium and Finite Element Methods for Slope Stability Analysis.

Morgan, R.P. and Rickson, R.J., 1995. Slope stabilization and erosion control: a bioengineering approach. Taylor & Francis.

Morgenstern, N.U. and Price, V.E., 1965. The analysis of the stability of general slip surfaces. Geotechnique, 15(1), pp.79-93.

Nakamura, H. (1988) “Landslide control works by horizontal Drainage works”. Proc. 5th International Symposium on Landslides, Lousanne, Vol. 2.

Ni, J., Leung, A.K. and Ng, C.W., 2019. Unsaturated hydraulic properties of vegetated soil under single and mixed planting conditions. Géotechnique, 69(6), pp.554-559.

Nilaweera, N.S. and Nutalaya, P., 1999. Role of tree roots in slope stabilisation. Bulletin of engineering geology and the environment, 57(4), pp.337-342.

Nilaweera, N.S., 1994. Effects of tree roots on slope stability: the case of Khao Luang Mountain area, So Thailand. Dissert. No. Gt-93-2.

Nonveiller, E. (1981), Efficiency of Horizontal Drains on Slope Stability, Proceedings, International Conference on Soil Mechanchanics and Foundation Engineering, Stockholm, Vic 3, 495-500.

Pathmanathan, M.L., 2009. Numerical Simulation of the Performance of Horizontal Drains for Subsurface Slope Stabilization (Doctoral dissertation, Washington State University).

Rabie, M., 2014. Comparison study between traditional and finite element methods for slopes under heavy rainfall. HBRC Journal, 10(2), pp.160-168.

Rahardjo H, Leong EC, Rezaur RB (2002) Studies of rainfall-induced slope failures. Proceeding of the National Seminar Slope 2002, April 27, 2002, Bandung, Indonesia, pp 15–29

Rahardjo, H., A. Satyanaga & E.C. Leong. 2012. Unsaturated Soil Mechanics for Slope Stabilization. Geotechnical Engi-neering Journal of the SEAGS & AGSSEA 43(1)

Rahardjo, H., Hritzuk, K.J., Leong, E.C. and Rezaur, R.B., 2003. Effectiveness of horizontal drains for slope stability. Engineering Geology, 69(3-4), pp.295-308.

Rahardjo, H., Li, X.W., Toll, D.G., Leong, E.C., 2001. The effect of antecedent rainfall on slope stability. Geotechnical and Geoenvironmental Engineering 19, 371– 399.

Rahardjo, H., Nio, A. S., Leong, E. C., and Song, N. Y. (2010). "Effects of groundwater table position and soil properties on stability of slope during rainfall." Journal of Geotechnical and Geoenvironmental Engineering, 136(11), 1555-1564.

Rahardjo, H., Santoso, V.A., Leong, E.C., Ng, Y.S. and Hua, C.J., 2011. Performance of horizontal drains in residual soil slopes. Soils and foundations, 51(3), pp.437-447.

Rahardjo, H., Satyanaga, A. and Leong, E.C., 2012. Unsaturated soil mechanics for slope stabilization. Southeast Asian Geotechnical Journal, 43(1), pp.48-58.

Riestenberg, M.M. (1987) Anchoring of thin colluvium on hillslopes by roots of sugar maple and white ash. PhD Dissertation, University of Cincinnati, Cincinnati, OH.

Santi, P.M., Crenshaw, B.A. and Elifrits, C.D., 2003. Demonstration projects using wick drains to stabilize landslides. Environmental & Engineering Geoscience, 9(4), pp.339-350.

Santoso, V.A., Rahardjo, H., Leong, E.C., Ng, Y.S. and Tam, C.P.H., 2011. Horizontal drains in residual soil slopes.

Schwarz M, Preti F, Giadrossich F, Lehmann P, Or D (2009) Quantifying the role of vegetation in slope stability: a case study in Tuscany (Italy). Ecol Eng (in press). doi:10.1016/ j.ecoleng.2009.06.014

Sidle RC (1992) A theoretical model of the effects of timber harvesting on slope stability. Water Resour Res 28:1897– 1910

Sidle RC, Pearce AJ, O'Loughlin CL (1985) Hillslope stability and land use. Am Geophysical Union, Water Resour Monogr 11. Washington, DC, p 140

Spencer, E., 1967. A method of analysis of the stability of embankments assuming parallel inter-slice forces. Geotechnique, 17(1), pp.11-26.

Stokes A, Ball J, Fitter AH, Brain P, Coutts MP (1996) An experimental investigation into the resistance of model root systems to uprooting. Ann Bot 78:415–421

Sujeevan V, Kulathilaka SAS (2011) Rainfall infiltration analysis in unsaturated residual soil slopes. J Sri Lankan Geotech Soc 6:9–19

Taylor, D.W., 1937. Stability of earth slopes. J. Boston Soc. Civil Engineers, 24(3), pp.197-247.

Tsukamoto Y, Kusakabe O (1984) Vegetation influences on debris slide occurrence on steep slopes in Japan. Proc Symp Effects of forest land use on erosion and slope stability, Environment & Policy Institute, Honolulu, Hawaii

Veylon G, Ghestem M, Stokes A, Bernard A (2015) Quantification of mechanical and hydric components of soil reinforcement by plant roots. Can Geotech J 52:1839–1849

Wu TH (1976) Investigation of landslides on Prince of Wales island. Geotechnical Engineering Report 5, Civil Engineering Department, Ohio State University, Columbus, Ohio

Wu W, Sidle RC (1995) A distributed slope stability model for steep forested basins. Water Resour Res 31(8):2097–2110

Wu, T. H., Mckinnel, W. P. & Swanston, D. N. 1979. Strength of tree roots and landslides on Prince of Wales Island, Alaska. Canadian Geotechnical Journal. 16(1): 19-33.

Wu, T.H., McOmber, R.M., Erb, R.T. and Beal, P.E., 1988. Study of soil-root interaction. Journal of Geotechnical Engineering, 114(12), pp.1351-1375.

Yildiz, A., Graf, F., Rickli, C. and Springman, S.M., 2018. Determination of the shearing behaviour of root-permeated soils with a large-scale direct shear apparatus. Catena, 166, pp.98-113., Yildz, Springman,, 2018

Yu, K., Pypker, T.G., Keim, R.F., Chen, N., Yang, Y., Guo, S., Li, W. and Wang, G., 2012. Canopy rainfall storage capacity as affected by sub-alpine grassland degradation in the Qinghai–Tibetan Plateau, China. Hydrological Processes, 26(20), pp.3114-3123.

Zapata, Claudia Elena. "Uncertainty in soil-water-characteristic curve and impacts on unsaturated shear strength predictions." (1999),PhD Dissertation, Arizona State University, Tempe, USA 5661-5661.

Zhan, T. L., Ng, C. W., and Fredlund, D. G. (2007). “Field study of rainfall infiltration into a grassed unsaturated expansive soil slope.” Canadian Geotechnical Journal, 44(4), 392-408.

ZHOU, W.ANDMAERZ, N. H., 2002, Identifying the optimumdrilling direction for characterization of discontinuous rock:Environmental Engineering Geoscience, Vol. 8, No. 4,pp. 295–307

Ziemer RR (1981) The role of vegetation in the stability of forested slopes. Proceedings of the International Union of Forestry Research Organizations, XVII World Congress. Kyoto, Japan. Vol. I, pp 297–308